SELF-CRACK HEALING OF ENGINEERING CERAMICS

by

ISRAA ARIF HAMMOOD

A dissertation submitted in partial fulfillment of the
requirements for the degree of

DOCTOR OF PHILOSOPHY IN MECHANICAL ENGINEERING

2022

Oakland University
Rochester, Michigan

Doctoral Advisory Committee:

GARY BARBER, Ph.D., Chair
ROBERT ADAMS, Ph.D.
DAVE SCHALL, Ph.D.
DEBATOSH DEBNATH, Ph.D.
SHIHAB AHMED ZAIDAN, Ph.D.
ANKUN YANG, Ph.D.

To remind myself how precious I am, I dedicate this dissertation to myself.

ACKNOWLEDGMENTS

I would like to acknowledge the HCED/Higher Committee for Education Development in Iraq, the director David Archbold and all the staff in the ISSO/the International Students and Scholars Office and the Graduate Office/School at Oakland University, administrative, advisers, directors, and all workers.

I would like to appreciate/acknowledge the Dean of the School of Engineering and Computer Science (SECS), Dr. Louay M. Chamra, at Oakland University, and both Qian (Beth) Zou, Associate Dean and Professor, and Katie Loodeen, Administrative Assistant to the Associate Deans and the workers at the Dean's Office for their support towards the completion of the Ph.D. Program.

My deep appreciation and gratefulness would go to my advisor, Prof. Dr. Gary Barber, and the Doctoral Advisory Committee Members Dr. Robert Adams, Dr. J Dave Schall, Dr. Ankun Yang, Dr. Debatosh Debnath and Dr. Shihab Ahmed Zaidan for their tremendous support, guidance and mentorship. I would also like to thank Dr. Meir Shillor, the Professor in the Mathematics and Statistics Department at the College of Arts and Sciences. Special Thanks would go to Brenda Bond, Administrative Assistant, Chair Department, Dr. Brian P. Sangeorzan, at the Mechanical Engineering in the SECS and Dr. Hongwei Qu, the Professor at the Electrical Engineering Department in the SECS at Oakland University for facilitating the research and paperwork and their assistance. I also would like to specially thank Steven Thrush, Bingxu Wang, all friends and colleagues at the Automotive Tribology Center and Matt Bruer, the Lab Manager.

I would like to thank the faculty members at the Branch of Materials Science in the College of Applied Science at the University of Technology, mainly Dr. Balqees M. Al-Dabbagh, Dr. Zaid Saleh, Noor Sabah, Dr. A. Sattar & Dr. Ranah M. Salih, and the technicians and Engineers at the Machine Shop in both Oakland University and the University of Technology.

 The samples prepared at the UOT, University of Technology and the selection process of particles, were prepared and done by Dr. Sh. A. Zaidan, the Professor of Ceramics and Materials Science at the branch of Materials Science in the College of Applied Science at the University of Technology; the heat treatment of the samples using the Tig process were done by the engineers and technicians at the machine shop in the UOT. The SEM images were taken at Al-Khora Company located in Baghdad, Iraq.

And finally, I would like to thank all those who have supported me towards achieving the PhD including family members, my mother, my siblings and their families, uncles and their families, mentors and friends.

Israa Arif Hammood

PREFACE

About the passion, motivation, level of sophistication, uniqueness, elegance yet simplicity, and reconciliation that can inspire/be the inspiration to dive into the field of research/research field; those altogether can be the key to an overwhelming success in most cases if not to exaggerate or manage the priorities which can be daunting; without the support, patience, persistence, passion, and motivation, nothing can be achieved and completed.

This work can be the node or the bridge for other findings or may facilitate or be considered as the base from which the shuttles can be launched for more innovations towards a more sustainable and clean future. Developing a better understanding towards the healability, theory, applications and mechanisms, of different types of materials is the main focus in this dissertation.

Thanks from the bottom of my heart to all who have stood by me and supported me.

ABSTRACT

SELF-CRACK HEALING OF ENGINEERING CERAMICS

by

ISRAA ARIF HAMMOOD

Adviser: GARY BARBER, Ph.D.

Healability and recyclability of materials; replicating nature in its beauty, where everything beautiful comes out of nature. The self-crack healing mechanism inspired by the natural healing ability of the biological and eco-systems can be categorized into either extrinsic or intrinsic, autonomous or non-autonomous. In the case of extrinsic healing, the system requires healing agents. On the other hand, intrinsic healing is inherent, the healing process is inherent in the material itself.

The purpose in its simplicity is to heal the damage in a sample composed of ceramic particles through the heat treatment or through applying another source to heal the damage might be through using a laser source at room temperature to reduce the cost of wasting efforts and materials. The system can be designed to include a sensor to sense the damage in the component and a healing agent like loose particles or a specific source that provides an immediate treatment through the heating in order to create or generate the glassy phase. Self-crack-healing materials are able to sense the crack and heal it. The notion of not giving up on things can be considered as the motive for such type of research.

Most ceramics are brittle and hence they are sensitive to flaws and cracks. Ceramics are subjected to thermal and mechanical stresses during service. Residual stresses may eventually cause microcracks (internal and surface cracks) and the failure of the component in use. This limits their use as structural engineering materials, and thus applying or inducing a self-crack healing ability would be a solution to overcome this problem. Great benefits can be expected from the components in use while applying the self-healing ability, such as reducing maintenance, inspection, and the cost of machining and polishing as well, which enhances the reliability of the component in use, and hence achieving a higher structural integrity*.

Developing new materials with increasing resistance to wear and corrosion is the goal for many researchers and manufacturers as well. Consequently, an attempt to imitate the mechanisms employed by nature through the biological systems have been made to design self-healing materials and coatings for corrosion protection which can result in complete recovery*.

Ceramics can be used in many applications including aeroengine turbine blades, gas turbine blades, high performance bearings and many other applications that require high temperature service and extreme environments like space shuttles*. However, these ceramics have low fracture toughness, which means that they are brittle and sensitive to flaws such as micro and macro cracks, which limit their applications as structural components. Crack-healing in ceramics is considered as a sustainable way, hence the present research is focused on the self-crack healing ability of Spinel nanocomposites and SiC bonded Kaolinite. The self-crack healing behavior was investigated as a function of

the healing conditions (time, temperature, and chemical composition) as well as the mechanism responsible for healing the cracks.

TABLE OF CONTENTS

TABLE OF CONTENTS—Continued

TABLE OF CONTENTS—Continued

LIST OF TABLES

LIST OF FIGURES

LIST OF ABBREVIATIONS

TBC	Thermal Barrier Coating
YPSZ	Yttria Partially Stabilized Zirconia
SPS	Suspension Plasma Spray
MAX	M denotes an early transition metal, A is a III A or IV A group elements, and X is either C or N
NMR	Nuclear Magnetic Resonance Spectroscopy
XRF	X-Ray Fluorescence
XRD	X-Ray Diffraction
FEA	Finite Element Analysis
EMA	Polyethylene-co-methyl acrylate
EMAA	Polyethylene-co-methacrylic acid
UF	Urea-Formaldehyde
DCPD	Dicyclopentadiene
TEM	Transmission Electron Microscopy
EDS	Energy Dispersive X-Ray Spectroscopy

CHAPTER ONE

INTRODUCTION

1.1 Relevance

Self-crack-healing materials are able to sense the crack and heal it. The notion of not giving up on things can be considered as the motive for such a type of research.

Ceramics can be used in many applications including aeroengine turbine blades, gas turbine blades, high performance bearings, and many other applications that require high temperature service or extreme environments like space shuttles. However, Ceramics are subjected to thermal and mechanical stresses during service. Residual stresses may eventually cause microcracks (internal and surface cracks) and the failure of a component in use. This limits their use as structural engineering materials, and thus applying or inducing self-crack healing ability would be a solution to overcome this problem. Great benefits can be expected from the components in use while applying self-healing ability, such as reducing maintenance, inspection, and the cost of machining and polishing, which enhances the reliability of the component in use*.

Developing new materials with increased resistance to fracture wear and corrosion is the goal for many researchers and manufacturers as well. Consequently, many attempts have been made to imitate the mechanisms of biological systems to design self-healing materials and coatings which can result in complete recovery. These research studies are reviewed and summarized. Self-crack-healing materials have the capability of partial or complete healing of the cracks and the damage imposed on them as well as the capability of recovering the functionality and the integrity of the structure [1, 2]. The self-

crack healing mechanism inspired by the natural healing ability of biological systems can be categorized as either extrinsic or intrinsic which, this categorization, is more applicable for polymeric composites; however, it can be used for ceramics or ceramic composites. In the case of extrinsic healing, the system requires healing agents. On the other hand, intrinsic healing is inherent, the healing process is inherent in the material itself. Autonomic self-healing would make the materials ideal for aerospace and automotive applications. Among the many types of healing only self-crack healing induced by oxidation can attain complete recovery. The crack healed zone should be mechanically as strong as the original material to achieve complete strength recovery, thus the crack healed zone should satisfy the following requirements*:

- The volume between the crack walls should be completely filled with the product formed by the self-healing reaction.
- The formed product should have the same or higher strength as the base material.
- The formed product should strongly bond to the crack walls.

For intrinsic self-healing, the healing agent is embedded into the matrix and the healing process is due to physicochemical reaction. The damage triggers the healing process through the healing agent. The mechanical properties can be recovered upon the healing process. In the case of extrinsic self-crack healing, the healing agent would be foreign particles added to the material during the manufacturing process. In this case, the healing agent is encapsulated and dispersed within the matrix. Upon cracking, the healing agent in the capsules flows into and fills the gap between the crack faces causing the

bridging of these crack faces (the healing agent interacts with the cracks). The crack causes the rupture of the capsules, releasing the healing agent, which flows to fill the cracks. This is followed by a physical or a chemical reaction to mend the crack faces, consequently resulting in the mechanical integrity of the component/composites [1].

Ceramics have low fracture toughness, which means that they are brittle and sensitive to flaws such as micro and macro cracks, which limit their applications as structural components. The present research is focused on the self-crack healing ability of different materials and composites. Self-crack healing behavior is reviewed as a function of the healing conditions (time, temperature, and chemical composition) as well as the mechanism responsible for healing the cracks.

A preliminary study, research and review on self-healing was conducted in the current research. A new method was used in this research to heal the damage on the surface of the samples using the heat treatment at elevated temperatures around 3000 ºC. and through using the electrical arc method, known as the traditional tig, Tungsten Inert Gas. The heat treatment for the samples to heal the damage on the surface of the samples was done through using an electrical arc method or tig, it's mainly a type of welding used to weld metals and alloys yet in the current research it has been used as a process to heal the cracks or the damage in ceramics. Through this process the damage could be healed through the heat generated by the electric arc; an inert gas like argon is used in this process as a shielding gas; during this process, the arc is formed between the tungsten electrode and the workpiece.

In this dissertation, Chapter 1 discusses the definition and the mechanisms of the self-crack healing process in ceramics, their composites and in materials in general; a literature review on the self-healing behavior in different classes of materials was conducted. Chapter 2 discusses the mechanisms and the requirements of self-crack-healing in ceramics and their composites and the objective of the current research. It also describes numerical models/computational models on self-healing systems conducted by previous researchers and the thermodynamics of the healing reaction. Chapter 3 focuses on materials/particles used in the current research and the experiments. Chapter 4 discusses pest oxidation of $MoSi_2$ nanocomposites, definition, studies, and factors/conditions. Chapter 5 includes results and a corresponding discussion. Chapter 6 consists of a summary, conclusion, and suggestions for future research.

1.2 Literature Review

Degradation, damage and failure can occur as a consequence of materials use, transport or processing, and hence designing a system with a self-crack healing ability to repair the damage and recover the structural integrity as well as prolonging the service life has been the goal for many researchers. The phenomena of self-healing behavior for structural materials as well as for coatings has a positive economic impact on society*.

T. Osada et al. gave a historical background on self-healing materials in their paper entitled "Focus on Self-healing materials: recent challenges and innovations.'' [2]. A review on the experimental and numerical studies on self-crack healing in materials was made in this chapter as categorized below:

1.2.1 Self-healing in ceramics, thin films and its composites/ concepts and previous studies

Inspired by nature, inducing crack healing capability in ceramics can bring many benefits including less maintenance, enhancing the reliability and the structural strength, and reducing maintenance [3].

Designing a self-healing system with self-crack healing ability has been a research topic for many researchers in the field of science and engineering. Investigations on the self-crack healing can be traced back to 1958 by Hummel and Bush [4]. They showed that the mechanical properties (Strength and Young's Modulus) of magnesium dititanate increased at high temperatures (1000 °C) and the healing of the cracks was the reason behind enhancing the properties. The self- healing of the cracks was investigated by several researchers; Lange, Petrovic and Jacobson [5]. They showed that at high temperatures, SiC reacts with oxygen to form SiO_2, which flows to fill the cracks.

Fig 1. Wound healing in the human body compared to crack healing in ceramics

Fig 1. shows the analogy of the self-healing process to wound healing in human bodies. In a self-crack healing process, the first step is the sintering process, which is an external stimulus to trigger the self-healing. The next step is the grain growth phenomenon and crack closure, and finally the formation of new bonds and healing of the crack [6]. The crack healing behavior of Spinel ($MgAl_2O_4$) ceramics has been investigated by several researchers. F. Tavangarian and G. Li investigated the crack healing behavior and the strength recovery of SiC/Spinel nanocomposites. The results of their work showed that the complete healing of the induced cracks was attained at a temperature of 1545 °C in a holding time of 1 min in an air atmosphere. A strength recovery was achieved for the samples heat treated at a temperature of 1550 ºC and 1 min holding time. A healing efficiency of about 99% was recorded for the samples healed at a temperature of 1550 ° C and 1 min holding time [6, 7, & 8]. In another study, F. Tavangarian et al. made a review on the crack-healing behavior in materials. In their publication they mentioned the recent developments in the area of crack-healing in materials, its applications and other future perspectives in this field [9].

Justyna K. et al. investigated the self crack-healing of YPSZ/$MOSi_2$ composites; the results of their study showed that the healing process occurs at high temperatures through the decomposition of the $MoSi_2$ leading to the formation of the reaction products which bridge the cracks to seal/mend it[10]. The self-healing behavior of $MoSi_2$ dispersed in YSZ/ and their oxidation behavior was studied at temperatures ranging from (1000 - 1300) °C [11]. G. Zhu et al. investigated the crack healing behavior of $MoSi_2$ and $(MoNb)Si_2$, the results of their research showed that the cracks can be healed through the

formation of an oxide layer (SiO_2) on the surface of the specimens at high temperatures [12].

Takahashi et al. [13] investigated the self crack-healing behavior of SiC/Al_2O_3 composites. Their results showed that healing was achieved at a temperature of 1200 °C with a holding time of 1 h in air, whereas partial healing was achieved for the samples healed at 1100 °C. The self-healing behavior of SiC/Al_2O_3 and $SiC/Al_2O_3/Y_2O_3$ composites was investigated by Kim et al. [14]. They demonstrated that self-healing of cracks occurs by a sintering process. In the case of the SiC/Al_2O_3 composite, the healing process of the cracks was achieved by the reaction of SiC with the oxygen to form SiO_2. However, in the case of a $SiC/Al_2O_3/Y_2O_3$ composite, the SiC oxidized to either amorphous or cristobalite silica. This was due to the reaction of silica and alumina, a mullitization reaction occured at temperatures above 1400 °C. However, adding yttrium oxide as a sintering additive lowers the temperature at which this reaction occurs. Kim et al. found that cracks can be healed through the sintering process of pre-cracked specimens at a temperature above 1400 °C for 1 h holding time. In the ternary systems they studied $SiC/Al_2O_3/Y_2O_3$, a liquid eutectic compound ($Y_2Si_2O_7$) was formed which flowed due to the low viscosity to fill the cracks and heal the surface.

Self-crack healing behavior of SiC was investigated by Osada et al. [15, 16] at temperatures ranging from (1000-1500) °C for different pressures of oxygen (1 atm, 5×10^{-4} atm, and 0.05 atm). The strength was recovered completely owing to the passive oxidation of the SiC. Ando et al. [17, 18] investigated the self- healing ability of SiC/Si_3N_4 composite; they demonstrated that cracks can be healed completely at temperatures

ranging from (900-1400 °C) in an air environment. The optimum conditions for healing the cracks were (1200-1300) °C for 1h in air only. Also, the crack healing behavior of Si_3N_4/SiC was investigated by Ando et al., at high temperatures under cyclic stress. Their results showed that the composite has an excellent healing ability, a complete healing of the cracks can be achieved at temperatures (1100-1200 ºC) regardless of the healing time [19].

Several studies on self-crack healing linked the self-crack healing phenomena and the oxidation behavior of the crack healing agent. The structural integrity can be enhanced through inducing the healing ability through the chemical reaction of the healing agent. The rate of the chemical reaction is affected by the temperature. Tikare and Choi [20] showed that the healing process can occur in different environments around 800 °C through mass transport. Haung and Wen [21] investigated the self-crack healing mechanism of Al_4SiC_4 ceramics. They showed that the healing process occurs through oxidation and release of the residual stresses (Sintering process at 1300 °C in air rather than in vacuum). Radford and Lange [22] showed that the healing of cracks can be achieved through the sintering process of samples fabricated from alumina, at a temperature of 1700 °C for a healing time of 1 h (the healing process is a result of the grain growth from one side to the other side of the crack surface). In other cases, the healing process can be achieved by the pore evolution of the microstructure during the annealing process of alumina as demonstrated by Gupta [23]. After sintering for 1 h, most of the cracks were healed and around 95% of the strength was recovered. M. Nakatani et al. studied the crack healing ability of SiN/SiC nanolaminated films at elevated temperatures ranging from (600-1200) ºC in an air environment. Their results showed

that the inserted layers of SiC may heal the cracks in SiN thin films. They also reported that the healing ability can be enhanced upon increasing the time and temperature [24]. Chen et al. investigated the crack healing ability in $Zr_2Al_4C_5$ composite ceramics at high temperatures ranging from (800-1200) ºC. They reported that this composite has an excellent ability to heal induced cracks and damage through the oxidation process. Their results showed that the optimum temperature to heal the cracks was 1000ºC. They reported that the cracks could be healed completely at a temperature greater than 1000 ºC in an air environment, the main mechanism to heal the cracks was found to be the oxidation process and forming of the oxides mainly t-ZrO_2 and α-Al_2O_3 [25]. Chu et al. [26] investigated self-healing of SiC ceramics, and showed that the strength of the healed samples increased as a result of the residual stresses due to the thermal expansion mismatch of SiO_2 and SiC. The self-crack healing ability was investigated by Chuo et al. [27]. They showed that cracks in SiC/Al_2O_3 ceramic can be partially healed in an argon atmosphere. Thompson et al. [28] investigated the self-healing ability of SiC/Al_2O_3 nanocomposites. They showed that pre-cracked specimens could be healed at 1300 °C for 2h holding time in an argon atmosphere. Adhesion of the cracks was the responsible mechanism for healing of the pre-cracked specimens. Self-crack healing ability was investigated by Wang and Steven [29]. They showed that Zirconia has excellent self-healing ability. At 1700 °C the ZrO_2(m) transforms into ZrO_2(t), which heals the cracks and recovers the strength. The responsible mechanisms for healing the cracks are the rearrangement of the grains through the transformation as well as the diffusion process. Takahashi et al. investigated the crack healing ability of mullite/SiC multi-composite under stress. The results of their work showed that the composite has an excellent healing

ability. The induced cracks healed under cyclic and static stresses at a temperature of 1473 k [30]. The self-healing of C/SiC composites modified with Si-B-C was investigated by Zuo et al. [31].

The phenomena of self crack healing was investigated based on numerical simulations using finite element analysis [32, 33]. The self-healing of cracks was investigated to extend the lifetime of thermal barrier coatings through the oxidation and decomposition of $MoSi_2$(B) healing particles at high temperatures leading to the formation of amorphous silica which flows to seal the cracks and/or fill the gap between the crack faces. This is followed by the reaction of ZrO_2 based thermal barrier coatings(TBC), which leads to the formation of $ZrSiO_4$, and this reaction leads to strong bonding between the healing agent and the matrix material and hence filling/sealing/mending the cracks [34]. The self-healing behavior of thermal barrier coatings fabricated by spark plasma sintering was investigated by F. Nozahic et al. The coating consists of yttria partially stabilized zirconia (YPSZ) with dispersed core-shell particles of MoSi2-Al_2O_3 as a healing agent (Self-healing TBC made of YPSZ and core-shell encapsulated $MoSi_2$(B) based particles). The coating was applied on MCrAlY coated Ni based superalloys through SPS)[35]. The self-healing ability of carbon composites containing B_4C and SiC particles has been investigated by Kobayashi et al [36]. T. Osada et al. [37] made a universal kinetic model of strength recovery which they considered a key parameter in the design of self-healing ceramics. In their study or self-healing design, they depend on the oxidation induced self-healing of surface cracks in composites containing a healing agent. Their prediction model of the strength of the healed composites was confirmed to be

identical to the experimental values and that could facilitate the design of self-healing ceramics suitable for various applications.

The self-healing ability of C/SiC composites modified with Si-B-C was investigated by Cao X. et al. at elevated temperatures and due to the thermal mismatch, the cracks can be healed [38]. Li et al.[39] investigated the crack healing ability of Ti_2AlC ceramic at high temperature. Their investigation showed that the cracks could be healed completely at 1200ºC for 2h in air and the Ti_2AlC shows significant crack healing ability as the cracks can be completely healed and filled with the oxidation products and the flexural strength can be recovered or even slightly enhanced. Rajesh et al. made an investigation on manufacturing of the self-healing materials. In this paper, they searched the modern approaches to self-healing [40]. The crack healing behavior in yttria stabilized zirconia thermal barrier coatings was investigated by Z. Derelioglu et al. through embedding the encapsulated particles of $MoSi_2$(B) as a healing agent. They reported that the cracks healed through the oxidative decomposition of the embedded particles at high temperatures and the formation of silica, which flows to the gap between the crack faces and reacts with zirconia to form $ZrSiO_4$ to adhere or seal the crack surfaces [41].

The mechanism behind the self-healing of the cracks can be attributed to the oxidation, diffusion and grain growth during the sintering process. During the sintering process the particles diffuse through the grain boundaries and as a consequence bridge the crack planes. During the sintering process, the system can fill the induced cracks with the formed transition compounds (glassy phases) and heal it. The generation of the mobile glassy phase is a necessity for the self-healing process. The crack healing behavior of mullite/SiC/Y_2O_3 composite was investigated by Lee et al. They showed that

the cracks can be healed due to sintering at temperatures ranging between (1200-1400) °C in an air environment [42]. S. Yoshioka et al. made an investigation using TiC particles as a healing agent to heal the induced cracks in Al_2O_4 based composites at high temperatures. In their study, they reported that TiC has potential to heal the cracks in ceramic systems extrinsically [43]. The crack healing behavior of SiC/Al_2O_3 composites was investigated by Ando et al. They showed that the cracks can be healed completely at healing conditions of 1300°C for 1 h healing time in an air environment. As a result of the reaction between SiC and O_2, the oxide SiO_2 forms, which is responsible for healing the cracks [44]. $MoSi_2$ was found to be a self-healing agent in TBCs by Sloof and Kochuby. When the crack is initiated, the healing agent reacts with O_2 to form the mobile phase which flows to fill the cracks [45]. The self-healing behavior of structural ceramics was investigated by K. Ando and W. Nakao. In their research they investigated the crack healing conditions (temperature, time, and chemical composition), and their influence on the healing behavior. They also showed that it is important to induce the self-healing ability in ceramics to improve the reliability and induce the structural integrity and reduce the machining and maintenance cost [46]. K. Houjou et al.[47] studied the self-healing behavior of Si_3N_4/SiC composites as a function of temperature, time, crack size and environment and the oxidation behavior as a function of the temperature and time. They reported that cracks could be healed completely in an air environment but not in N_2, Ar nor in vacuum. The optimum temperature to heal the cracks completely ranged between (900-1400) ºC, the maximum size of the cracks to be healed completely was reported to be 200 μm in diameter. The crack healing ability of Al_2O_3/Ti_2AC was investigated by B. J. Pedimonte et al. The addition of the MAX (where M denotes an early transition metal,

A is a III A or IV A group elements, and X is either C or N) phase served as a healing agent which reacts with the O_2 present to form oxidation products which flow to fill the gap between the crack faces. The oxidation products were Ti_2AlC and Ti_2SnC [48]. The crack healing behavior of Al_2O_3/SiC composite was investigated under various conditions by Masata Ono et al. The healing process was accomplished through the sintering of the composites. The heat treatment conditions to heal the cracks completely ranged from (1000 °C- 1400 °C) in air. Various healing conditions were applied to heal the surface cracks of the machined specimens [49]. The self-crack healing performance of Ti_2AlC ceramics was investigated by H. J. Yang et al. Their results showed that cracks can be healed after heat treatment of 1200 °C in air for 10 min, the healing of the cracks was due to an oxidation process [50]. The analysis of the self-healing effect of the crystalline admixtures in concrete was studied in 4 different environments. The results showed that the healing behavior differs depending on the exposure and the presence of the crystalline admixtures [51]. The crack healing ability of Al_2O_3/SiC was investigated by Takahashi et al. Complete healing of the induced cracks was achieved at temperatures of 1200 °C or 1300 °C for a holding time of 1hr. A partial healing of the cracks was observed [52]. Lu X. et al. reported in their article the oxidation process and the formation of the oxide (α-Al_2O_3) as the main mechanism to heal the cracks [53]. SiC is one of the most investigated self-healing agents when a crack occurs, SiC reacts with the oxygen in an air environment during the sintering process at high temperatures to form SiO_2, which flows to fill initial cracks or cracks induced upon service [5, 54, 55, 56, and 57]

The crack self-healing in ceramics has been investigated by many researchers on single oxide crystals, amorphous silicates, polycrystalline oxide and non-oxide materials.

A number of studies can be found in the literature regarding self-healing behavior of engineering ceramics, such as Al_2O_3/SiC composite, Si_3N_4 composite, ZrB_2/SiC ceramics and ternary carbides (e.g. Ti_3AlC_2, $Zr_2Al_4C_5$.etc.). Many of these studies showed that the crack healing ability of these materials was induced by surface oxidation. Oxidation products, such as SiO_2, Al_2O_3, and TiO_2 can easily penetrate into the defects and flaws, which leads to the closure of cracks and healing. Systems like Si_3N_4/SiC, Mullite/SiC, and Al_2O_3/SiC have been investigated and showed significant self-healing abilities [17, 49, and 58]. The crack healing behavior in Al_2O_3 was investigated by Kim et al. Their results showed that cracks can be healed by sintering the samples above 1400 ºC for 1h [59]. The crack healing behavior of Cr_2AlC ceramic as a function of temperature, time, and crack size was investigated by Li et al. In their study they showed that healing of the cracks was due to annealing of the specimens at temperatures above 1000 °C [60]. The crack behavior of UO_2 has been investigated by Bain. The responsible mechanism for healing cracks is the grain growth due to the irradiation of UO_2 at conditions of 1400 °C and 600 h [61]. Roberts and Heuer showed that the healing ability in monolithic Al_2O_3 can be attributed to the sintering process at temperatures above 1000 °C, whereas Kim et al. showed that cracks were healed at temperatures above 1400 °C for 1h [62]. The topic of self-healing has gained considerable interest for many researchers for the purpose of sustainability [63]. A Farle et al. studied the crack healing behavior of Ti-containing materials and composites under combustion chamber conditions. The mechanism that is responsible for healing the cracks is oxidation induced sintering. The main ceramics that they used in their study were Al_2O_3, Ti_2AlC and Cr_2AlC. The results of their research showed that the MAX phase ceramics Ti_2AlC and Cr_2AlC have an intrinsic ability to heal the cracks. In

alumina, the healing was achieved through the dispersion of the TiC particles. In Al_2O_3/TiC, the crack closure was achieved through filling of the cracks with the oxides, TiO_2. In Ti_2AlC, the main oxides formed were TiO_2 and Al_2O_3. In the case of Cr_2AlC, the cracks were filled with Al_2O_3 [64].

In general, the healing process is triggered by a chemical oxidative reaction while specimens are being sintered/heat treated. The size of the particles play a role in the self-healing process, the smaller the particle size, the more efficient the healing process, and the better the mechanical properties. The size of the nanoparticles used should be similar.

Some studies have shown that the healing process or the rate of healing depends on the crack width; the healing rate or the degree is reduced as the cracks width is increased [65]. Sloof et al. [66] reported the oxidation process and the formation of the oxides, mainly Al_2O_3 as the main mechanism to heal MAX phase ceramics, Ti_3AlC_2, Ti_2AlC and Cr_2AlC upon the heat treatment at elevated temperatures. X. Tao et al. [67], investigated the self-crack healing behavior of $MoSi_2$/borosilicate glass composite by comparing the flexural strength of the pre-scratched specimens before and after healing treatment. The strength could be recovered partially after heat treatment higher than 800ºC, and the healing of the scratch was observed after healing treatment at 900ºC and 1400 ºC . X.-P. Zhans et al. [68] investigated the crack healing behavior and strength recovery of ZrO_2 (Y_2O_3)-Al_2O_3-$MoSi_2$ ceramics in air at different conditions (heat treatment, time, and the content of the base material $MoSi_2$ in the composite). The results of their investigation showed that cracks could be healed completely at 1100 ºC for 3h in air and the strength recovered. The oxidation products such as SiO_2 (glassy phase) were

responsible for healing the cracks and recovering the strength (the glassy phase formed by the oxidation reaction is responsible for closing the cracks and rebinding the crack walls). Increasing the $MoSi_2$ content increased the flexural strength, however it was lower than that of the original samples. K. Takahashi et al. [69] studied the crack-healing behavior of Si_3N_4/SiC composites under cyclic stress of 210 MPa at temperatures: 900, 1000, 1100, and 1200 ºC in an air environment. The results showed that the samples healed at temperatures of 900 ºC and 1000 ºC. Brochu et al. [70] made a review on the self-healing biomaterials in which they introduce new approaches to the self-healing in biomaterials.

Recently, ternary carbides and nitrides such as Ti_2Alc, Zr_2AlC_5, and Cr_2AlC, also called MAX phase, have received much attention due to their unique combination of properties including low density, high modulus and strength, high electrical conductivity, good thermal conductivity, low coefficient of friction, good thermal stability and oxidation resistance, and have shown efficient crack healing capability at 1100 ºC and 1200 ºC in air. [24, 71, & 72]. S. Li et al. [73], investigated the crack healing of Ti_2SnC ceramic in an air environment at low temperature and within a short period of time. At a temperature of 800 ºC, Ti_2SnC showed a capability of repairing the cracks induced by thermal shocks within just 1h. Their study showed a full recovery of the strength and conductivity; filling the cracks by the formation of the solid oxides, such as Al_2O_3, TiO_2 and Cr_2O_3 was identified as the main mechanism for healing surface cracks. K. Ando and W. Nakao applied the concept of self-healing ability to ensure the reliability of ceramic materials through the service life of a component [74]. W. Nakao et al. [75] studied the self-healing ability of mullite/SiC whisker/SiC particles multi composites. In their paper, they

reported the oxidation process of SiC admixture as a healing mechanism. They reported that the cracks healed by only the $SiC_{(W)}$ was weaker than the matrix (base), unlike the cracks healed by the oxidation of $SiC_{(W, P)}$, which yielded a part superior in mechanical properties to the matrix at every tested temperature. K. W. Nam studied self-healing behavior to heal the large cracks in SiC ceramics as a function of the heat treatment, coating method and coating times [76].

Cracks were healed [77] through the heat treatment at high temperatures of 1000 ºC or above which causes a chemical reaction that mends the induced flaws and cracks. Electrochemical anodization was used to heal the cracks induced in Al_2O_3/Ti composites, a full recovery of the strength to its original level was reported.

Self-crack healing of Al_2O_3/SiC nanoparticles was investigated by using a kinetic model. The crack healing was investigated under different conditions. A complete recovery of the strength was achieved at conditions of 1000 °C-1550°C in partial oxygen pressure above active to passive pressure transition $PO_2{}^{t}_{min}$; their results made a contribution to design materials with self-healing capabilities for gas turbine applications [78]. During the sintering process, the nanoparticles bond together to enhance the mechanical and physical properties of the final product. A percentage of shrinkage of about 10-20 % and deformation occur during the physical process [79]. L. Jun et al. [80] studied the crack healing behavior of Al_2O_3 matrix composites mainly TiC_p/Al_2O_3, SiC_w/Al_2O_3 and ZrO_2/Al_2O_3, which are used in many applications, such as heat engines, cutting tools, etc. The prepared specimens of these composites were indented at different loads of 49, 98, and 196 N and were annealed for 1h at different temperatures of 1000, 1200, and 1400 ºC

in an air environment and at 1200 ºC for 1h in vacuum. For this process, the main healing mechanism is a chemical reaction, and in the case of vacuum it is stress relaxation, which produces less strength recovery. However, the main mechanisms to heal the cracks in ZrO_2/Al_2O_3 composite were believed to be the existence of the eutectic phase and the rearrangement of the grains which is caused by the phase transformation of zirconia from monoclinic to triclinic, $ZrO_{2(m)} \rightarrow ZrO_{2(t)}$, when increasing the healing temperature.

L. Bontemaa et al. studied the autonomous healing of the cracks of Al_2O_3 at high temperature through the use of SiC as a healing agent which forms silica, which serves as a healing agent to heal the cracks at high temperatures. In their study they selected healing particles composed of transition metals and their carbides and nitrides to heal the damage and restore the strength. They reported oxidation as a healing mechanism through the filling of the cracks with the transition metal oxide. The oxidation process is accompanied with a volume expansion of 50% or higher. The selected oxides were TiO_2, ZrO_2, ZnO, HfO_2, N_2O_5 and Y_2O_3 [81].

Nakao et al. [82] studied the self-healing behavior of mullite/SiC whisker multi composites and mullite/SiC whisker composites. They reported that a mullite/15% SiC whisker 10 Vol% SiC particle multi composite (MS15W10P) to be used as a material for springs, could heal the cracks at a temperature of 10h at heat treatment temperatures ranging from (1273-1473) K. They reported a superior healing ability of MS15W10P to that of MS25W. The healing ability of silicon carbide particles and whiskers multi-composite compared with whiskers only was attributed to the difference in the distribution and geometry of SiC.

Kilicli et al. [83] studied the self-healing behavior in metallic materials and their composites. In their study they reviewed, summarized and evaluated the healing mechanisms involved in the healing process. They reported the lack of studies on the self-healing in metallic materials/MMCs. X.-P. Zhang et al. [84] studied the self-healing behavior of TZ3Y20A-SiC ceramics and $ZrO_2(Y_2O_3)$-Al_2O_3-SiC ceramics as a function of temperature, time, crack size and SiC content. They reported crack healing through the oxidation mechanism in which the SiC reacts with the oxygen in the atmosphere and forms SiO_2. They reported optimum healing conditions of 0.54 μm crack size, 10 h healing time, 10 Vol% SiC, and 1000 ºC healing temperature. They also reported a complete healing ability of the composite at conditions of 10 Vol% SiC at a heat treatment temperature of 1073 K for a holding time of 30 h, 1273 K for 10 h or 1373 K for 5 h for a crack width of 0.45 μm. Francois et al. [85] studied the self-healing of cracks in glass-boron composites. Their results showed that the healing occurs at 700 ºC by the oxidation process of boron in molten B_2O_3, which flows to fill the crack walls. They observed the healing behavior through using X-ray nanotomography. They reported that the healing process occurs through the chemical reaction between the boron oxide (B_2O_3) and the glass matrix as observed using coupled NMR, electron microscopy and nano-XRF analysis which leads to the diffusion of barium and calcium and the formation of borosilicate phases, which heal the cracks. This behavior was observed using 2D and 3D observations, x-ray nanotomography, nano-x-ray fluorescence imaging, electron microprobe and NMR. E. J. Barbero and K. J. Ford conducted research to characterize the self-healing of fibre-reinforced polymer matrix, laminated composites [86].

Z. Illhan et al. [87] studied the self-healing behavior of plasma sprayed spinel coatings through the incorporation of silicon carbide and yttria as healing agents. They reported that after 1h of the heat treatment, the silica reacted with Y_2O_3 to form a crystalline phase Y_2SiO_5 and vitreous phase $Y_2Si_2O_7$. They reported that the results obtained from the experiments are the same as the results obtained from the microstructural simulations. The oxidation process was reported as a healing mechanism to heal the cracks in $MgAl_2O_4$ coatings. N. Z. Muhammad et al. [88] performed an analysis and comparison of several methods and tests that were developed to evaluate the efficiency of healing in concrete. They reviewed, analyzed and compared the different methods tests that are available. W Nakao and S Abe studied the effect of the nanosizing of reinforced dispersed particles on the healing behavior. They found this was an effective mechanism for healing damage through the oxidation process. The range of temperature at which the strength could be completely recovered for nanosized particles was (950-1300) ºC [89].

K. W. Nam and J. S. Kim studied the self-healing behavior of SiC ceramics as a function of temperature and crack size. The cracks could be healed at optimum conditions of 1100 ºC for an hour in an air environment. The strength could be recovered after heat treatment of the specimens. They reported that a combination of SiC ceramics with SiO_2 as an additive had excellent healing ability [90]. E. Baranger et al. [91] proposed a model to predict the behavior and lifetime of crack-healing behavior of ceramic composites; this model can be used to compare experimental and numerical results. S. Ozaki et al. [92] developed a constitutive model to analyze the behavior of self-crack healing ceramics. L. Boatemma et al. [93] studied the healing behavior of embedded Ti particles to heal cracks

in alumina through the oxidation process at elevated temperatures. They reported that the optimum conditions for healing the cracks and recovery of the strength are 800ºC and 900ºC for 1h and 30 min respectively. Upon heat treatment at high temperatures, the cracks in Ti_2AlC ceramics could be healed through the oxidation process and the formation of the oxides/oxidation products, Al_2O_3 and TiO_2. They reported that the outward diffusion of the Al-atoms in the Ti_2AlC is much faster than the diffusion of Ti atoms due to the covalent bonding/covalent nature of the bonding between the atoms. W. Kunz and H. Klemm studied the crack healing behavior of Environmental Barrier Coating for non-oxide ceramic matrix composites and the healing mechanism. They reported an oxidation process as the healing mechanism, which was the transformation of the microstructure and the formation of SiO_2 and its reaction with ytterbium silicate [94]. S. Yoshioka and W. Nakao studied the crack healing behavior of Al_2O_3/TiC ceramic composite. The self-healing behavior was investigated as a function of the temperature and time. They reported strength recovery at a temperature of 800 ºC for a holding time of 1h. The cracks were filled with the formed TiO_2 [95]. M. Stumpf et al. [96] studied the crack healing behavior of ZrO_2 composites with the addition of MAX phase as a healing agent to the ZrO_2 matrix composites. They reported the oxidation process as the healing mechanism upon annealing at a temperature of 1200 ºC in an air environment with a healing time of (10-20) min. G. M. Sloof studied the crack healing behavior in advanced machinable Ti_3AlC_2 through oxidizing the cracked samples. The results of their study showed that the ceramic has an excellent ability to heal the cracks through the oxidation process at elevated temperatures, they reported a complete healing of the cracks time through the oxidation and the formation of the oxides after heat treatment at a

temperature of 1100 ºC in an air environment for 2 h [97]. D. S. Burton et al. [98] proposed a constitutive model to simulate the crack healing behavior of a shape memory alloy composite. F. Liu et al. [99] studied the self-crack healing behavior/ability of SiBCN ceramics and its composites as well as their application in aeronautics, aerospace and nuclear power industries. For ceramics derived from the hyperbranched polyborosilazaes in a high temperature and oxidation environment, they reported the effect of the healing temperature on the crack healing behavior. They found that the healing process occurs at a temperature of 1000 ºC in an air environment. Increasing the content of the boron in the ceramic increases the healing efficiency in the ceramic in the presence of O_2 at high temperatures. The main oxides formed which heal the cracks are SiO_2, B_2O_3 and $B_2O_3.SiO_2$. These oxides fill the cracks and prevent further damage of the substrate.

S. T. Nguyen et al. [100, 101] studied the self-healing behavior of ytterbium disilicide. In their study, they reported that the composite ($Yb_2Si_2O_7$- Yb_2SiO_5/SiC) has the ability to heal the cracks. The cracks could be healed owing to the reaction between the monosilicate and the silica which yields the formation of Si_2 (disilicide). Nakao et al. [102] studied the healing behavior of surface cracks, in ceramics as well as the mechanical behavior. They stated that inducing the healing ability to heal these cracks can ensure the integrity of the structural ceramics. M. W. Keller and M. D. Crall described the methods of self-healing in composite materials [103]. L. Boatemma et al. [104] studied the crack healing behavior of Al_2O_3/Ti_2AlC composite. They studied the addition of Ti_2AlC particles as a healing agent to the Al_2O_3 ceramics. They reported that the induced cracks could be healed through the oxidation process and formation of oxides. TiO_2 formed as a result of the decomposition of the matrix phase. Ti_2Al formed after the annealing at

temperatures ranging between (800-1000) ºC/at high temperatures in an air environment. The healing behavior was studied at temperatures ranging between (800-1000) ºC for a holding time of 0.25, 1, 4 and 16 h. The recovery of the strength was about 90% after annealing/heat treatment of 1000 ºC for a holding time of 15 min. A full recovery of the strength was attained after annealing at 1000 ºC for 1h. They reported the oxidation process as the healing mechanism. In their paper, S. V. Prabhu et al. [105], they made a comparative study and assessment on the crack-healing ability of conventional electrical sintered and microwave sintered Al_2O_3/SiC ceramic composites. The heat treatment was conducted at a temperature of 1200 ºC. for a 1h holding time in an air environment. The recovery of the strength after the microwave sintering process was reported to be better than that of the conventional electrical sintering. The phases that were detected through the XRD are: SiO_2, Al_2O_3 and SiC. B. Wang et al. [106] studied the self-healing behaviour of SiC-Al_2O_3-B_4C ceramic composites at low temperatures lower than 800 ºC. in an air environment; the best healing performance was recorded at a temperature of 700 ºC in an air environment for 30 min. They also reported the oxidation process of B_4C as the main healing mechanism. K. S. Lee et al. [107] studied the crack-healing SiC-SiC ceramic composites fabricated or prepared using different methods or processes in order to be used in or employed in application at extreme environments. In their study, T. Osada et al. [108] concluded that the previously proposed damage-healing constitutive model which was employed to the FEA of a series of damage and healing processes of Al_2O_3/SiC ceramic could be applied to study the self-healing behaviour linked with the simulation of stochastic fracture caused by the microstructure distribution. In their finite element model, they used a commercial software package LS-DYNA. C. S. Obayi and P. S.

Nnamchi [109] presented the challenges in the characterization of self-healing materials in their chapter entitled “Exploits, Advances and Challenges in Characterizing Self-Healing Materials”. They discussed the methods, challenges and prospects towards self-healing property at different length scales.

1.2.2 Self-healing in concrete and cementitious materials

The self-healing behavior of smart construction material was investigated by employing tailored additives. The so-called crystalline admixtures were used where active chemicals react with water and cement particles in concrete to form calcium silicate hydrates [110]. Self-healing of cementitious material has also been investigated using numerical models [111].

Y. Li performed a review on the concepts and approaches related to autonomous and autogenous self-healing in cementitious materials using different healing agents as well as analyzing the advantages and disadvantages of the diverse self-healing strategies [112]. G. Yildirim et al. [113] reviewed the ability of intrinsic healing in engineered cementitious composites. They reported the factors that affect/influence the healing efficiency and the effect of the healing behavior on the mechanical properties of cementitious composites.

K. Vijay et al. [114] reviewed the use of bacteria as a healing agent in concrete as well as the variation of the properties based on the addition of bacteria. In their study, they reported that using the bacteria as a healing agent increases the durability and strength of the concrete. They also mentioned that using encapsulation methods yield better results than the direct application method. The self-healing ability of hybrid

engineered cementitious composites was studied by Moncef AL. Nehdi [115]. The rapid ability to heal the multiple damage autonomously of the superamphiphobic surfaces based on a smart two layer self-healing network was investigated by Hao Zhang et al [116]. M. Roig-Flores et al. [110] studied self-healing behavior in concrete. They analyzed the effect of the crystalline admixtures in four different environments and compared the results with a reference concrete. They reported that the presence of water is required to heal the damage. R. Davies and A. Jefferson proposed in their work a numerical/ analytical model to simulate the self-healing behavior in cementitious materials [117]. L. Ferrara et al. [118] studied the self-healing ability of high performance fiber-reinforced cementitious composites upon exposure to different environmental conditions. They investigated the healing ability as a function of the composition, the maximum crack width and the environmental conditions. J. Qiu et al. [119] studied the effect of several factors (slag content, crack width, and environmental alkalinity) on the efficiency of the self-healing in engineered cementitious `composites, these fiber-reinforced strain hardening cementitious composites have the ability to heal the cracks. H. Huang et al. studied the self-healing mechanisms in cementitious composites and analyzed the required environmental conditions for each healing mechanism. They reviewed the healing mechanisms in cementitious materials and the conditions of the healing agents, aspects, applications and perspectives in engineering practice [120]. A. Beglarigale et al. [121] studied the self-healing behavior in cementitious materials through the micro-encapsulation of the healing agent. In their research, they used sodium silicate as a self-healing agent, which is encapsulated through the polymerization of the monomer on the

aqueous sodium silicate droplets/microencapsulation of the sodium silicate with polyurethane shell. The optimum ratio of the sodium silicate and water was 50%.

B. Hilloulin et al. [122] analyzed the healing ability and efficiency and the nature of healing products as well as the mechanical regains obtained as a consequence of the healing process in cementitious materials. They quantified the healing capability and kinetics of low water to cement ratio concrete. They found that concrete structures subjected to premature cracking can heal with mechanical regains while immersed into water.

N. Kringos et al. [123] studied the self-healing ability of bitumen. In their work, they proposed a finite element based model based on a thermodynamic approach to heal the bitumen. They proposed a finite element model to simulate the healing process in bitumen based on a thermodynamic approach. The model employed a 3D-finite element system CAPA-3D. B. Hilloulin et al. [124] investigated self-healing behavior in ultra-high performance concrete. In this study, they proposed a hydro-chemo-mechanical model implemented in finite element code Cast3M to calculate the self-healing potential of a damaged concrete beam after cracking. The model predicted lower strength of the self-healing concrete in the healed region than the strength of the original concrete. They compared the results obtained from the numerical model with that obtained from experiments. Hickman and Evans [125] studied the crack healing ability of $CaCO_3$. They showed that the complete healing of the cracks was found to be at 850 °C with a healing time of 25 h. M. R. Hoosain et al. [126] reviewed in their paper the self-healing

technologies in concrete for more sustainable buildings such as mineral mixtures, bacteria, and adhesive liquids.

1.2.3 Self-healing in polymers, coatings and its composites

In polymers, self-healing methods have been developed to include the techniques of microencapsulation and macroencapsulation whereby the polymeric healing agent is released into the cracks.

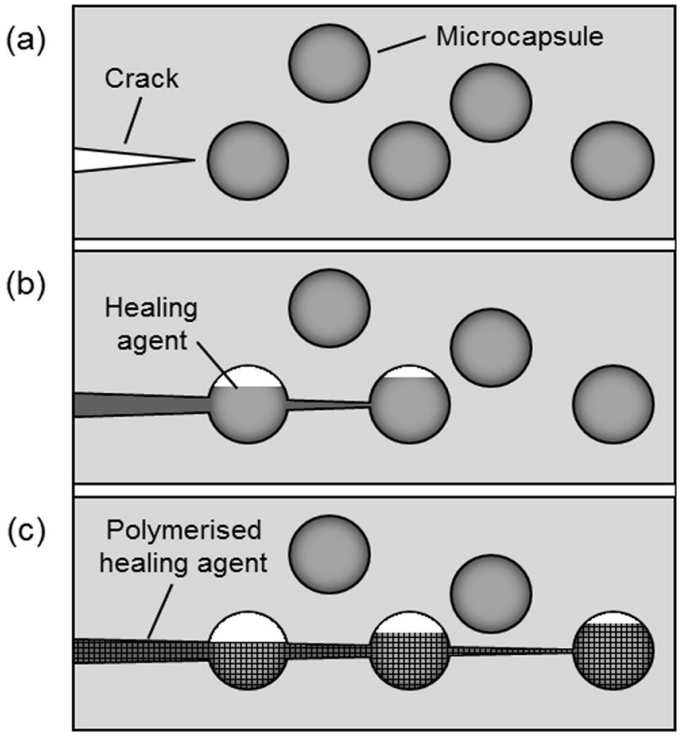

Fig 2. The self-healing process using embedded microcapsules. (a) the crack forms in the matrix due to the inflicted damage (b) the growing crack ruptures microcapsules in its path, hence releasing the healing agent into the crack plane (c) polymerization process occurs and the crack faces are sealed [127].

Polymer based macrovascular networks/macrovascular network self-healing polymers have shown ability to heal cracks autonomously [128, 129]. The crack healing mechanism of carbo-fibre-epoxy composites containing mendable polymer stitches was investigated by Pingkarawat et al [130]. S. van der Zwaag et al. demonstrated the self-healing behavior in man-made engineered materials inspired by the natural materials [131]. Jang S. et al have shown that cracks in polymers are mendable upon healing. These polymers or mendomers have the capability/ability to heal the cracks upon heating to temperatures close to the T_g thermally reversible Diel- Alder reaction. In their research, the focus was on using these mendomers as a matrix to remend graphite fiber reinforced composites [132]. These additives were added to the epoxy resin network and carbon epoxy composite to heal the cracks and delaminations [133]. The self-healing behavior of high performance structural fiber reinforced polymer composites was investigated by Amael C. et al [134]. H. Jin et al. investigated autonomic healing in epoxy by using a dual-microcapsule system which utilized epoxy-amine chemistry in a cured thermosetting epoxy polymer at high temperature [135]. Y. C. Zhang et al. studied the self-healing behavior in polymeric materials, they reported a self-healing polymeric system that is capable of healing/repairing itself to 100% multiple times. This system provides a new concept to the recycling process of the thermosetting polymers through a sequence of Diels-Alder and Retro-Diels-Alder [136]. S. R. White et al. [137] studied the crack healing ability of polymeric materials. They reported that the healing agent is encapsulated and upon the rupture of the microcapsules, the healing agent is released, then a polymerization reaction occurs with the catalyst, which bonds the crack faces and heals it. Upon the healing process, about 75% of the strength is recovered. A cohesive

constitutive model which was implemented in a finite element framework to capture multiple healing events was designed by S. A Ponnusami et al. [138] which was developed originally to model the fracture; this model is designed to model both the intrinsic and extrinsic healing materials. Chun H. Wang et al. [139] investigated the self-healing of carbon fiber epoxy composite combined with the toughening effect. The composite was toughened with two copolymers EMA (Polyethylene-co-methyl acrylate) and EMAA (Polyethylene-co-methacrylic acid) . EMAA thermoplastic was investigated as a healing agent to mend the damage in epoxy based composites [140].

The healing ability and mechanisms of anti-biofouling materials as well as their potential applications were investigated by Lia Shuo and Weiwei Guo [141]. The self-healing behavior of superhydrophobic films manufactured by the liquid repellent glue + particles was investigated by Hao Zhang et al. [142]. The rapid, multiple, and repeatable self-healing of the superoleophobic surfaces was achieved by the infiltration of a liquid fluoroalkylsilane coayin into the substrate. The self-healing effect of carbon-epoxy laminate and the toughened effect of the delamination was investigated by K. Pingkarawaat et al [143]. Bay B. Ladani et al. investigated the healing behavior of composites reinforced with hybrid Z-fibre [144]. The crack healing mechanism of carbon fibre epoxy composites containing mendable polymer stitches was investigated by Pingkarawat et al [145]. The self-healing of wetting surfaces has been investigated by Kunlin Chen et al. In their studies they introduced several wetting surfaces and their healing behavior, these wetting surfaces include superhydrophobic surfaces, superamphiphobic surfaces, underwater superoleophobic surfaces, and high hydrophilic antifouling surfaces [146].

Self-healing coatings are based on nanocontainers or fiberic systems that store the healing agents. Upon mechanical damage, the self-healing agent's release microvascular network/microchannels 3D system distributing the healing agent into the polymeric system. F. Micchiche et al. studied the self-healing of a multi-layer coatings (two layers) system made of montmorillonite clay. They reported a healing process of the damage at the surface through the volume expansion of montmorillonite upon a mild heat treatment under moist air conditions [147]. Lv Z et al. [148] studied the effect of capsule morphology on self-healing ability and its efficiency in capsule based self-healing materials. In their study, they developed an analytical model to characterize the amount of the released healing agent, then a comparison was made between the results obtained from the published numerical simulation study for verification. Steven D. Mookhoek et al. [149] investigated an encapsulated self-healing system with a high aspect ratio of the polymer to improve the healing efficiency. The healing of the cracks was achieved through dispersing of the capsules that contain the healing agent and the solid catalyst within the polymeric base material (matrix) microencapsulated healing agent which are incorporated into the polymeric material/polymers and composites to heal the cracks. The strong bonding to the matrix (host material) and long shelf-life are required when dealing with the microcapsules upon cracking, these embedded microcapsules rupture and hence cause the release of the healing agent, which flows to the crack plane to heal it. B. J. Blaiszik et al. [150] studied the healing behavior of UF (urea-formaldehyde) nanocapsules containing/ filled with a healing agent, DCPD, dicyclopentadiene. These capsules were fabricated using sonication techniques and an ultrahydrophobe to stabilize the healing agent droplets.

A numerical study on an elongated microcapsule self-healing polymeric system filled with a liquid healing agent was conducted by S. D. Mookhoek et al. [151] and compared with one based on spherical capsules. They reported that the release of the liquid healing agent is affected by the high aspect ratio and the proper spatial orientation of the elongated capsules. The degree of the healing as a function of capsule concentration and dimensions and the crack opening distance was predicted by the model. Many researchers have obtained good results so far for healing the damage in polymeric systems. C.I. Idumah studied the self-healing behavior of polymer nanocomposites and their applications [152]. F. Alizadegan et al. studied the healing behavior in polymeric systems, polyurethane coatings, which contained nano-clay and embedded microcapsules. The healing efficiency was increased by increasing the content of the microcapsules. Their results showed that the best healing was achieved for coatings with 1 wt% nano-clay and 5 wt% or 10 wt% microcapsules [153]. J. M. Lucci et al. conducted a study that combined both the theoretical and computational analysis on the healing process/behavior of a microencapsulated healing agent, DCPD, dicyclopentadiene, in a polymer matrix with a microvascular network. In their study, they simulated the healing process of polymeric systems [154]. I. L. Hia et al. studied the self-healing behavior of multicore microcapsules, which provides multiple healing cycles. They studied the self-healing of capsules based composites that are capable of providing multiple healing cycles. This system is based on epoxy and hardener encapsulated into an alginate biopolymer based on self-healing multicore microcapsules formed from epoxy and hardener [155]. H. Jin et al. [156] investigated autonomic healing in epoxy through using a dual-microcapsule system which utilized epoxy-amine chemistry in a cured

thermosetting epoxy polymer at high temperature. Ponnusami et al. [157] developed a numerical model of the crack propagation in encapsulated healing agents embedded into TBCs. M. A. Zadeh et al. [158] proposed in their work the 1st generation of the sol-gel based polymer coating, which was an intrinsically healable hybrid organic-inorganic crosslinked network coating containing non-reversible crosslinks and reversible tetra-sulphide groups. N. Zhong et al. [159] studied intrinsic healing in polymer matrices. They reported that the efficiency of the healing decreases with the particle content regardless of the high degree of the healing. In this paper, they summarized the work on the development of highly efficient and reliable thermal interface materials.

In their study, S. An et al. [160] discussed self-healing technologies and urged that more efforts be made on self-healing structural materials, their performance and their application and taken into consideration under different conditions, especially extreme conditions.

1.2.4 Self-healing in metallic materials and its composites

M. Nosonovsky and P. K. Rohatgi discussed in a book the thermodynamic principles of the healing behavior in metallic materials. In this book, case studies of the development of the metallic and metal matrix composites and self-healing process in metallic composites with embedded low melting temperature solders were discussed [161].

N. H. van Hijk and S. van der Zwaag studied self-healing behavior in metallic systems. They reported that the healing process in these systems is due to the fact that the solute atoms act as a healing agent. They reported various approaches to heal the cracks autonomously through intrinsic solid state diffusion [162].

M. V. Manuel and G. B. Olson studied the self-healing alloy biomimetic composites of Sn-based metal matrix composites (MMCs) reinforced with (SMA) wires. After the heat treatment, the SMA wires partially melt and weld the damage causing the welding of the cracks. After the healing process, 95% of the strength recovered [163]. A finite element model was used by D. S. Burton et al. to simulate the crack healing behavior of shape memory alloy composites. The SMA wires were modeled using a constitutive model that implemented a user-defined truss element in ABAQUS [164].

S. Danzi et al. [165] studied self-healing behavior/capability in metals. They reported that the healing process in metals requires thermal activation. They reported that thermal activation is required for the healing process in metals through heat treatment in furnaces. The cracks were welded in different metal films through the solid state reactions in a heat source. In their research, they designed Ni/Al multilayers as on- chip heat sources. The healing of these metal films were found to be based on an external annealing process. The healing behavior of Al_2O_3/Ti composites and their applications was studied using the electrochemical approach by Shi et al [166]. S. Thomas et al. [167] proposed a way to protect zinc coatings through using self-healing oxides, chromium based surface layers. These oxides have the ability to heal the damage owing to the aqueous nature/properties of the chromium ions. The chromium ions exist in dual oxidation states and these are Cr (III), which forms Cr_2O_3 which acts as a protective layer, and Cr (VI), which exists as a soluble CrO^{-2}_4. As a consequence it can self-heal the induced damage. They investigated the short term protection of zinc, then long term protection is affected by the corrosion products of the zinc.

The healing of the surface damage in metallic materials is difficult, and the main reason is that there is no means for the healing agent's delivery in metallic materials and alloys/delivery of the healing agent. The metallic atoms are strongly bonded and have low diffusion rates. The basic requirements for the healing agent in the case of the metallic materials are:

- High wettability in respect to the matrix (low content angle between the healing liquid agent and the solid matrix)
- The contact angle <80 º,
- The MP < 280 ºC.

The commonly used metals as a solder are Zn, Sn, Bi and In. One example of a solder composition is 42 Sn-58 Bi. In a healing situation, SMA wires transfer from martensite to austenite upon healing to achieve crack healing. Hollow spheres filled with low melting point metal are embedded in the matrix/Zn, Sn, or Sn-Bi-eutectic filled Al_2O_3 hollow spheres. In a Cu-matrix, upon heating, Bi-Sn eutectic melts and flows to mend flaws [168,169,170,171,172,173].

CHAPTER TWO

MECHANISMS AND REQUIREMENTS OF SELF-CRACK-HEALING IN CERAMICS

2.1 Self-healing Mechanism In Ceramics [174, 175, 176]

In ceramics, the self-healing of the damage is initiated through the thermal activation followed by the sintering process, rearrangement of the particles/atoms, viscous flow of the glassy phase(s) and hence sealing of the cracks and/or the solid-state oxidation reaction.

The healing temperatures for ceramics have generally been found to be in the range of the sintering temperatures (> 1400 ºC) although some studies reported lower temperatures of < 1000 ºC. The healing reaction of the induced cracks was reported to occur through the annealing process in an oxidation environment at temperatures in the range of 1000 ºC-1200 ºC for ceramics such as SiC, Al_2O_3, ZrO_2, Si_3N_4, ZrB_2, $3Al_2O_3.2SiO_2$ at low oxygen partial pressures and under constant or cyclic stresses. The oxidation process is accompanied by volume expansion of an estimated percentage of greater than 50% with the lowest possible values of the thermal stresses. TiO_2, ZrO_2, Al_2O_3, SiO_2, HfO_2, Nb_2O_5 and Y_2O_3 are amongst the most effective oxides to result in an effective healing process.

After the sintering process, residual stresses are formed due to the mismatch of the thermal expansion/coefficients of the constituents components, the matrix and the healing agent/particles. The volume expansion upon the oxidation process is a prerequisite for the healing process and filling of the crack gap.

The oxidation reaction can be expressed as:

$$MX_n + (a+b)\ O_2 \rightarrow MO_{a/2} + n\ XO_{b/2} \quad (1)$$

Where:

MX- Carbide or nitride

$MO_{a/2}$ & $XO_{b/2}$ - The oxidation reaction products

Examples of elements with high volume expansion of up to 100% are Nb, Ta, Cr, NbC, and SiC and those with volume expansion of less than 100% are Ti, Hf, Zr, TiC, TaC, Cr_3C_2, TiN, ZrN, TaN, Cr_2N, and Si_3N_4. These are considered elements with positive volume expansion; however, these may not be able to heal the cracks/damage completely. The size of the healing particles and the crack dimensions are among the factors that have an impact on the self-healing process.

The most important criteria to heal the damage is the strong bonding between the crack faces. Hence, the adhesion energy/bonding energy can be described using a macroscopic atomic model and can be defined as the work of adhesion/bonding/the work done to bond or adhere the surfaces

$$W_{Bonding} = -(\gamma^{surf}{}_{matrix\ (Al2O3)} + \gamma^{\ surf}{}_{oxide}) + \gamma^{\ interface}{}_{Al2O3} \quad (2)$$

Where:

$\gamma^{surf}{}_{matrix\ (Al2O3)}$: The surface energy of Al_2O_3

$\gamma^{\ surf}{}_{oxide}$: The surface energy of the oxide and can be determined from the enthalpy of the surface of each of the constituents/elements which composes the interface weighted by the molar density of the system.

$\gamma^{interface}_{Al2O3}$: The interface energy Al_2O_3 which can be determined or estimated from the energies of the interactions of the atoms on the sides of the interface, or from the enthalpy of the solutions.

All oxides have both high surface and bonding energies which enable them to bond well to the matrix. The residual stresses are generated due to the mismatch between the coefficients of thermal expansion of the constituent components or the matrix, the main substance and the healing agent.

For MAX phase materials, the main approach to heal the cracks is the intrinsic self-crack-healing, in which a decomposition reaction of the matrix occurs. In contrast to the approach used to heal the cracks/damage in alumina or other oxides, in which the material is at its lowest energetic state, wherein the most applicable approach to heal the cracks is the extrinsic self-crack-healing.

Most of the research on self-healing in ceramics focused on using SiC, TiC, Al_2O_3, and MAX phase ceramics as healing agents to heal the damage and surface cracks, which decompose upon the heat treatment to their main oxides. Other ceramics with too low of a melting point such as AlN/ceramics like AlN aren't considered as healing agents due to their too low volume expansion (<25%), which yields an insufficient healing process.

2.2 Requirement of Self-healing: [3, 174]

- The healing must be triggered by cracking.
- Healing occurs at high temperatures.
- The strength of the healed zone must be superior to the base material.

- In ceramics, the healing particles located at the crack walls react with the oxygen in an air environment to produce healing products/resulting in the healing action.
- The volume between the crack walls should be filled with the self-healing reaction products.

The healing methods that are applied to polymer and ceramics are difficult to be applied to metallic materials and its alloys. In metals the atomic mobility is limited and hence the healing process in metals is not easy to achieve.

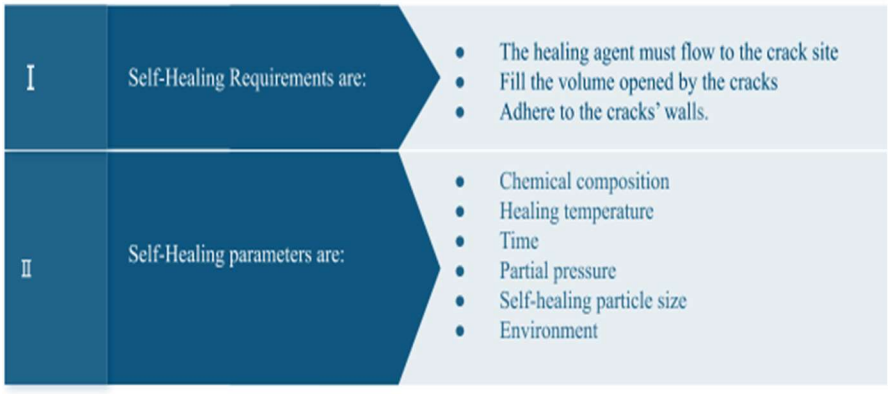

Fig. 3 Self-Healing Requirements and Parameters

2.3 Numerical Models On Self-healing Systems

The concept of damage management was used in most of the research on self-crack-healing rather than the concept of damage prevention. The self-crack healing

concept is based on the notion that an autonomous healing of the cracks once the damage inflicted on the material occurs.

The oxidation products fill the gap between the crack faces and adhere to the crack surfaces.

The gain in mass due to oxidation can be given by [175, 176, 177, 178]:

$$\Phi = V_o V_{P/} V_P \quad (3)$$

Where:

V_{o-} The healing oxide' molar volume.

V_{P-} The healing particle' molar volume.

$$P = d\, A_u / V_a \quad (4)$$

P-The probability that a crack crosses a healing particle.

d-The diameter of the healing particle.

V_a- the volume of the self-healing composite.

A_{u-} The area of the crack plane, which can be represented as:

$$A_u = V_a^{2/3} \rightarrow P = d/V_a^{1/3} \quad (5)$$

$$n_p = N_p\, P \quad (6)$$

Where n_p is the number of the healing particles.

$$N_p = \varphi\, V_a / V_p \quad (7)$$

$$V_p = \pi d^3 / 6 \quad (8)$$

N_p is the total number of the particles present inside the unit volume element and φ is the volume fraction of the healing particles added to the volume of the composite, V_a.

$$n_p = d/V_a^{1/3} \;\; 6\varphi V_a / \pi d^3 = 6\,\varphi\, V_a^{2/3} / \pi d^2 \quad (9)$$

The volume of the oxide filling the crack can be given by:

$$V_f = \psi_p \varphi n_{pVp} = \psi\varphi\Phi dv^{2/3} \quad (10)$$

Where:

ψ_p- the fraction of the particles converted into the oxide.

The volume of the gap with a width ω to be filled is defined as:

$$V_g = \omega\, A_a = \omega\, V_a^{2/3} \quad (11)$$

Ψ = the fraction of the crack gap filled.

$$\Psi = Vf / Vg \quad (12)$$

$$\Psi = \beta p\, \varphi\Phi d / \omega \quad (13)$$

βp = βp (T, t), which represents the oxidation of the healing particles. The concentration of the healing particles into the healing oxide can be represented as βp, which is dependent on the temperature and time.

The oxidation reaction can be represented as:

$$B = (Mt - M_o)/ (M_\infty - M_o) \quad (14)$$

Where:

Mt – The mass at time t.

M_o- The mass at time 0.

M_∞- The mass at an infinity time.

Engineers and researchers have employed some of the numerical models to simulate engineered self-healing abilities within the materials. One of the methods that is used to engineer self crack healing capability is to incorporate a second phase as a healing agent within the material. Only a limited number of studies have focused on simulating the phenomena in this proposed system of nanoparticles.

Tony Jefferson et al has presented a model on the self-healing behavior:

Assuming that the damage variable is a scalar variable (ω)

$$\alpha = (1- \omega)\, De : \varepsilon \tag{15}$$

Where

α -Stress tensor

ω –Damage tensor

ε –Strain tensor

De –Elasticity tensor

A broad form of the damage constitutive relationship

$$\alpha = (I4s- \omega).\, De : \varepsilon \tag{16}$$

Where

I4s -Identity tensor

It follows that

$$\bar{\alpha} = \alpha / (1- \omega) D_e : \varepsilon \quad (17)$$

Where

$\bar{\alpha}$ = the effective stress

Introducing the Helmholtz energy potential (ψ)

$$\Psi = \frac{1}{2} \alpha / (1- \omega): \varepsilon: D_e : \varepsilon \quad (18)$$

Differentiating with respect to the damage tensor

$$Y = - \partial\Psi/\partial\omega = \frac{1}{2} \varepsilon: D_e : \varepsilon \quad (19)$$

By adding the healing term, the stress, strain relationship is given as follows

$$\alpha = (I^{4s}- \omega). D_e : \varepsilon + h_\omega . \omega . D_e : \varepsilon (\varepsilon - \varepsilon_h) \quad (20)$$

Where

h_ω – the healed zone in the material

ε_h - the healing strain

Schimmd and Remmers introduced a 1D model to simulate the self-healing process whereby they introduced a time dependent healing function $h_\omega(t)$ which is ranging between 0 and 1

The model presented by them can be described as follows

$$\tau = (1- \omega)\, K_{u+} (1- \omega_h)\, rh_{\omega}(t)\, \omega_k(u-u_b) \quad (21)$$

Where

τ –the normal tractions

u –crack opening displacement

k- elastic stiffness

r-parameter gives the limit of healing

ω_h- redamages of the healed material

The effective stress concept was employed by the model that Barbero et al proposed on self-healing

An expression presented by Garner et al that gives the redamage of the healed material and relates the stress to the strain is given by:

$$\alpha = (1- \omega)\, E\, \varepsilon + (1- \omega_h)\, E_h\, (\Gamma_h)\, \varepsilon \quad (22)$$

Where

E – Young Modulus

E_h –the effective Young Modulus of the healed material

Γ_h – curing parameter

Voyiadjis et al proposed a thermodynamic framework that utilized damage, healing, and plasticity parameter, where he introduced two healing variables:

$$\bar{E}_{h\upsilon} = E\,[(1-\omega) + \omega\,(1-h_{\upsilon})]^2 = E\,[(1-\omega) + \omega\,h_{\omega})]^2 \quad (23)$$

Where

h_{υ} – the healing variable, which can be either 0 for complete healing or 1 for no healing,

$$h_{\upsilon} = 1 - h_{\omega} \quad (24)$$

$$h`_{\upsilon} = \bar{E}_{h\upsilon} - E_{\omega} / E_{\omega} \quad (25)$$

$$E_{\omega} = (1-\omega)\,E \quad (26)$$

2.4 Thermodynamics Of The Healing Reaction [174,175, 176, 177, 178]

In order to have a healing process of the induced cracks to initiate the healing process in ceramics, an oxidation process has to occur. Consider A as healing agent particles dispersed within the matrix, an oxide ceramic matrix, M; the stability criteria requires that A oxidizes to AO by reducing the matrix oxide.

The oxidation reaction of the healing agent can be summarized as follows:

$$A + M^{X+}O_{x/2} \leftrightarrow A^{y+}O_{y/2} + M \quad (27)$$

Provided that the following condition is achieved/the free energy of the reaction is:

$$\Delta_r G\,(T) = \Delta_f G^{o}_{(AOy/2)} - \Delta_f G^{o}_{(Mox/2)} \quad (28)$$

And

$$\Delta_r G\,(T) > 0$$

$$\Delta_f G^{o}_{(Aoy/2)} > \Delta_f G^{o}_{(Mox/2)}$$

The healing agent/particles react with the oxygen on the crack surface/surface of the crack.

$$2/y\ A + O_2 \rightarrow A_{2/y}O_2 \quad (29)$$

The exothermic reaction enthalpy, the enthalpy of the oxidation reaction is given by the free energy formation of the oxide and the formation entropy and can be expressed as follows:

$$\Delta_f H^o = \Delta_f G^o_{(Aoy/2)} - T\Delta_f S^o \quad (30)$$

$$\Delta_r G\ (T) > 0$$

Hence

$$\Delta_f G^o_{(Aoy/2)} > \Delta_f G^o_{(Mox/2)}$$

A strong bonding between the crack faces and the formed oxides is favored in this reaction.The kinetic Triplet [120], the activation energy E_A, the Arrehenius Constant, and the reaction model, were used by researchers working on self-healing to predict the healing parameters of the used healing agent.

The rate of transformation of any substance for non-isothermal experiments is represented by:

$$d\alpha/dt = d\alpha/dt.\ Dt/dT \quad (25)$$

Where α can be defined as the function converted at any time and is given by:

$$\alpha = m_t\text{-}m_0/m_\infty\text{-}m_0 \quad (26)$$

m_0, m_t, m_∞ are the masses at time 0, t and ∞ respectively.

$$\beta = dT/dt \text{ -the heating rate} \quad (27)$$

$d\alpha/dt$ represents the isothermal conversion rate and is given by:

$$d\alpha/dt = A\ e^{-EA/RT}\ f(\alpha) \quad (28)$$

From Eq 25 & 26 we have the non-isothermal conversion rate:

$$dT/dt = A/\beta\ e^{-EA/RT}\ f(\alpha) \tag{29}$$

Integrating Eq. 28 yields the non-isothermal transformation rate law:

$$g\ (\alpha) = A/\ \beta \int_0^T e^{-EA/RT}\ dT$$

Rewriting Eq. 27 and Eq. 29 yields:

$$d\alpha/d\boldsymbol{\xi} = A\ f(\alpha) \tag{30}$$

$$g(\alpha) = A\ \boldsymbol{\xi} \tag{31}$$

The experimentally determined conversion rate can be given by:

$$d\alpha/d\boldsymbol{\xi} = d\alpha/dt\ e^{EA/RT} \tag{32}$$

$$d\alpha/d\boldsymbol{\xi} = \beta\ d\alpha/dT\ e^{EA/RT} \tag{33}$$

The Arrhenius Constant can be determined from non-isothermal experimental data.

The reaction time required or generalized time can be determined from:

$$\boldsymbol{\xi} = E_A/\beta\ T\ .\ P_{(X)} \tag{34}$$

$$P_{(X)} = \int_x^\infty\ \ e^{-x}/x^2\ dx\ dT \tag{35}$$

Where

$$X = E_A/RT \tag{36}$$

From the non-isothermal transformation rate law, we have:

$$g(\alpha) = A/\beta \int_0^T \exp\ (E_A/RT) \tag{37}$$

Which yields

$$\int_0^T \exp\ (E_A/RT)\ dT = E_A/R \int_x^\infty\ \ e^{-x}/x^2\ dx \tag{38}$$

The equation that governs the activation energy is given by:

$$\ln(\beta/T^2_P) + (E_A/RT_P) = C \tag{39}$$

Where

T_P – The peak temperature, which represents the temperature at which the reaction rate is at its maximum

R – Gas constant

C – Constant

E_A -Activation energy and can be obtained by plotting

$$\mathrm{Ln}(\beta/T^2_P) \text{ vs. } 1/T_P \tag{40}$$

Upon the sintering process chemical and physical reactions occur, which result in conversion process of the substances; the solid-state reaction can be described using an analytical model, an example of such model is the master curve plot which uses the generalized time ($\boldsymbol{\xi}$),which is the time required to obtain a function converted at infinite temperature and describes the isothermal or non-isothermal reactions respectively:

$$\boldsymbol{\xi} = \int_0^T \exp(E_A/RT)\, dt \tag{41}$$

$$\boldsymbol{\xi} = 1/\beta \int_0^T \exp(E_A/RT)\, dT \tag{42}$$

2.5 Objective

Degradation, damage and failure can occur as a consequence of materials use, transport or processing, and hence designing a system with a self-crack healing ability to repair the damage and recover the structural integrity as well as prolonging the service life has been the goal for many researchers. The phenomena of self-healing behavior for structural materials as well as for coatings has an economic impact on society. Inspired by nature, inducing crack healing capability in ceramics can bring many benefits including less maintenance, enhancing the reliability, and the structural strength, and reducing the maintenance, or replacing the parts or the components in use [3]. Studies on

the oxidation behavior, mechanical properties, and the synthesis process of $MoSi_2$ composites were done, yet limited resources or research on the self-crack healing, and modeling of the healing process were found on $MoSi_2$ composites, and only limited research exists on the self-healing behavior of $MoSi_2$ composites. No studies were found on the self-healing behavior of Spinel/ $MoSi_2$ composites and no computational studies on this phenomena of these nanocomposites have been carried out.

Therefore, the objective of the conducted research focuses on investigating the self-crack healing ability of the Spinel/$MoSi_2$ tribosystem both analytically and experimentally. This research will be accomplished by:

- Investigating the optimum conditions for self-crack healing.
- Investigating the main method to be used in healing the cracks in ceramics and its composites
- The main mechanisms for healing the cracks.
- Characterization/morphology and structure tests (SEM).

CHAPTER THREE

MATERIALS AND METHODS/EXPERIMENTAL PROCEDURE

3.1 Raw Materials And Powder Processing

3.1.1 Molybdenum disilcide ($MoSi_2$)

Molybdenum disilicide powder is a gray powder with the chemical formula $MoSi_2$. Its molecular weight is 152.11, density 6.3 g/cm^3, coefficient of thermal expansion 5.1 * 10^{-6} K^{-1}, resistivity rate 21* 10^{-6} Ω.cm, and microhardness 1200 kg/mm^2. It has a high melting point (2030 °C), high corrosion resistance, high oxidation resistance, excellent thermal and electrical conductivity, high temperature ductility, excellent optical properties, high temperature creep resistance and high strength at high temperatures.

3.1.2 Spinel (MgAl2O4)

Spinel is a silver powder with the chemical formula $MgAl_2O_4$, it has a high melting point (2135 °C); it is chemically inert, and has excellent optical and electrical properties, good thermal shock resistance, and high strength.

3.1.3 Yttrium Oxide (Y2O3)

Yttrium Oxide nanopowder is a white powder with the chemical formula Y_2O_3, spherical morphology, unique physical and chemical properties, and excellent dielectric properties. Its density is 5.0 g/cm^3, and is chemically stable, it also has: a high melting point (2440 °C), low coefficient of thermal expansion 8.0 μm/m.K, good heat and corrosion resistance, high thermal conductivity and high strength at elevated temperatures.

3.1.4 Silicon Nitride (Si3N4)

Silicon Nitride is a white powder with the chemical formula Si_3N_4, spherical morphology, a narrow range particle size with large specific surface area; its melting point is 1900 **º**C, its bulk density is 0.15 g/cm^3, its thermal conductivity rate is 16.7 W/(m.k), its hardness is ≅ 9-9.5, its compressive strength is 490 MPA. It does not dissolve in water but it is soluble in hydrofluoric acid. At high temperatures, Si_3N_4 provides good lubrication, wear resistance, corrosion resistance and oxidation resistance. It withstands thermal shocks/hot and cold shocks. It has high mechanical strength and good dimensional stability.

3.1.5 Silicon Carbide (SiC)

Silicon Carbide is a grayish to black powder with the chemical formula SiC; its melting point is about 2830 **o**C, its density is around 3-3.2 g/cm3; it has an excellent thermal conductivity of around 300 K (W/m. K), excellent corrosion resistance, high temperature resistance and abrasion resistance, very low coefficient of thermal expansion of 4.0 $\times 10^{-6}$ /K; and is insoluble in water. It is mostly used as abrasives, in automotive industry as brakes, clutches and as bearings; one of its applications also is bullet proof vests; a semiconductor material; it is also used in electronic applications such as LEDs and detectors.

3.1.6 Kaolinite (Al2O3.2SiO2.2H2O)

Kaolinite is a clay mineral; its color is white to creamy. The chemical formula/stoichiometry of Kaolinite is $Al_2O_3.2SiO_2.2H_2O$/ $Al_2(OH)_4Si_2O_5$; Its melting

point is in the range of (740-1785) ºC; its density is 2.65 g/cm^3. It is insoluble in water. Its hardness on the Mohs Scale is in the range of 2-2.5.

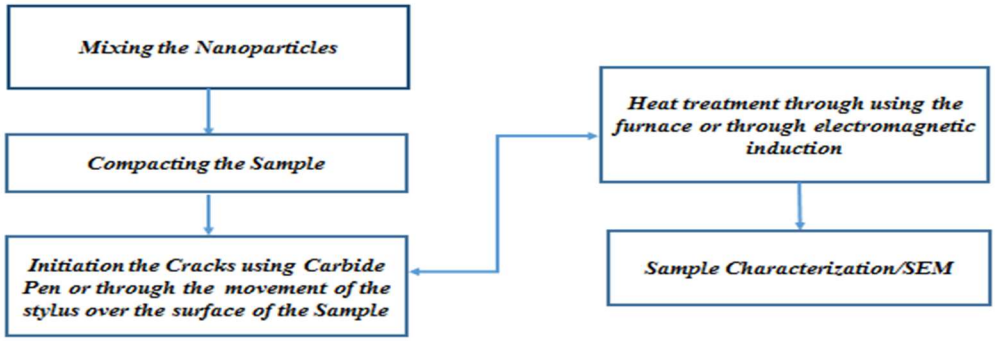

Fig. 4. Procedure of Sample Preparation

3.2 Experimental Procedure

3.2.1 Procedure for Sample Preparation

After the selection process of the particles/nanoparticles and designing the crack-healing ceramic composites/mixtures, the particles were mixed in specific percentages through using a Mortar and Pestle and compacted into small pellets in order to be investigated for their healability. The steps are shown in detail through the following bullet points:

- Mixing the nanoparticles
- Compacting the powders
- Initiation of the crack/scratch using carbide pen.
- Heat treatment through a box furnace, the heat generated through friction using a tribotester or a tig welding process.
- Characterization of the samples using SEM.

Fig. 4 shows the procedure of sample preparation starting from mixing the particles through the compaction process of the mixed particles and forming the pellets/compacts/green bodies and ending with the heat treatment through the traditional/conventional methods and other methods.

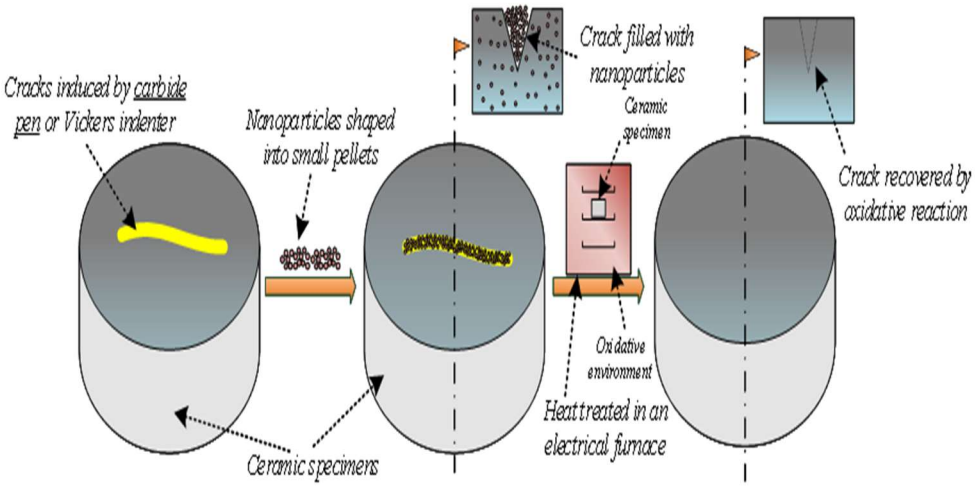

Fig. 5. The Steps for the Preparation of Self-Crack-Healing Ceramics

Many researchers studied the self-healing behavior in ceramics. For this class of materials, self-healing occurs at a specific temperature. The healing process in ceramics occurs at temperatures greater than 800 ºC. Fig. 5 shows the process of inducing/initiating the crack on the surface of the sample using a carbide pen and the healing process of the crack through the heat treatment.

3.2.2 The chemical composition in wt. % of the nanoparticles

The following combinations/mixtures were prepared to investigate the crack-healing ability of these mixtures:

$MoSi_2$ (25 %) + $MgAl_2O_4$ (70%) + Y_2O_3 (5%)

$MoSi_2$ (30 %) + $MgAl_2O_4$ (70%)

$MoSi_2$ (70%) + $MgAl_2O_4$ (30%)

$MgAl_2O_4$ (25 %) + $MoSi_2$ (70%) + Y_2O_3 (5%)

Si_3N_4 (70%)+ $MgAl_2O_4$ (25%) + Y_2O_3 (5%)

$MgAl_2O_4$ (50 %) + $MoSi_2$ (50%).

SiC (90%) + Kaolinite (10%).

The produced compacted samples (green body) were then sintered at various temperatures for different holding times in an argon and air environment for the sake of investigating self-crack healing ability in the furnace at heating/cooling rate of 10 °C/min. In order to investigate the self-crack healing ability of the proposed mixtures of nanoparticles, the specimens were subjected to different healing conditions to determine the optimum conditions for the healing process.

Twelve combinations of the nanoparticles were prepared. The samples prepared at OU Labs, their chemical compositions as well as the different healing conditions are summarized in Table 1.

Table 1 The Chemical Compositions and the Healing Conditions of the Prepared Nanoparticles

Sample Code	Chemical combination (% of mixture)	Compact press (klbf)	Sintering condition 1st step process			Sintering condition 2nd step process / healing conditions		
			Temp (°C)	Time (min)	Environment	Temp (°C)	Time (min)	Environment
S_1	Si_3N_4(70%)+ Spinel+Y_2O_3	17.50	1000	120	A_r	1000	120	O_2
S_2	Si_3N_4(70%)+ Spinel+Y_2O_3	18.50	1000	120	A_r	1000	120	O_2
S_3	Si_3N_4(70%)+ Spinel+Y_2O_3	19.50	1000	120	A_r	1000	120	O_2
S_4	$MoSi_2$ (80%) + Spinel	20.00	1000	120	A_r	750/850	60/180	O_2
S_5	$MoSi_2$ (80%) + Spinel + Y_2O_3	22.00	1000	120	A_r	700	120	O_2
S_6	Al_2O_3 (70%) +$MoSi_2$ + Spinel	19.00	1000	120	O_2	1000	60	O_2
S_7	Al_2O_3 (70%) +$MoSi_2$	16.75	1000	120	O_2	_	_	_
S_8	Al_2O_3 (80%) +MoSi2	17.00	1000	120	O_2	_	_	_
S_9	Al_2O_3 (50%) +$MoSi_2$	16.00	1000	120	O_2	_	_	_
S_{10}	Spinel (70%) + $MoSi_2$ + Y_2O_3	17.50	1000	120	O_2	1000	120	O_2
S_{11}	$MoSi_2$ (70%) + Spinel	17.00	1000	120	O_2	850	120	O_2
S_{12}	Spinel (80%) + $MoSi_2$	20.00	1000	60	A_r	850	120	O_2

During the sintering process, the formed transition compounds (glassy phases) should fill the cracks and heal the specimens. Cracks were induced on the surface of the specimens using a carbide pen. In ceramics, it's difficult to heal the cracks at temperatures less than 1000 °C, and for this reason the sintering additives are added to the mixture of the nanoparticles [100]. The formed compounds and phase transformations were investigated using the SEM.

3.3 A Methodology of Designing Self-Crack-Healing Ceramics

This section summarizes the design, manufacturing and characterization of self-crack-healing ceramics as follows:

- Selection of particles/nanoparticles
- Preparation method of the samples/compaction and shaping process
- Setting the conditions/healing parameters
- Specific analysis to predict the healing/initiation of the healing reaction, thermogravimetric analysis etc.
- Healing method/approach; oxidation and diffusion upon heat treatment at moderate or high temperature, activator or healing particles at moderate to low temperatures, electromagnetic induction at room temperature etc.
- Assessing the healing process through characterization.

Figure 6- Mortar and Pestle

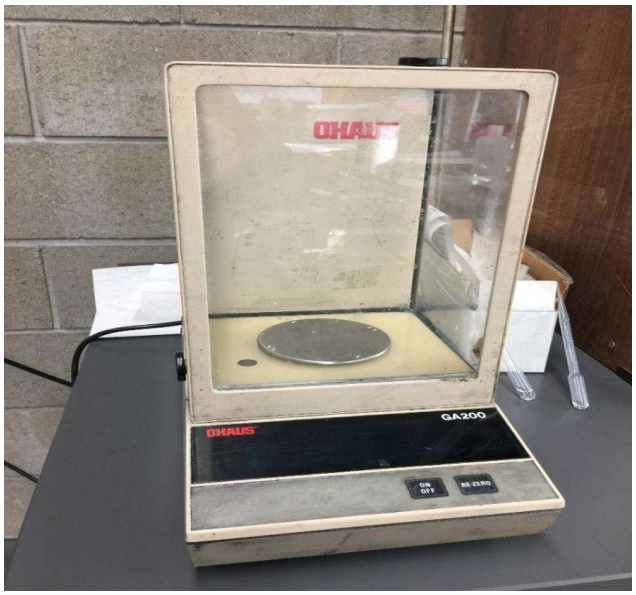

Figure 7- Electronic Balance

Fig. 8- Dry Pressing Die Set

3.4 Equipment

3.4.1 Mortar and Pestle

A traditional mortar and pestle was used to mix the powders together to have a homogenous and a well distributed mixture of particles as shown in Fig. 6.

3.4.2 Electronic Balance

An OHAUS GA 200 Electronic Balance, Fig. 7, with dimensions (20.6 cm *30.7 cm *44.5 cm), weighing range 40 g/200 g was used to weigh the nanoparticles; the calibration was checked before using the balance.

3.4.3 Dry Pressing Die Set

As shown in Fig. 8, a set of 13 mm diameter (ID) hardened steel dry pressing die set was used to make cylinder-shape pellets. The pressing die had a maximum load of 15 metric tons, Rockwell Hardness: Rc 62, Diameter: 13 mm, Height: 75 mm, Sleeve

Height: 40 mm, Material: W18Cr4V hardened carbon tool steel. The die set includes: two 13 mm ID cylinder-shape core dies made of highly polished hardened steel, one steel support sleeve, one steel support plate, one push rod, one pellet ejector.

3.4.4 Lindberg/Blue Laboratory Box Furnace

As seen in Fig. 9 Trade name: Moldatherm//®Insulation, The Lindberg/Blue Box Furnace M BF51732 with a maximum operating temperature of 1200 °C and with the dimensions of the chamber: 33 cm* 27.9* 12.7 cm was used for the sintering process. Different temperatures were used to heal the samples. No treatment or polishing was carried out on the samples' surfaces before the sintering process.

3.4.5 CARVER® Laboratory Equipment

A hydraulic Press was used to compact the samples into round small pellets, the maximum applied load that was used to compact the samples is about 10.9 ton. Fig. 10 shows the CARVER Hydraulic Press.

After the compaction, the green products/bodies are sintered through two steps. The preliminary stage of sintering causes the burn out of the binder, decomposition and oxidation, and elimination of the gaseous products. During the sintering process, the particles are joined together and adhere into an aggregate. Shrinkage and densification occur during this process; however, densification may not always occur. During the sintering, the compact is heated to ½ or ⅔ of its melting point through which atomic diffusion occurs*. Diffusion, chemical reaction, decomposition of the binder and viscous flow of the liquid phase occur during the solid state sintering*. The stress and

the differential thermal expansion of the phases should not lead to the failure of the product. An increase in the volume expansion occurs during the burn out process.

A binder or plasticizer is added to the matrix of the nanoparticles to prevent the friction and wear of the die and prevent the air from escaping, a lubricant is added between the punch and die wall; the deformation during the dry pressing decreases the porosity and enhances the adhesion.

The intragranular and intergranular pores are reduced through the dry pressing; these granules are plastically deformed through this process. Sometimes defects such as lamination or end capping result from the poor lubrication of the die walls or

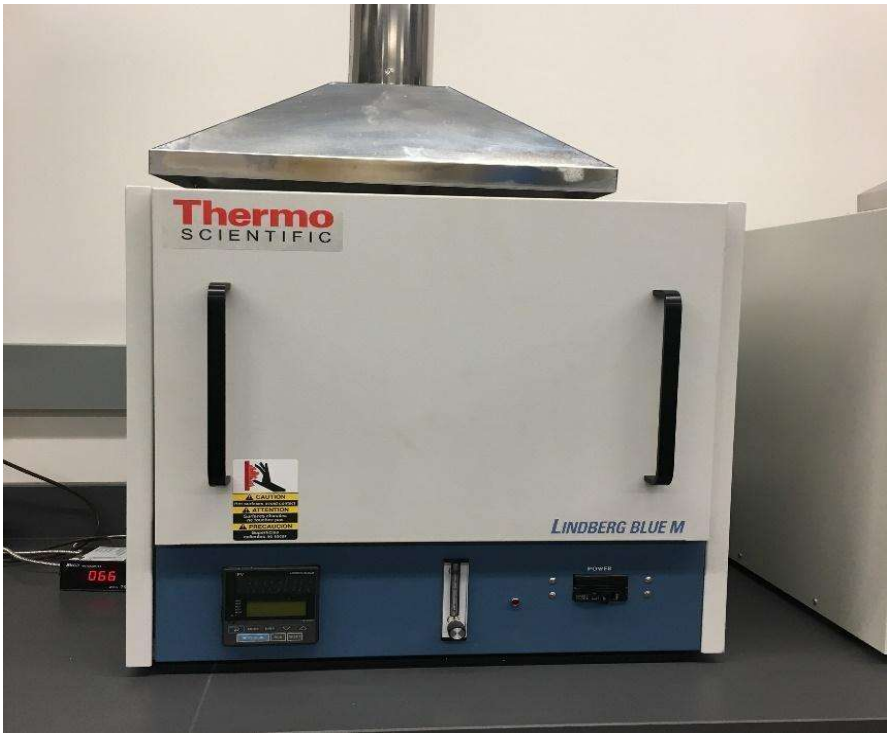

Fig. 9- Lindberg/Blue Laboratory Box Furnace

Fig. 10- CARVER Hydraulic Press

gradient in the pressure transmitted within the compact as a result of friction; lubrication reduces the gradient pressure*.

3.4.6 Bruker Tribotester

The tribo-sintering test was performed on a pin on disc UMT Bruker Multi Specimen System. The tribological test was conducted in a reciprocating sliding regime. Fig. 11 shows UMT Bruker. The Parameters that were used to conduct the test:

Reciprocating rate: 1 HZ

Normal Load: 70 N

Stroke: 10 mm

Duration of Test: 30 min.

3.4.7 Power Tig, LTR160 ESAB Welding Equipment[192]:

In the process of Tungsten Inert Gas Welding, the electrode is placed on the workpiece or the specimen composed of ceramic particles in order to heal the crack/damage which originated on the surface of the sample due to the high strains after applying the pressure or stress. The heat is generated between the sample and the electrode from the arc. The arc forms between the tungsten electrode and the workpiece/specimen in an inert environment. After pressing the trigger, the arc is produced; the torch is tilted a bit and lifted in order to produce the electrical arc, then the trigger is released in order to stop the arc. In this mode, the torch electrode is positioned where the crack is located in order to initiate the welding; pressing the trigger and releasing the torch causes the arc to strike. To stop the welding, the switch is released and hence the current is decreased. Four modes are available using this technique, the most common are the lift arc which utilizes a current at low levels and HF, high frequency, which consists of a high voltage spark that lasts for a few microseconds. When the current flows, an ionization or an ion cloud forms. Fig.12 shows the welding device, Power Tig 160.

3.4.8 Scanning Electron Microscopy, SEM:

The characterization process of the samples was conducted through using the SEM at Oakland University Labs and at Alkhora Company SEM Lab located in Baghdad, Iraq. Fig. 13 shows the Scanning Electron Microscope.

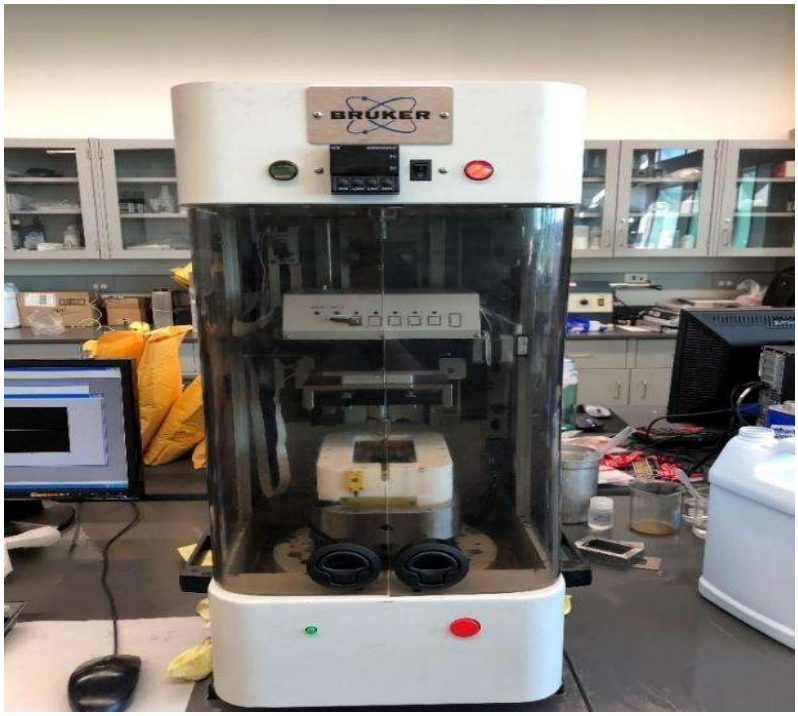

Figure 11- Bruker Tribotester

Fig. 12- Power Tig 160

ALKHORA COMPANY SEM LAB - BAGHDAD -IRAQ

INSPECT F 50 FE-SEM

Fig. 13- Scanning Electron Microscope

CHAPTER FOUR

PEST OXIDATION OF $MoSi_2$ NANOCOMPOSITES

At elevated temperatures, $MoSi_2$ possesses excellent mechanical, optical and thermal properties, such as excellent oxidation resistance, excellent corrosion resistance, and high electrical and thermal conductivity. At high temperatures, $MoSi_2$ undergoes a brittle to ductile transition reaction. It has a high melting point of about 2030 ºC and density of 6.3 g/cm^3. Pest oxidation can be defined as unwanted phenomena that occurs during the heat treatment of $MoSi_2$ and its composites, which can be described as the decaying or fragmentation of the sample into powdery product and/or flakes or clusters of SiO_2 and Whiskers of MoO_3/decomposes of $MoSi_2$ into MoO_3 and SiO_2. Pest oxidation or accelerated oxidation can also be defined as the process that occurs in $MoSi_2$ and its composites/nanocomposites. In this process, $MoSi_2$ decomposes into clusters of MoO_3 and whiskers or flakes of SiO_2. The diagram in Figure 14 below shows the decomposition of $MoSi_2$ upon the heat treatment due to pest oxidation.

Studies on the pest oxidation are insufficient; however, the researchers that have been working on this phenomena reported that the pest oxidation occurs at temperatures below 700ºC, specifically in the temperature range between (400-600) ºC owing to the cracks and porosity in the material, unlike what have been proven in the present study since the pest oxidation occurred at temperature above the range of temperatures that have been observed by other researchers; in the current research the conditions at which

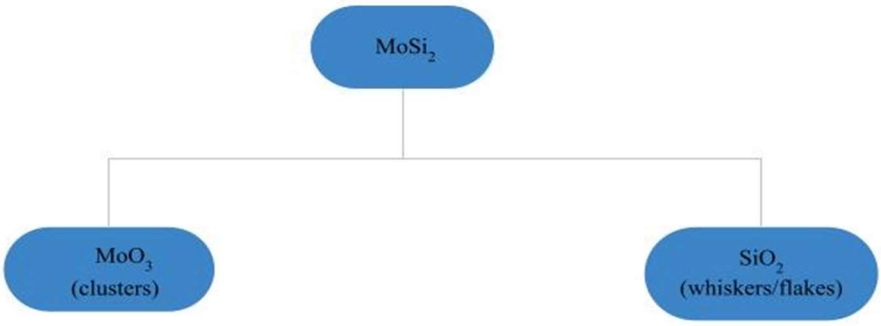

Fig.14 Diagram shows the decomposition of $MoSi_2$

the pest oxidation occurred were at 1000 ºC for a holding time of 1h and 2hrs in an O_2 environment. The pest oxide, MoO_3, formed in the $MoSi_2$ composites regardless of the Si- content in the composite. The phenomena of pest oxidation was known and described in 1955 by Fitzer [179].

The current chapter sheds light on the main conditions and mechanisms responsible for the pest oxidation. The pest oxidation was observed by other researchers in the range of the temperature between (400-600) ºC, which was described as the disintegration of a sample due to fracture and oxidation. Through this process, the oxygen reacts with $MoSi_2$ to form MoO_3 and SiO_2 ($MoSi_2$ decomposes into MoO_3 and SiO_2), and owing to the formation of MoO_3 and as a result of the volume expansion internal stresses are initiated, which causes the disintegration to powder. The reaction can be described as follows [179]:

$$2\ MoSi_2 + 7\ O_2 \rightarrow 2\ MoO_3 + 4\ SiO_2 \qquad (43)$$

Some of the researchers described the pest oxidation as a yellowish-green oxide (MoO_3) formed at the surface; the current research showed that the sample disintegrated to a grayish powdery and flakey structure. The pest oxidation can be described as an ashy product, flakey structure, or islands of the pest oxides as a result of the pest oxidation as shown in Figure 15 below.

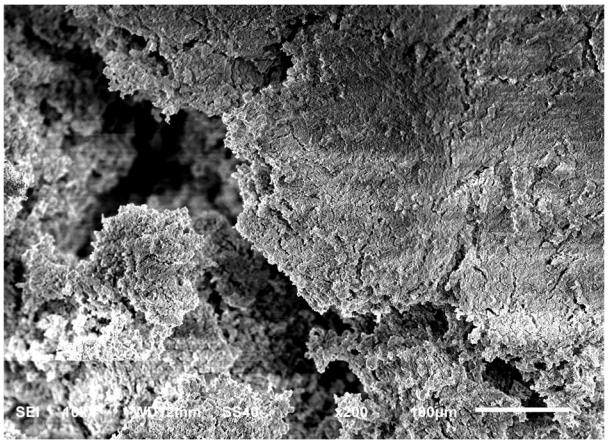

Fig. 15 The pest oxidation

C. G. McKamy et al.[169] studied the pest oxidation of polycrystalline $MoSi_2$; the results of their study showed that the pest oxidation occurs at the temperature range between (400-600) ºC, in their research they studied the conditions and mechanisms involved in the formation of the pest oxidation. C. G. McKamy et al. showed that the rich

Si-content composites don't disintegrate, yet form a protective gray silica layer on the surface of the samples.

The main reason that led to the pest oxidation is the presence of cracks and pores. The presence of cracks and pores are the main factors that determine the pest oxidation. In an air environment, the $MoSi_2$ reacts with the O_2 to form the pest oxide MoO_3 with the formation of a porous silica layer. Lee et al. reported the mechanisms behind the pest oxidation, they described it as the disintegration to fine powder within 24 h; the two main mechanisms reported by Lee et al. are:

- The adsorbed O_2 on the crack walls decreases the surface energy of the crack leading to faster crack growth.
- In the crack area, oxidation occurs leading to the accumulation of the oxide products along the cracks, and hence internal stresses initiate which causes accelerated crack opening.

Previous studies postulated the main mechanisms of the final stage of the pest oxidation:

- Diffusion of the O_2 into the grain boundaries to form MoO_3 leading to pushing of the grains apart and
- The formation of microcracks along the grain boundaries through the internal high stresses induced by the oxidation process.

Chou and Nieh described the pest oxidation as blisters formed as a result of the formation of MoO_3 owing to combined internal stresses and large volume expansion upon the formation of MoO_3 and SiO_2. T. S. R. Ch. Murthy et al. [180] described the pest

oxidation as the disintegration of the structure; they mentioned that $MoSi_2$ undergoes pest oxidation at a temperature range of (400-600) ºC. At a temperature range of (400-600) ºC, $MoSi_2$ decomposed into MoO_3 and SiO_2 in a phenomenon known as the pest oxidation wherein whiskers of MoO_3 and clusters of SiO_2 formed. The sample was oxidized for 24h. The vapor pressure at 500 ºC is high and the formed volatile MoO_3 enhanced the disintegration. T. S. R. Ch. Murthy et al.[180] reported that the formation of MoO_3 whiskers and SiO_2 clusters occurs through the nucleation and growth mechanisms. P Srikari Tantri et al.[181] described pest oxidation as an undesirable phenomenon that occurs at low temperatures. They mentioned that the main reasons behind the pest oxidation are the presence of defects, such as microcracks, pores and intergranular boundaries. T. C. Chou and T. G. Neih reported that the pest oxidation occurs at low temperatures in their observations of the pest oxidation in $MoSi_2$ specifically in the temperature range of (400-600) ºC; they describe it as the disintegration of the sample, which results in a powdery product [182]. K. Yanagihara et al.[183] reported that the inward diffusion of the O_2 affects the oxidation process of $MoSi_2$. They reported the similarity of the oxidation behavior of (Mo, Ta)Si_2 and $MoSi_2$.

S. Knittel et al.[184] studied the oxidation behavior of hot pressed $MoSi_2$ in the temperature range of (400-1400) ºC; they categorized it in five different regimes. A. Stergiou et al. reported that the addition of aluminum to $MoSi_2$ suppresses the pest oxidation of $MoSi_2$ at a temperature around 773 K (the suppression of the pest phenomena at a temperature of 773 K through the addition of aluminum to $MoSi_2$). They reported that at this temperature, a mixed oxide of Al/Si formed/the formation of a mixed oxide at this temperature with the formation of traces of Al/Mo oxide. An enrichment in

the Al for the scale was reported at higher temperatures. On the surface of $Mo(Si_{1-X}\ Al_X)_2$ and at a temperature of 1623 K, a layer of α-Al_2O_3 formed. Two-oxide layers of the mullite and silica with dissociated alumina as the outer layer and alumina as the inner layer were formed at a temperature of 1873 K. They suggested that the main mechanisms that contribute to the pest oxidation weren't only the oxidation of the cracks, but also the diffusion of O_2 to the grain boundaries [185].

K. Yanagihara et al. [186] studied the pest oxidation/pest mechanism and Al effect on the pest phenomena of $MoSi_2$ and $Mo(Si, Al)_2$ at 773K in an air environment. On the external surface of $MoSi_2$, platelet-like oxide formed along the initial cracks, pores and scratches. A. Stergiou et al. reported that the pest oxidation can be suppressed through the addition of aluminum/alloying. Al. K. Yanagihara et al. [186] studied the pest oxidation of Mo-Si-X, where X= Al, Ta, Ti, Zr and Y at a temperature range of (673-973) K in an air environment. They evaluated the effect of the 3rd element on the pest oxidation. They reported the disintegration of $MoSi_2$ at a temperature of 773K. The formation of SiO_2 is accompanied by the volume expansion of up to 85%, which results in internal stresses at the grain boundaries of $MoSi_2$. They reported the pesting of $MoSi_2$ through the addition of Al. They reported the selective oxidation of the third element at the grain boundaries. They reported the suppression of the pest oxidation when the volume expansion is small. Both $MoSi_2$ and $(Mo, Ta)Si_2$ disintegrate into powder unlike $(Mo, Ta)Si_2$, $(Mo, Zr)Si_2$, and $(Mo, Y)Si_2$ wherein kept their initial shape. They reported that the main mechanism responsible for the pest oxidation is the volume expansion as a result of the selective oxidation of the silicon at the grain boundaries.

In a patent related to the pest oxidation of $MoSi_2$ and its composites, the pest oxidation was observed at an intermediate range of temperatures, and was described as accelerated oxidation leading to the disintegration of the sample or the product into powdery product, which has been observed at a temperature of 500 ºC; the powdery product consists of whiskers of MoO_3 and clusters of SiO_2 and the residual is $MoSi_2$. In the same patent, it was reported that the pest oxidation could be suppressed by the addition of (30-50) Vol.% of the Si_3N_4 to the $MoSi_2$ [187].

T. C. Chou and T. G. Nieh studied the pest phenomena of $MoSi_2$ and its composites at the temperature range of (350-700) ºC in an air environment; they described the phenomena as the disintegration of the bulk into powder; the phenomena were observed for the samples oxidized at a range of temperatures between (375-500) ºC. The pest product, or the powdery product consisted of whiskers or platelets of MoO_3 and clusters of the silica, and the residual or the remnant is $MoSi_2$. The main mechanisms for the pest oxidation were found to be the volume expansion, nucleation and grain growth [188]. A complete disintegration to powder was observed for the samples composed $MoSi_2/Al_2O_3$ and oxidized at a temperature of 500 ºC for holding time of 142h, whereas the pest oxidation for the samples composed of $MoSi_2$/AlN was observed after oxidation/heat treatment at the same temperature for holding time of 22h revealing the fact that the time required for the pest oxidation of $MoSi_2/Al_2O_3$ is longer than that of $MoSi_2$/AlN. For polycrystalline $MoSi_2$, the pest oxidation was observed after oxidation/heat treatment at a temperature of 375, 400, 425, 450, and 500 ºC. The pest products were found to be whiskers of MoO_3, clusters of SiO_2, and crystals or particulates of $MoSi_2$. For the single crystalline $MoSi_2$, the pest oxidation was observed for the

samples oxidized at a temperature of 500 ºC; the main pest products were found to be whiskers of MoO_3, clusters of SiO_2 and crystals of $MoSi_2$. For the composite $MoSi_2$/AlN, the pest oxidation was observed after heat treatment at a temperature of 500 ºC, and the main reaction products were found to be whiskers of MoO_3, clusters of (SiO_2+ AlN) and particulates of $MoSi_2$. For the composite $MoSi_2/Al_2O_3$ oxidized at a temperature of 500 ºC, and the main pest reaction products were found to be whiskers of MoO_3, clusters of (Al_2O_3+ SiO_2), and particulates of $MoSi_2$ [189]. K. Natesan and S. C. Deevi addressed in their paper the oxidation behavior at a wide range of temperatures covering the range from (500-1400) ºC of $MoSi_2$ and its composites, specifically Mo_5Si_3 based composites and $MoSi_2$-Si_3N_4 composites. At low temperatures around 500 ºC, the molybdenum silicides' composites exhibit a non-protective scale of the oxide or pesting [190]. H. Zhang et al. [191] in their paper on the oxidation behavior of CNTs/$MoSi_2$ Composites at low temperature, reported that the pest oxidation could occur at a temperature of 400 ºC in an air environment, yet not at temperature of 500 ºC. In their study, they used the SEM and XRD to analyze the microstructure and to identify the formed phases; they reported that the main characteristics of the pest phenomena is the formation of whiskers of MoO_3 and microcracks on the surface of the composite, which caused the disintegration of the sample.

During the pest oxidation, the disintegration of the mixture into powder and the formation of the pest oxide (MoO_3), a chemical reaction occurs between the oxygen and molybdenum, which yield the formation of MoO_3 and SiO_2 in the range of temperatures (400-800) ºC. At higher temperatures, the formed MoO_3 vaporizes with the formation of

a protective layer of the silica, which seals the cracks. Si-rich composition (80%) doesn't disintegrate. During this process, the oxygen moves to the crack walls. The volume expansion results in the formation of stresses and causes the separation of the sample as a consequence a fine disintegrated powder forms, yellow green pest oxide grows as a result of the pest oxidation [179-190].

CHAPTER FIVE

RESULTS AND DISCUSSION

The objective of the research in its simplicity is to fill out the induced cracks with the reaction products, in other words to heal the damage or the crack induced on the surface of the specimens and investigate the healability of the prepared mixtures of ceramic particles. Different conditions were used to investigate the healing ability and the mechanism responsible for self-healing as well. The prepared crack-healing tribosystem showed partial to complete healing of the intentionally induced cracks on the surface of the prepared specimens. Twelve combinations of the nanoparticles were prepared at OU's Labs and one combination was prepared at the UOT/University of Technology Labs.

In the case of the combination Si_3N_4 (70%) +Spinel+ Y_2O_3, two different combinations of the same mixture were prepared, one was based on processing particles in two sintering steps, the oleic acid was used as a binder in this mixture of particles; for this combination, the particles were dissolved in the metal die during the compaction process. For the same combination yet without using the processed or the sintered particles, the process of preparing, compacting, and sintering the mixture of the particles was successful; the compaction pressures for this combination of particles was between (9.5-10.90) Ton. The sintering conditions were fixed at a temperature of 1000 ºC and a holding time of 120 minutes in an oxygen environment for most prepared samples except those that have been prepared at the UOT Labs. For some samples, the excessive pressure

during the compaction process leads to some noticeable cracks as a strain due to the stress applied on the surface which are definitely considered as manufacturing defects. For this combination of particles, the Si_3N_4 particles, not the samples used in this research, the sintering process of ceramics are in a range of temperatures greater than 1200 **º**C, and hence the samples were sintered in two steps before the mixing process; the first step of the sintering process was conducted at conditions of 350 ºC and 30 min holding time, and the second step of the sintering process was conducted at conditions of 400 ºC for 30 minutes holding time. For the same combination, a sample was compacted at a pressure of 9.6 Ton and another at a pressure of 9.8 Ton were damaged due to initiated cracks during the compaction process of the specimens, which resulted in separation of the prepared samples into layers which suggests a need to study the morphology of the particles before the compacting process or using an analytical software to investigate the healability of the mixtures of the particles and the conditions at which the compacting and healing process occur in order to reduce the waste of particles. The texture of the prepared samples of this combination was smooth and soft without polishing the surface. For most prepared combinations of the particles, the shaker was run for a time ranging between (3-5) hrs to produce a well mixed and distributed mixture of particles.

In the case of the combination $MoSi_2$ (80%) + Spinel+ Y_2O_3, the yttria was added in small amounts of about 5% of the combination, the compaction pressure used for the samples was in a range between (9.5 –11.0) Ton. For most of the prepared samples the sintering conditions were fixed as mentioned above. Most of the combinations were

sintered in one process; however, some of the samples needed to be sintered in two sintering steps. From the same above-mentioned combination, the compaction pressure for one of the prepared samples was 20 Kibf and a two step sintering process was applied with conditions of 1000 ºC for a holding time of 35 minutes as the first step in an argon environment. The second step of the sintering process was fixed at a temperature of 750 ºC for a range of time (30 min-1h) in an O_2 environment. Heat treatment conditions as a healing process were applied for this sample as follows: 700 ºC for a holding time of 1h in an O_2 environment. No healing was observed for this sample regardless of several discontinuous heat treatment periods including cooling and heating. Another sample prepared from the same combination was compacted at a pressure of 17.50 klbf. The first sintering process was at a condition of 1000 ºC for a holding time of 1h in an argon environment. Full densification was achieved, yet a long crack initiated along the side of the specimen. The applied healing conditions were as follows: 250 ºC for 2 hrs holding time in an oxygen environment and slight to partial healing was achieved. The mixture of the particles was first processed to eliminate the shrinkage, a pre-sintering process for the mixture of the particles was conducted at a condition of 350 ºC for a holding time ranging between (30 min- 1h). Another sample from the same combination of the particles was sintered in two steps; the first sintering step was conducted at a condition of 1000 ºC for a holding time of 2 hrs. The second sintering step was applied at conditions of around 850 ºC for a holding time of 3 hrs. One sample was sintered at conditions of 1000 ºC for a holding time ranging between (30-45) min as a first step sintering process, the second sintering process was conducted at conditions of 675 ºC for a holding time of 30 min. For

this sample a healing condition of 700 ºC and 1 h holding time was applied; however, no obvious healing was observed.

For some of the combinations, a two step sintering process was conducted on the particles before the preparation process of the samples, the first step of the sintering process was conducted at conditions of 1000 ºC for a holding time of 30 min- 45 min, the second step was at conditions ranging between (650- 850) ºC for a holding time ranging between (15- 45) min. All the samples were left in the furnace to cool down after the sintering and heat treatment processes.

A sample prepared from the same combination compacted at a pressure of 20 klbf was damaged and cracks were formed on the surface of the sample as a result of the poor lubrication. The sample compacted at a pressure of 19.5 klbf. was sintered at a condition of 1000 ºC for a holding time of 2 hrs in an O_2 environment. In most of the cases, the shaker was run up to (3-5) hrs, and the mortar and pestle was used to obtain a well mixed and distributed mixture of the particles.

In all cases, the shaker and mortar and pestle were used to mix the particles. The sintering process of the green compacted samples can be defined as the heat treatment of the system to a temperature about 0.5 -0.75 of the melting point in order to eliminate the porosity; the driving force for the sintering process is the reduction of the surface free energy, which can be achieved through the diffusion process of the atoms, in which mass transportation of the matter from the grains to the pores, or coarsening of the

microstructure occurs. During the sintering process, the additives can impede the grain growth of the ceramics [197,].

The sintering process of the samples was carried out in an air and an argon environment. For most of the samples, the conventional process of sintering the samples was conducted in an air environment for different conditions, the first sintering step temperature was fixed at 1000 ºC for a holding time ranging between 30 min and 2 hrs. Some studies have mentioned the difficulty of sintering spinel at temperatures lower than 1600 ºC; to reach the densification stage of the materials specific sintering additives are added. A double stage or two steps sintering process is required for some of the ceramic particles as it is hard to obtain a dense phase in just a single sintering step and to eliminate the shrinkage and obtain homogenous particles or mixture of particles. Hence, the sintering additives are added to improve the sinterability.

The tribological test was conducted in a reciprocating sliding regime to heal the sample consisting of a tribosystem which utilizes Spinel/$MoSi_2$ nanoparticles. The prepared mixture of the nanoparticles was uniaxially cold pressed using a hardened steel die (13 mm in diameter). Cracks were induced on the surface of the specimens through the reciprocating motion of the tribotester and partially healed by the action of friction and the heat generated. The heat generated by the friction resulted in partial sintering and or healing at some specific areas on the surface of the sample in a process called tribo-sintering. The results showed about 80% of the crack could heal through utilizing the tribotester at a room temperature by the action of the heat generated from friction.

Complete healing may not have occurred due to the nonhomogeneity of the mixture of the particles.

Figure 16 shows a sample at different magnifications after the tribo-sintering at room temperature, where a preliminary study was done on the healing process through the tribotester in this research. The mixture of the particles was uniaxially pressed into round specimens using a hydraulic press at different compacting pressures ranging between (15-20) klbf. The sintering process of the compacted green specimens was carried out using the conventional method. The sintered samples were left in the furnace to cool down to avoid the thermal shock and internal stresses which cause the initiation of cracks and lead to failure of the samples. The additives like yttria are added to reduce the temperature and time required for the sintering process. Oleic acid was used as a binder during the compaction process of the samples. The limited mobility of the atoms as a consequence of the strong and directional chemical bonds led to a difficult healing process in ceramics [197].

The higher crystal growth as a result of adding some of the metal oxides may cause an incomplete densification during the process of sintering some ceramics. Also, increasing the temperature may result in an increase in the sintered density of the heat treated samples [197]. To enhance the shrinkage and obtain a well distributed and homogenous mixture of particles before the mixing and compaction process to prepare the specimens, the particles were subjected to heat treatment conditions at conditions in the temperature range (350-400) ºC for a holding time ranging between 30 min to 1 h.

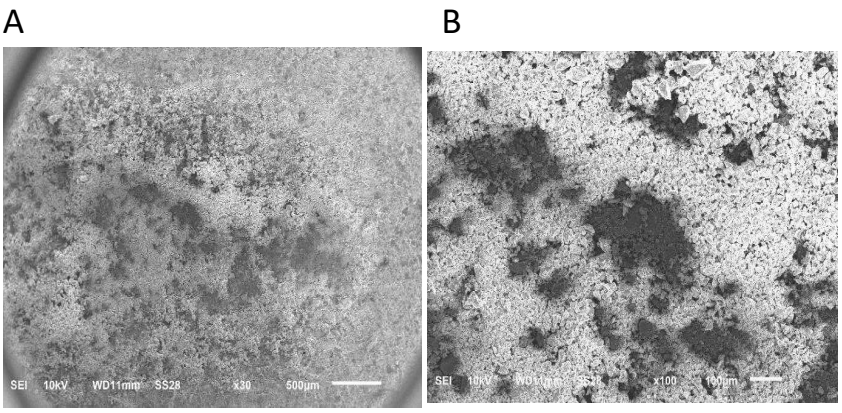

Fig. 16 (A) SEM image showing the tribo-sintering for the sample containing $MoSi_2$+ Spinel ($MgAl_2O_4$) (70%) at magnification of 30x. (B) SEM image showing the tribo-sintering for the sample containing $MoSi_2$+ Spinel ($MgAl_2O_4$) (70%) at magnification of 100x.

The green compacted particles or samples were sintered in two steps; the first step of the sintering process was fixed at a temperature of 1000 ºC at a time ranging between 30 minutes up to 2 to 3 hrs. in an argon or oxygen environment. The second sintering step occurred in the range of temperatures between 650ºC up to 850ºC for the time range of 30min up to 3hrs in an oxygen environment. In each sintering step the shrinkage rate is at least 5%. The first step of the sintering process defines the formation of the necks between the mixture' particles, while the second step or stage of the sintering process corresponds to the densification[195, 196]. The samples were left in the furnace after each heat treatment regime in order to cool down to avoid thermal shock and the formation of internal stresses. Some of the cracks were produced during the preparation, compaction process, the heat treatment and/or through using an external stimulus, mainly the carbide pen.

Cracks were healed by adding loose particles on the surface of the cracked specimen at the center of the induced crack. These loose particles have been added to seal the gap between the crack faces Figure 17 shows SEM micrographs at different magnifications of a crack induced on the surface of the sample through using a carbide pen before the healing process of the sample.

Figure 18 shows the healing process through adding loose particles, the particles were added to the sample after inducing the crack on the surface and baking or sintering/heat treating the sample in a box furnace. The loose particles were chosen from the same mixture of the particles of the sample. From an industrial view point, this process might be considered not useful unless the particles are embedded in the sample or a source included in the design component spraying these particles upon the cracking process after sensing or inspecting the crack.

Figure 19 and Figure 20 show the microstructure of the sample (Si_3N_4+Al_2O_3+Y_2O_3) before and after the healing process as shown through the SEM micrograph. The crack was healed through adding loose particles on the surface of the cracked specimen at the center of the induced crack.

In the Tig Process, the parameters that were used to heal the crack or the damage intentionally induced on the surface of the samples were as follows:-

Temp. was fixed at around 3000 ºC [192], the time was manipulated or was ranging between minute(s) and fractions of the seconds as follows:

The first sample, S_1, was treated or healed through using the tig using two steps, t_1=26 Sec, the power that has been used in this step is 100 Amp and 1.09 min. as a second step or t_2, the power that was used for this step was 80 Amp. The parameters for the second

sample, S_2, were time of 1.50 min and a power of 80 Amp. The temperature was fixed at approximately 3000 degrees C.

The procedure was as follows: Two samples were used to investigate the effect of the heat treatment through using the electrical arc to heal the crack/damage on the surface of the tested samples that are composed of SiC bonded Kaolinite with a percentage of (5-10%). The following SEM images/micrographs show the microstructure of the sample (SiC bonded $Al_2O_3.2SiO_2.2H_2O$) before and after the healing/treatment process through the tig process. The building block/unit cell of the clay mineral of kaolinite is composed of silica sheets of Si_2O that are linked to the aluminum oxide/hydroxide ($Al_2(OH_4)$ layers, which are called gibbsite. In other words, the structure of the kaolinite is composed of a sheet of Si-O tetrahedra which is arranged in a hexagonal network linked to a sheet of Al-(O,OH) octahedra[193,194]. Upon the treatment using the tig process, decomposition of the structure, diffusion and phase transformations induced-oxidation occur. Figures 21-24 show the crack, intentionally induced using a carbide pen, or generated by the stresses during the manufacturing processes of the samples, on the surface of a sample composed of SiC bonded kaolinite; different magnifications have been employed/used to show the size and depth of the crack. Several samples have been tested using tig welding, some of these samples failed due to the thermal shock upon the heat treatment using the tig process; two samples have been considered treated successfully. The structure of the samples composed of SiC bonded kaolinite is shown in Figures 25, 26, 27, 28, 29 & 30.

The structure of SiC bonded kaolinite is shown in Figure 31. The oxidation process is considered as the main mechanism to heal the damage or the crack induced on the sample alongside with diffusion/decomposition of the components to form the phases

which result in healing. Figures 32- 36 show the oxidation process upon the heat treatment using the tig welding process.

The main mechanisms which contributed to the healing process of the sample and bridging the crack after the heat treatment using the tig process can be considered as oxidation and diffusion[25, 31, 38]. Several images have been taken at different magnifications for the cracked and the treated samples through the tig welding process. The size of the crack has been minimized and considered sealed as shown in the SEM micrographs at conditions mentioned in the text in earlier pages.

Figure 37 shows the difference in the structure of the sample composed of SiC bonded Kaolinite before and after the heat treatment through the electrical arc using the tig welding process, the porosity is noticeable and significant before the tig process treatment suggesting that the porosity has been reduced by the heat treatment and the crack could seal upon the adhesion and healing process through the tig treatment. The crack healing in ceramics in general is induced through the thermal activation perturbation of the cracks followed by the sintering process or the heat treatment and particles rearrangement, viscous flow of the formed glassy phases to the crack gap or zone and healing process of the cracks [176].

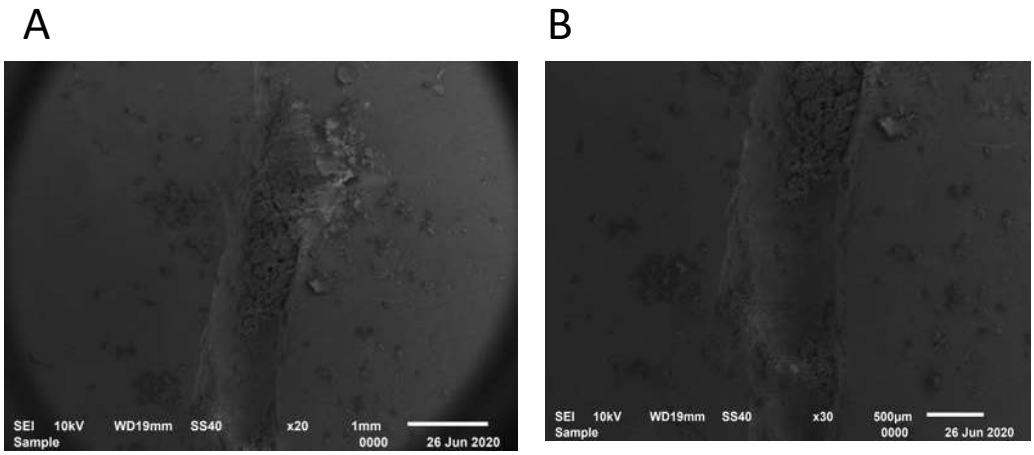

Fig. 17 (Left) SEM image showing the induced crack on the surface of the sample, Si_3N_4+Al_2O_3+Y_2O_3, at a magnification of 20x. (Right) SEM micrograph showing the induced crack on the surface of the sample, Si_3N_4+Al_2O_3+Y_2O_3, at a magnification of 30x.

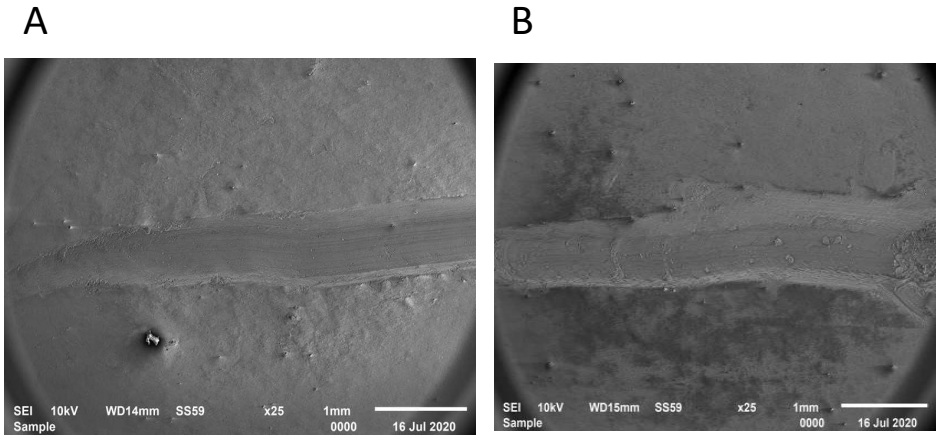

Fig. 18 (A & B) SEM images showing the healing process of the induced crack on the surface of a sample, Si_3N_4+Al_2O_3+Y_2O_3, and healing it through adding loose particles at a magnification of 30x and width of 14 mm & 15 mm.

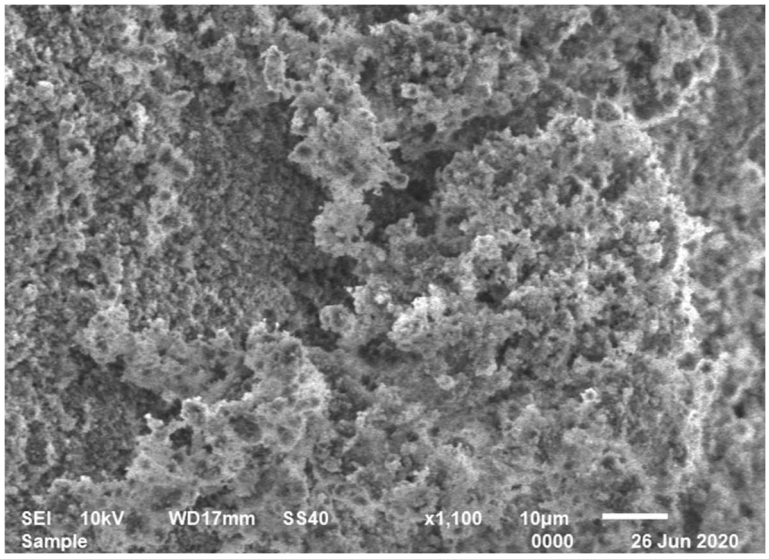

Fig. 19 SEM image/micrograph showing the morphology of, Si_3N_4+Al_2O_3+Y_2O_3, before the healing process.

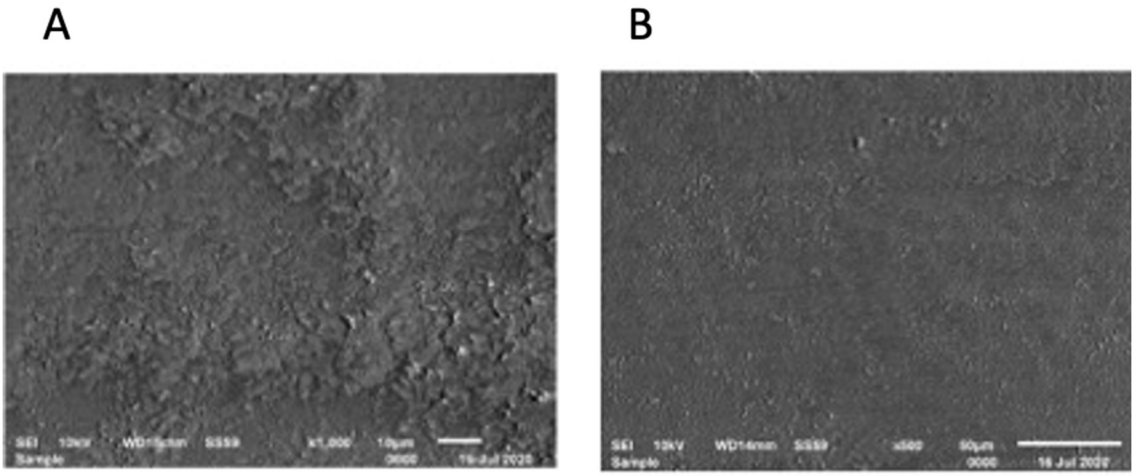

Fig. 20 (A) SEM image/micrograph showing the morphology of the healed combination, Si_3N_4+Al_2O_3+Y_2O_3, at a magnification of 1,000x. (B) SEM image/micrograph showing the morphology of the healed combination, Si_3N_4+Al_2O_3+Y_2O_3, at a magnification of 500x.

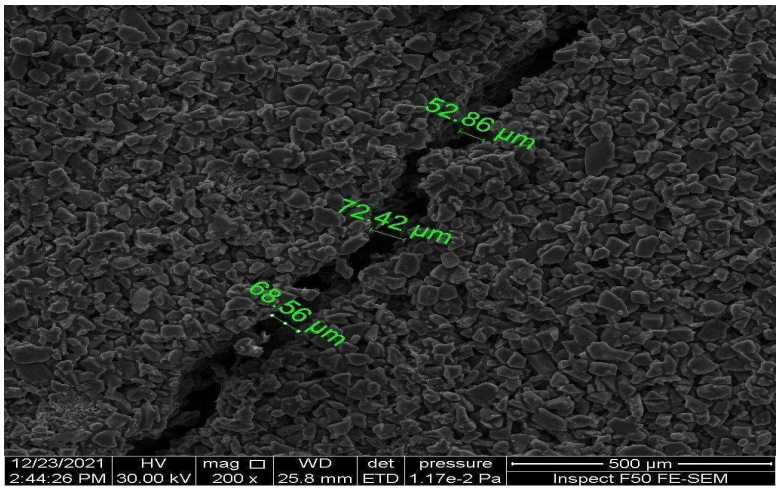

Fig. 21 SEM micrograph shows the size of the crack on the surface of a sample composed of SiC bonded kaolinite

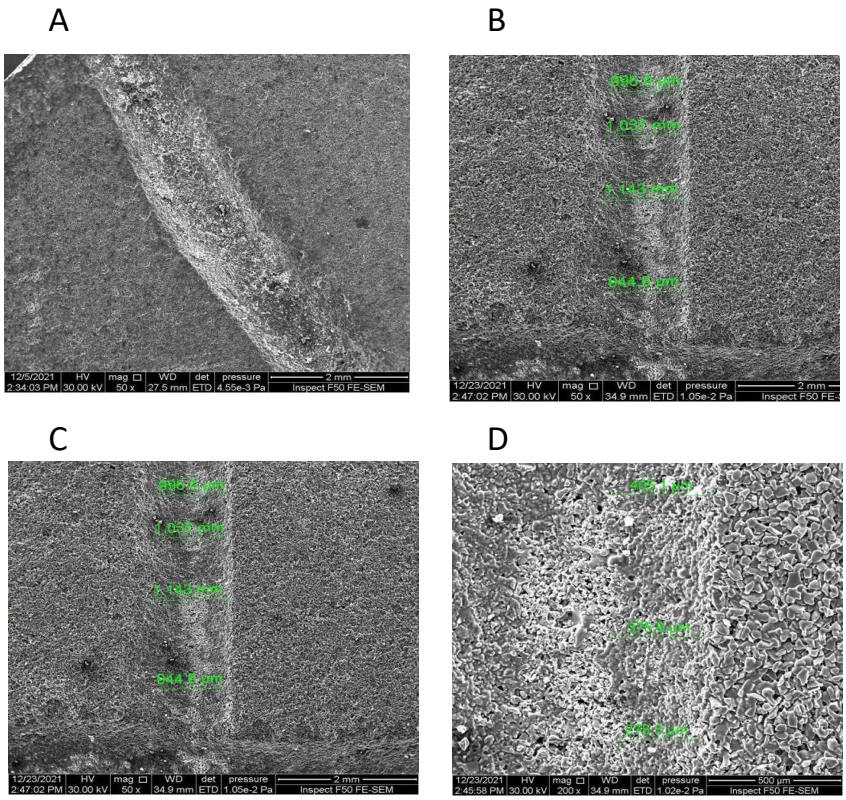

Fig. 22 (A, B, C & D) SEM images show the size of the crack induced on the surface of a sample composed of silicon carbide bonded kaolinite.

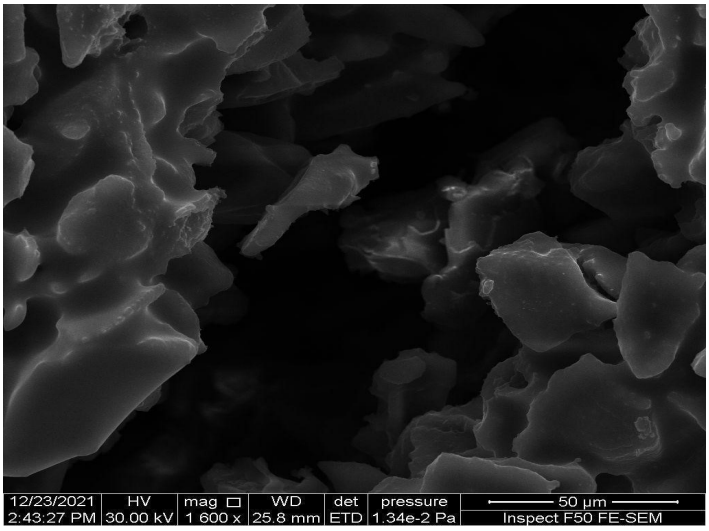

Fig. 23 SEM micrograph shows the crack depth of a sample composed of SiC bonded kaolinite

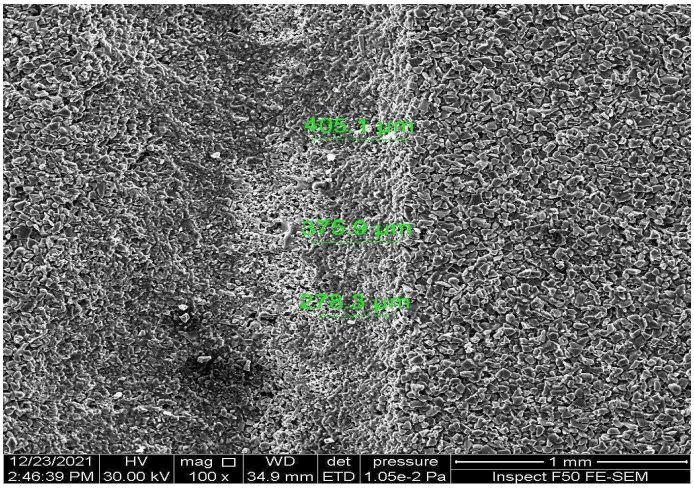

Fig. 24 SEM micrograph shows the width of the crack induced on the surface of a sample composed of silicon carbide bonded kaolinite.

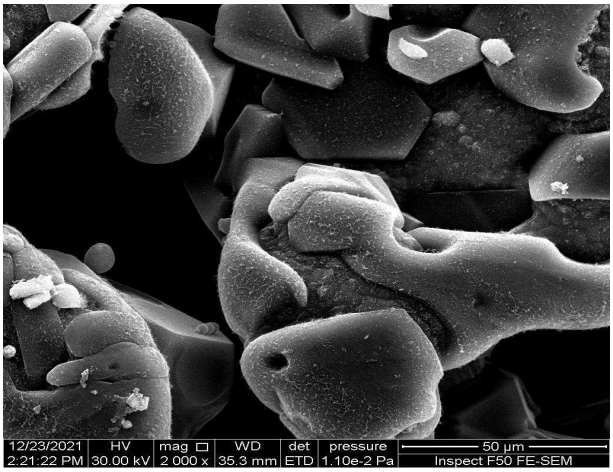

Fig. 25 SEM image shows the structure of a sample composed of silicon carbide bonded kaolinite.

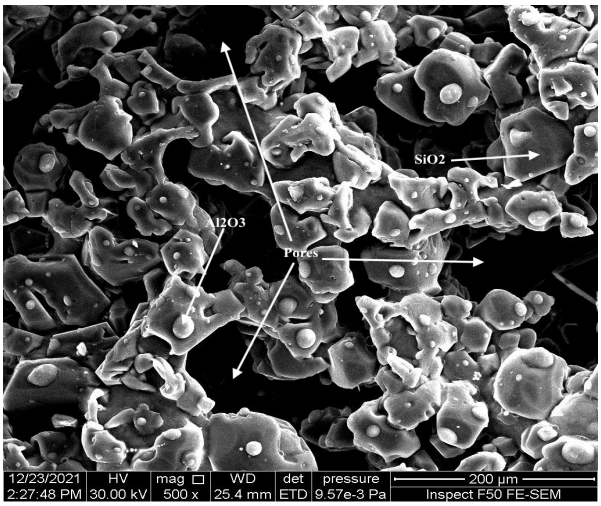

Fig. 26 SEM micrograph shows the porosity in the structure of a sample composed of silicon carbide bonded kaolinite.

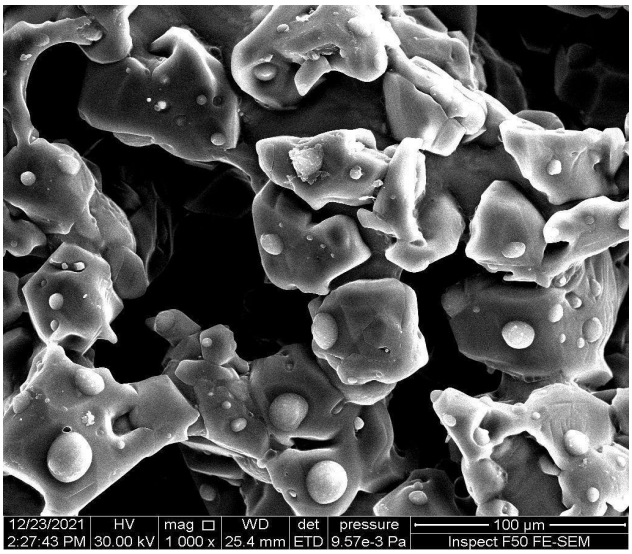

Fig. 27 SEM micrograph showing the structure of a sample composed of silicon carbide bonded kaolinite

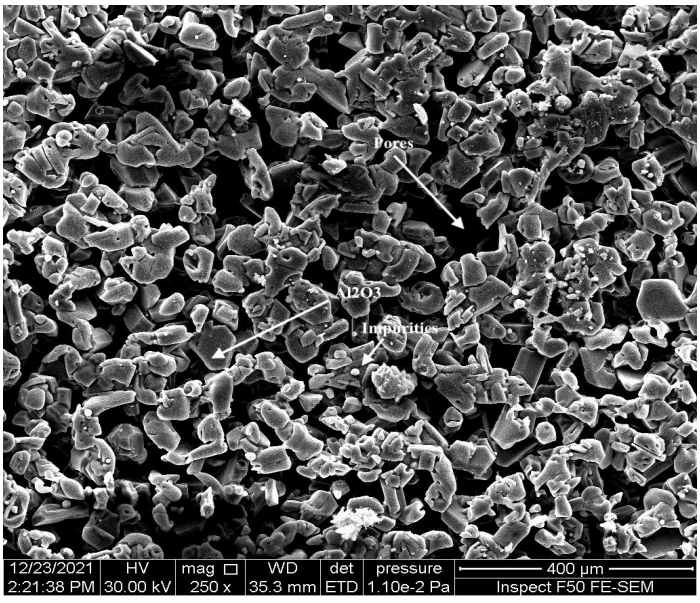

Fig. 28 SEM image shows the microstructure of the SiC bonded Kaolinite

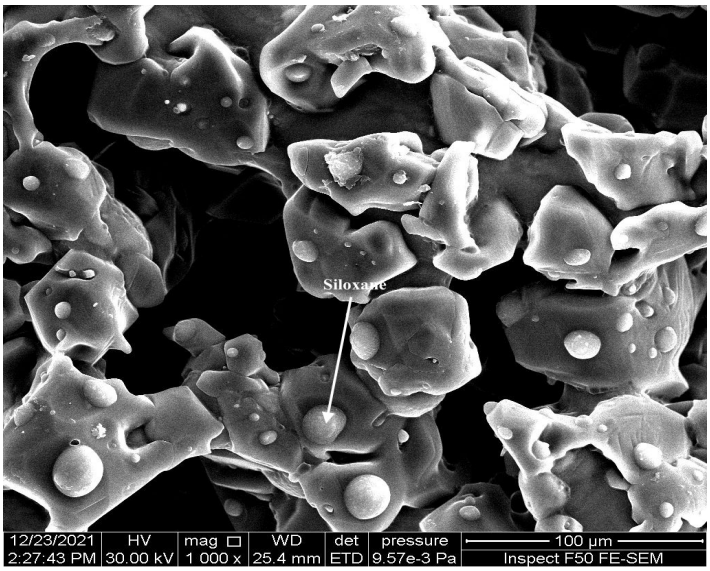

Fig. 29 SEM micrograph providing a closer view of the structure of SiC bonded Kaolinite

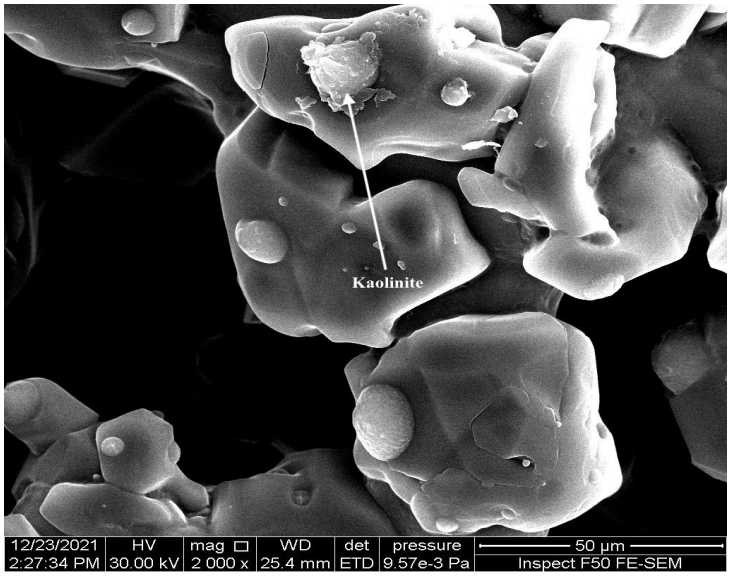

Fig. 30 SEM micrograph showing the structure of SiC bonded Kaolinite

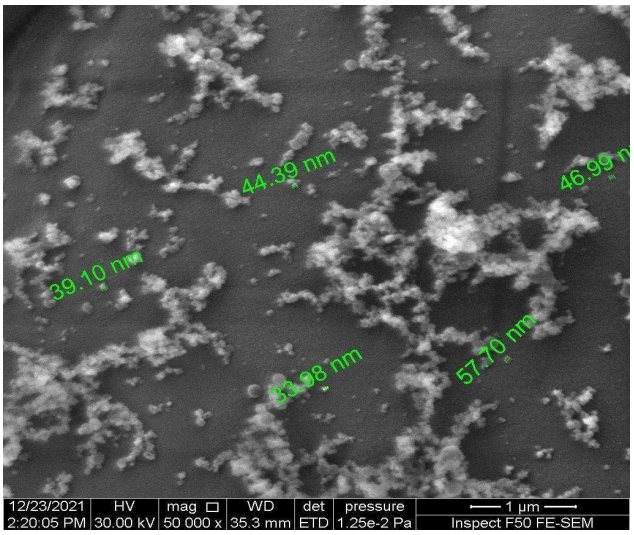

Fig 31 SEM micrograph shows the structure of the SiC bonded Kaolinite

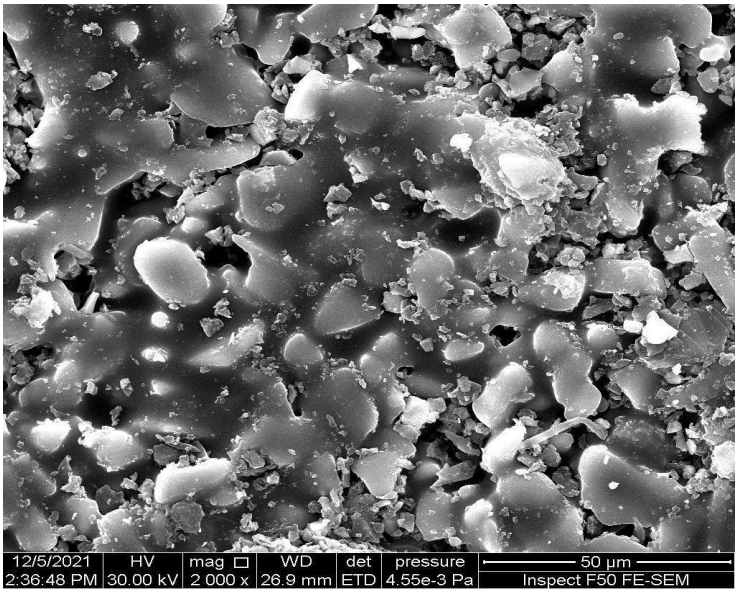

Fig 32 SEM micrograph showing the structure of the oxidized/treated SiC bonded kaolinite

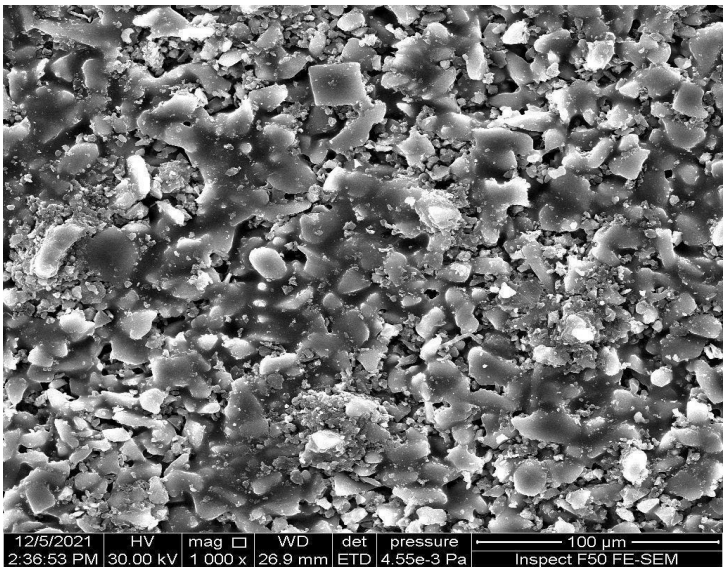

Fig 33 SEM micrograph showing the structure of the treated SiC bonded kaolinite, fusion and merging of the particles

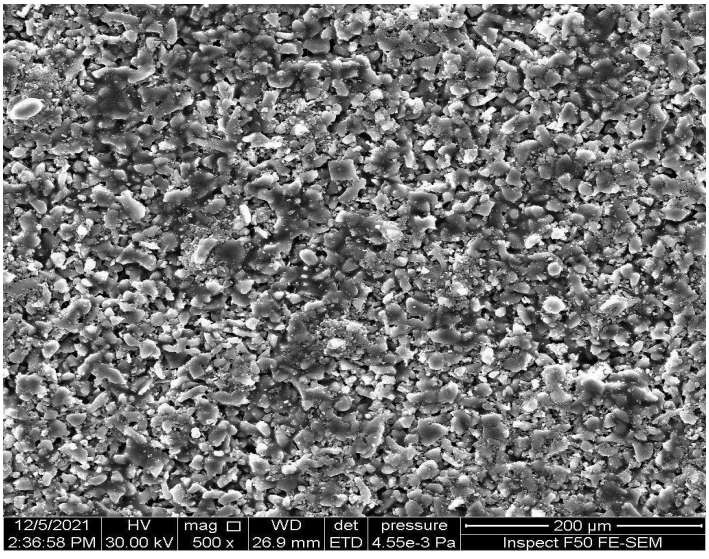

Fig 34 SEM micrograph shows the structure of the treated SiC bonded kaolinite

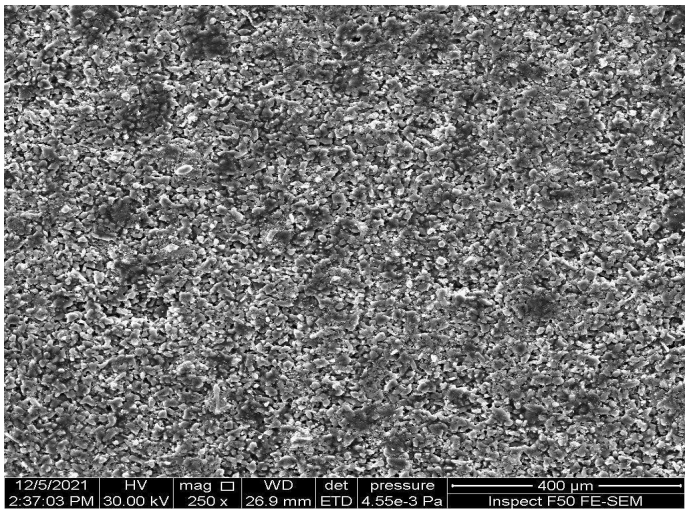

Fig 35 SEM micrograph shows the structure of the treated SiC bonded kaolinite

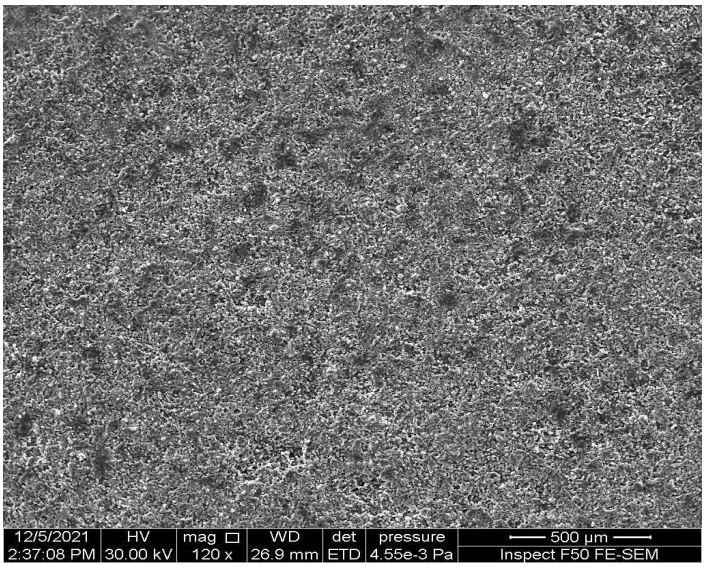

Fig 36 SEM micrograph shows the structure of the treated SiC bonded kaolinite

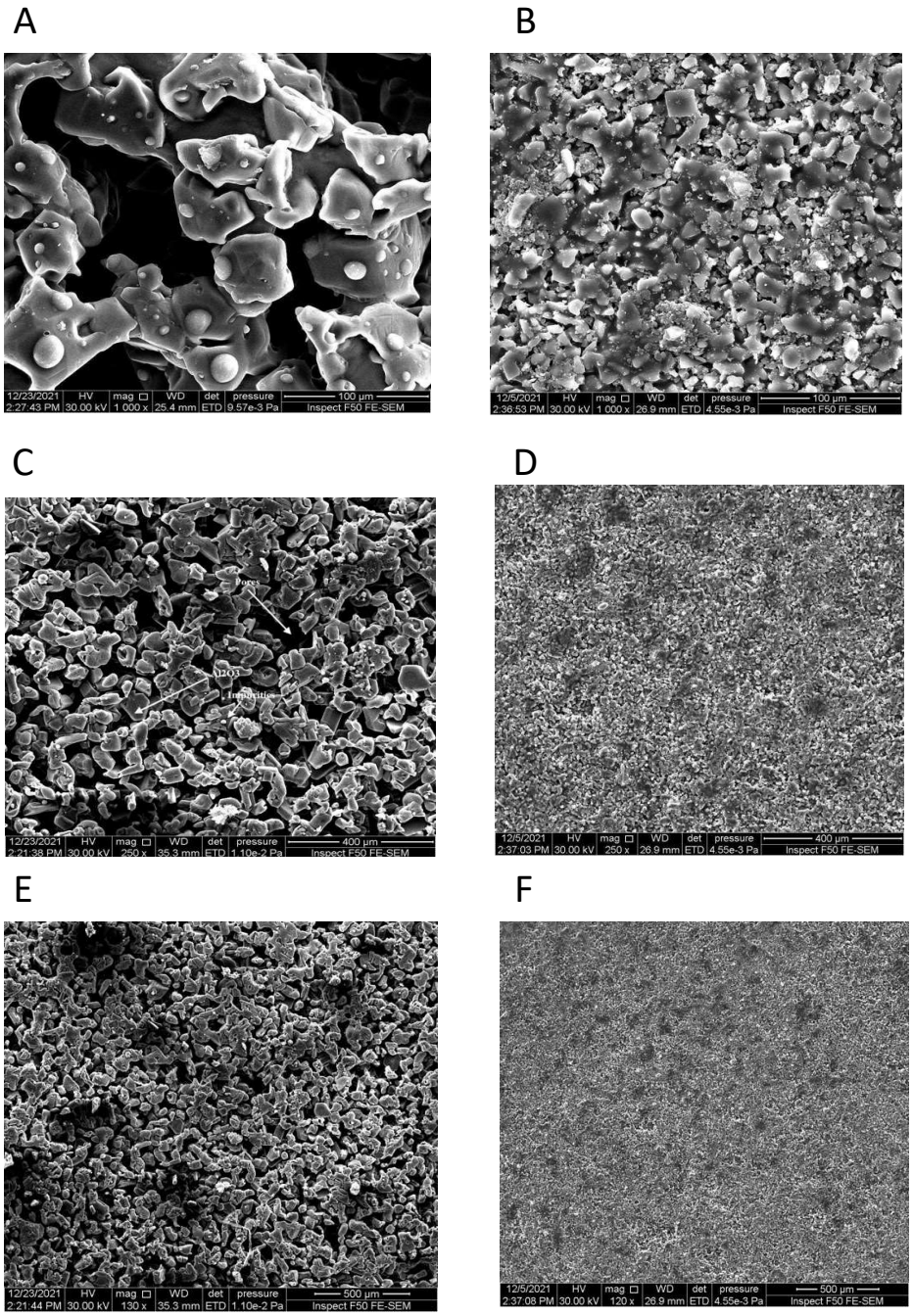

Figure 37 show the difference in the structure before and after the treatment using the electrical arc method generated via using the tig process for the sample composed of SiC bonded Kaolinite at different magnifications; (A) Shows the structure of the sample before the treatment at a magnification of 100 μm. (B) Shows the structure of the sample after the treatment or the healing using the tig process at a magnification of 100 μm. (C) Shows the structure of the sample before the treatment using the tig process at a magnification of 400 μm. And (D) Shows the structure of the sample after the treatment or the healing using the electrical arc method through using the tig process at a magnification of 400 μm. (E) Shows the structure of the sample before the treatment using the Tig process at a magnification of 500 μm. (F) Shows the structure of the sample after the treatment using the Tig process at a magnification of 500 μm.

CHAPTER SIX

SUMMARY AND FUTURE WORK

A review of the self-healing behavior, concept and processes, was done in this dissertation covering the research that has focused on the experiments related to this behavior in ceramics and its composites as well as investigating the healability of some ceramic mixtures through the conventional heat treatment in a box furnaces and through using a tig welding process.

Many researchers studied self-healing behavior in ceramics. For this class of materials, self-healing occurs at a specific temperature. The healing process in most ceramics occurs at temperatures greater than 800 ºC as reported by researchers. Few research studies have reported the occurrence of healing processes at temperatures below this range or at room temperatures. No studies have been reported or considered the healing process of the cracks or damage using the tig process.

Since some of the obstacles that might affect or have already affected the current research which mainly focuses on self-crack-healing can be summarized as follows:

- Difficulty of having consistency in the results not to mention a complete healing process for the induced cracks (100%), which can be attributed to:
- Not including a thermodynamic study or calculations of the prepared mixtures or a predictive model to predict the exact conditions and mixtures used to heal the damage, such software may be able to predict the optimum parameters for the healing process.

- Not having a well distributed mixture of particles as a result of not utilizing or ball milling for the mixtures.
- Not investigating the crystal structure of the particles individually.

And hence a broad study would be suggested in the near future that considers the above mentioned factors and parameters. Cracks were healed in this research through adding loose particles from the same combination of particles used in ceramic samples composed of Si_3N_4+Al_2O_3+ Y_2O_3 through the heat treatment in a box furnace. Some of the prepared samples of other mixtures failed during the compaction process due to the excessive pressure or upon the heat treatment owing to the volume expansion and internal stresses. The possible chemical reactions which occurred upon heat treatment of the samples can expressed through the following equations:

$$Si_3N_4+2Al_2O_3+ Y_2O_3 \rightarrow SiO_2+ 4AlN+Y_2Si_2O_7 \quad (44)$$

$$MoSi_2+ MgAl_2O_4 \rightarrow SiO_2+ MgO+Al_2O_3+ MoO \text{ (if pest oxidation occurred)} \quad (45)$$

$$4MoSi_2+ MgAl_2O_4 \rightarrow 4/2SiO_2+ MgO+Al_2O_3+ 4Mo \quad (46)$$

The samples prepared at UOT were treated using the Tig process in an air environment in order to heal the damage on the surface of the samples composed of SiC bonded kaolinite, suggesting that the tig welding can be considered process to heal the cracks in ceramics. The kaolinite is the least reactive clay mineral based on several studies; in this process the SiC reacts with the oxygen to form silica. The possible chemical reaction can be expressed in the healed regions as:

$$SiC+ 2O_2 \rightarrow SiO_2+ CO/CO_2 \quad (47)$$

A partial healing could be attained at room temperature in an air environment through using the tribotester or through the action of tribosintering using the UMT Bruker tribotester as a result of the heat generated upon friction owing to the reciprocating movement of the pin on the surface of the sample composed of spinel (70%) and molybdenum disilicide.

The suggestions for future research are:

- Studying pest oxidation of $MoSi_2$ nanoparticles and its composites over a wide range of temperatures covering the temperatures from 250 ^oC through 1600 ^oC or elevated temperatures using the HIP technique or the conventional one; other methodologies or methods might be considered as a source in the heat treatment of the samples.
- Conducting experiments on mechanical, electrical and tribological properties of the healed tribosystems at different conditions (chemical composition, temperature, time, and environment)
- Characterization/morphological studies (TEM, EDS, XRD, etc.)
- Modeling software (Abaqus, ANSYS LS-DYNA) to be utilized or another software to simulate or predict the crack healing behavior.
- Work on the self-healing: mechanism, characterization and modeling of hybrid systems/epoxy blends and ceramics nanoparticles/MAX phase ceramics. Work on the self-healing: mechanism, characterization and modeling of $MoSi_2$/and or Spinel + MAX phase (Ti_3AlC_2, Ti_2AlC, Nb_2AlC, Nb_4AlC_3, Ta_3ALC_2, Ta_4AlC_3, Ta_3AlC_2, V_2AlC, V_3AlC_2, V_4AlC_3, Zr_2AlC, Mo_2BC).

- Investigating the effect of the second phase on the sintering and healing process of the prepared nanocomposites through morphological studies.

Future work can also be carried out as follows:

- Studying the mechanical and the tribological properties of the prepared samples after the sintering process and after the healing cycles.
- Investigating the optimum conditions for the sintering process
- Investigating the optimum conditions for preparing ceramic samples or the preparation process of ceramic specimens, manipulating the conditions through increasing or decreasing the time of the heat treatment and the temperature.
- Studying the optimum conditions for the healing process of the cracks propagated during the compaction process, or intentionally induced on the surface of the samples, and the heat treatment process.
- Investigating the effect of inclusion 2^{nd} or 3^{rd} phase on the sintering process, the healing process, and the properties as the addition or inclusion of additives or other phases might enhance/improve or degrade the properties of the samples.
- Studying the effect of the binder on the compaction process of the sample or the particles/mixture of particles.
- Investigating the effect of increasing or decreasing the main component, and/or the sintering additives to the combination of the particles.

REFERENCES

[1] Hager M, Greil P, Leyens C, Van der Zwaag D, Schubert U. *Self-Healing Materials*. 2010.

[2] Wataro Nakao, Toshio Osada, Tomoya Nishiwaki, and Hideyuki Otsuka. *Focus on Self-healing materials: recent challenges and innovations*. Science and Technology of Advanced Materials 2021, Vol. 22, No. 1, 234.

[3] Van der Zwaag S, Van Dijk NH. Jonkeers HM. Mookhoek SD, Sloof WG. *Self-healing behavior in man-made engineering materials: bioinspired but taking into account their intrinsic character*. Philos Trans Royal Soc A 2009; 367: 1689-704.

[4] Bush EA, Hummel FA. *High temperature mechanical properties of ceramic materials: I, magnesium dititanate*. J Am Ceram Soc. 1958; 41 (6): 189-195.

[5] Petrovic JJ, Jacobson LA. *Controlled surface flaws in hot-pressed SiC*. J Am Ceram Soc.1976;59 (1-2) 34-37.

[6] Tavangarian F, Li G. *Crack-healing in Spinel ($MgAl_2O_4$) Ceramics.* Mater Sci Eng A. 2015; 641: 201-209.

[7] Tavangarian F and Li G. *Crack healing and strength recovery in SiC/Spinel nanocomposites*. Ceram Int. 2015; 41 (7) 8702-8709.

[8] Tavangarian F, Li G. *Bio-inspired crack self-healing of SiC/ Spinel nanocomposite.* Ceram Int. 2015; 41 (2) 2828-2835. ceramint.2014.10.103.

[9] Tavangarian F, Hui D, Li G. *Crack-healing in Ceramics*. Compos B Eng. 2018; 144: 56-87.

[10] Kukzyk-Malecha, Justyna & Zhang, Xun & Carr, James & Nozahic, Frank & Estournes, Claude & Monceau, Daniel & Combat, Alexandra & Sloof, Win G. & Zwaag, S & Withers, Philip & Xiao, Ping. (2018). *Thermo-mechanical properties of SPS produced thermal barrier coatings containing pure and alloyed $MoSi_2$ Particles.* Journal of European Ceramic Society

[11] Nozahic, Franck and Monceau, Daniel and Estournes, Claude, *Thermal Cycling and reactivity of a $MoSi_2/ZrO_2$ composite designed for self-healing thermal barrier coatings*. (2016) Materials and Design, Vol. 94, PP. 444-448.

[12] Gaoming Zhu, Xiaohong Wang, Qiong Lu, Guangzhi Wu, Peizhong Feng. *High-temperature crack healing behavior and strength recovery of (MoNb)Si_2,* Applied Surface Science, 343 (2015) 41-48.

[13] Koji Takahashi, Masahiro Yokouchi, Sang-Kee Lee, and Koji Ando. *Crack-Healing Behavior of Al_2O_3 Toughened by SiC Whiskers*. J. Am. Ceram. Soc., 86 [12]43-2143-47 (2003).

[14] K. Ando, B.-S. Kim, M.-C. Chu, S Saito, Koji Takahashi. *Crack-healing and Mechanical Behavior of Al_2O_3/SiC Composites at Elevated Temperatures.* Fatigue & Fracture of Engineering Materials & Structure. 27 (7):533-541.

[15] Osada T, Nakao W, Takahashi K, Ando K. Self-crack *healing behavior under combustion gas atmosphere.* Mechanical Properties and Performance of Engineering Ceramics and Composites IV. In: Singh D, Kriven WM, editors. The American Ceramic Society; 2010, p. 155-166.

[16] Osada T, Nakao W, Takahashi K, Ando K. *Kinetic of Self-Crack-healing of Alumina/Silicon Carbide Composite Including Oxygen Partial Pressure Effect.* J Am Ceram Soc 2009;92:864-9.

[17] Ando K, Chu MC, Yao F, Sato S. *Fatigue strength of crack healed Si_3N_4/SiC composite ceramics.* Fatigue Fract Eng Mater Struct 1999;22:897-903.

[18] Ando K, Ikeda T, Yao F, Sato S, Kobayashi Y. *A preliminary study on crack healing behavior on Si_3N_4/SiC composite ceramics*. Fatigue Fract Eng Mater Struct 1998;21:119-122.

[19] Kotoji Ando, Koji Takahashi, Shin Nakayama, Shinji Suito. *Crack-Healing Behavior of Si_3N_4/SiC Ceramics Under Cyclic Stress and Resultant Strength at the Crack Healing Temperature.* December 2004. Journal of the American Society 85 (9): 2268-2272.

[20] Choi SR, Tikare V. *Crack healing of alumina with a residual glassy phase: strength, fracture toughness and fatigue*. Mater Sci Eng A 1993; 171:77-83.

[21] Huang XX and Wen GW. *Mechanical properties of Al_4SiC_4 bulk ceramics produced by solid state reaction*. Ceram Int 2007; 33:453-8.

[22] Lange FF, Radford KC. *Healing of surface cracks in polycrystalline Al_2O_3*. J Am Ceram Soc, 1970; 53: 420-1.

[23] Gupta TK. *Crack healing and strengthening of thermally shocked alumina*. J Am Ceram Soc 1976;59:259-62.

[24] Masanori Nakatani, Junki Nishimura, Satoshi Hanaki, Hitoshi Uchida. *Crack-Healing behavior induced by oxidation in SiN/SiC nanolaminated films.* Thin Solid Films 556(2014) 68-73.

[25] Chen G, Zhang R, Zhang X, Zhao L, Han W. *Oxidation-induced crack healing in $Zr_2Al_4C_5$ ceramic.* Mater Des 2009;30:3602-7.

[26] Chu MC, Cho SJ, Lee YC, Park HM, Yoon DY. *Crack healing in silicon carbide*. J Am Ceram Soc 2004;87:490-2.

[27] Chou IA, Chan HM, Harmer MP. *Effect of annealing environment on the crack healing and mechanical behavior of silicon carbide-reinforced alumina nanocomposites*. J Am Ceram Soc, 1998;81:1203-8.

[28] Thompson AM, Chan HM, Harmer MP. *Crack healing and stress relaxation in Al_2O_3-SiC "nanocomposites".* J Am Ceram Soc 1995;78:567-71.

[29] Wang J, Stevens R. *Modification of indentation cracks in TZP ceramics by thermal treatment*. J Mater Sci Lett 1988; 7:560-2.

[30] Koji Takahashi, Kenichi Uchiide, Wataru Nakao, Kotoji Ando, *Crack-Healing Behavior of Mullite/SiC Multi-Composite under Stress*, Proceedings of the first International Conference on Self-Healing Materials 18-20 April 2007, Noordwijk aan Zee. The Netherland.

[31] Zuo X, Zhang L, Liu Y, Cheng L, Xia Y. *Oxidation behavior of 2D C/SiC modified with self-healing Si-B-C coatings in static air*. Cerros Sci, 2012:65:87-93.

[32] Jaulaprakash, Krishnasamy & A Ponnusami, Sathiskummar & Turteltaub, Sergio & Zwaag, S. (2018). *Modeling the fracture behavior of thermal barrier coatings containing healing particles*. Materials and Design.

[33] Dambi, Masoud & Abu Al-Rab, Rashid & Little, Dallas. (2012). *A continuum damage mechanics fracture work for modeling micro-damage healing*. International Journal of Solids and Stiches.

[34] W. G. Sloof, S. R. Turteltaub, A. L. Carabat, Z. Derelioglu, S. A. Ponnusami & G. M. Song. *Crack Healing in Yttria Stabilized Zirconia thermal barrier coatings.*(2015).

[35] Frank Nozahic, Claude estournes, Alexandra Lucia Carabat, William G. Sloof, Sybrand van der Zwaag, Daniel Monceau. *Self-healing thermal barrier coating systems fabricated by spark plasma sintering.* (2018) Materials & Design, Vol. 143. PP.204-213.

[36] Kobayashi K, Maeda K, Sano H, Uchiyama Y. *Formation and oxidation resistance of the coating formed on carbon material composed of B_4C-SiC powders.* Carbon 1995; 33:397-403.

[37] Toshio Osada, Toru Hara, Masanori Mitome, Shingo Ozaki, Taichi Abe, Kiichi Kamoda, and Takahito Ohmura. *Self-healing by design: Universal kinetic model of strength recovery in self-healing ceramics.* Science and Technology of Advanced Materials 2020, Vol. 21, No. 1, 593-608.

[38] Cao X., Yin X., Ma X., Fan X., Cheng L., Zhang L. *Oxidation behavior of SiBC matrix modified C/SiC composites with different PyC interphase thicknesses.* Ceram. Int. 2015;41:1695–1700.

[39] Li S, Xia L, Song G, Kwakernaak K, van der Zwaag S. *Multiple crack healing of a Ti_2AlC ceramic*. J Eur Ceram Soc 2012; 32:1813-20.

[40] Rajesh Purohit, Neelesh Kumar Gupta, Murli Raj Purohit, Akshat Patil, R. K. Bharilya, Swadesh Kumar Singh. *An investigation on manufacturing of self-healing materials*. Materials Today: Proceedings 2 (2015) 3371-3377.

[41] Z. Derelioglu, A. L. Carabat, G. M. Song, S. van der Zwaag, W. G. Sloof. *On the use of B-alloyed $MoSi_2$ particles as crack healing agents in yttria stabilized thermal barrier coatings*. Journal of the European Ceramic Society 35 (2015) 4507-4511.

[42] Lee S, Ono M, Nakao W, Takahashi K, Ando K, *Crack healing behavior of mullite/SiC/Y_2O_3 composites and its application to the structural integrity of mechanical components.* J Eur Ceram Soc, 2005; 25:3495-502.

[43] Shunsuke Yoshioka, Linda Boatemaa, Sybrand van der Zwaag, Wataru Nakao, Willem G. Sloof. *On the use of TiC as high-temperature healing particles in alumina based composites.* Journal of the European Ceramic Society 36 (2016) 4155-4162.

[44] Chlap Z, Flasar P, Ando K, Dlouhy I. *Fracture behavior of Al_2O_3/SiC nanocomposite ceramics after crack healing treatment.* J Eur Ceram Soc 2008:28: 1073-7.

[45] Kochuby V and Sloof W G. *Self-healing mechanism in thermal barrier coatings. In: ITSC proceedings*, Maas-tricht, 2-4 June. (2002).

[46] Kotoji Ando and Koji Takahashi, *crack-healing behavior of Si_3N_4/SiC ceramics under cyclic stress and resultant fatigue strength at healing temperature*. J. Am, Soc, 85 [9] 2268-72. (2002).

[47] Keiji Houjou, Kotoji Ando, Sung-Po Liu, Shigemi Sato. *Crack-Healing and Oxidation behavior of Silicon nitride ceramics,* Journal of the European Ceramic Society 24 (2004) 2329-2338.

[48] B. J. Pedimonte, G. Bei, D. Pourjafar, T. Fey, P. Greil. *Oxidative Crack Healing in Al_2O_3 Composites Loaded with Ti_2AC (A=Al, Sn) Repair Fillers*, J. Ceram. Sci, Tech., 05 [01]63-68. (2014).

[49] Masato Ono, Wataru Nakao, Koji Takahashi, Kotoji Ando and Shinji Saito. *Strength Recovery of Machined Al_2O_3/SiC Particle Composite Ceramics*, Proceedings of the first international conference on Self-Healing Materials 18-20 April 2007, Noordwijk aan Zee, The Netherland.

[50] H. J. Yang, Y. T. Pei, J. C. Rao and J. Th. M. De Hosson. J. Mater. Chem., 2012, 22, 8304-8313.

[51] Ferrara, Liberrto & Albertini, Isaia & Getta, Ravindra & Krelani, Visar & Moscato, Simone & Pirritano, Francesco & Roig Flors, Marta & Serna, P & Theeda, SM. *Self-healing of cement based materials engineered* (2015). Self-healing of cement based materials engineered through crystalline admixture: results from a multinational university network.

[52] Koji Takahashi, Masahiro Yokouchi, Sang-Kee Lee, and Koji Ando, *Crack-Healing Behavior of Al_2O_3 Toughened by SiC Whiskers*. J. Am. Ceram. Soc., 86 [12] 43-2143-47. (2003).

[53] Lu X, Li S, Zhang W, Yao B, Yu W, Zhou Y. *Crack healing behavior of a MAB phase: MoAlB.* J Eur Ceram Soc. 2019; 39 (14): 4023-4028.

[54] Lange FF. *Healing of surface cracks in SiC by oxidation.* J Am Ceram Soc 1970;53:290.

[55] Gulbransen EA, Jansson LA. *High-temperature oxidation, reduction and volatilization reactions of silicon and silicon carbide*. Oxid Metals 1972;4:181-201.

[56] McLean AF, Fisher EA, Bratton RJ. *Brittle materials design, high temperature gas turbine*. Tech Rept AMMRC 1973;73: 169-210.

[57] Korous J, Chu MC, Nakatani M, Ando K. *Crack healing behavior of silicon carbide ceramics*. J Am Ceram Soc 2000; 83:2788-92.

[58] K. Ando, M. C. Chu, K. Tsuji, T. Hirasawa, Y. Kobayashi, S. Sato, *Crack healing behavior and high temperature strength of Mullite/SiC composite ceramics,* J. Eur. Ceram. Soc. 22 (2002) 1313-1319.

[59] B. S. Kim, K. Ando, M. C. Chu, S. Saito, *crack healing behavior of monolithic alumina and strength of crack-healed member*, J. Soc. Material. Sci. Jpn. 52 (2003) 667-673.

[60] Li S, Xiao L, Song G, Wu X, Sloof WG, van der Zwaag S. *Oxidation and crack healing behavior of a fine-grained Cr_2AlC ceramic.* J Am Ceram Soc 2013; 96:892-9.

[61] Bian AS. *Cracking and bulk movement in irradiated uranium oxide fuel elements*. Trans Am Nucl Soc 1963; 6:352-3.

[62] Heuer AH, Robert JL. *The influence of annealing on the strength of corundum*. Cryst Proc Br Ceram Soc 1966;6:17-27.

[63] Van der Zwaag S. *Routes and mechanisms towards self-healing behavior in engineering materials* Bull Pol Ac Tech 2010; 8:227-36.

[64] A Farle, L Botemaa, L Shen, S Govert, J B W Kok, M Bosch, S Yoshioka, S van der Zwaag and W G Sloof. The Self-healing behavior of Some Selected Ceramics under Combustion Chamber Conditions. Smart Mater. Struct. 25 (2016) 084019.

[65] Hickman SH, Evans B. *Influence of geometry upon crack healing rate in calcite.* Phys Chem Minerals (1987) 15:91-102.

[66] Sloof WG, Farle AS, Shen L. *Intrinsic autonomous crack healing in MAX phase ceramics*. 2015.

[67] Xin Tao, Xiaojing Xu, Xiqing Xu, Wenhu Hong, Anran Guo, Feng Hou, Jiachen Liu. *Self-healing Behavior in $MoSi_2$/Borosilicate glass composites*. Journal of the European Ceramic Society 37 (2017) 871-875.

[68] Xiu-Ping Zhang, Jia-Hu Ouyang, Zhan-Guo Liu, Yu-Jin Wang, Ya-Ming Wang, *Crack-healing behavior and strength recovery of hot-pressed TZ3Y20A-$MoSi_2$ ceramics.* Material Science and Engineering A 648 (2015) 299-304.

[69] Koji Takahashi, Kotoji Ando, Shinji Sato. *Crack-Healing Under Cyclic Stress and Improvement of the Resultant Fatigue of Si_3N_4/SiC*. Key Engineering Materials (Volume 317-318) pp. 453-456. 2006. The Science and Engineering Ceramics.

[70] Alice B. W. Brochu, Stephen L. Craig and William M. Reichert. *Self-healing biomaterials.* J Biomed Mater Res A. 2011 February; 26 (2): 492-506.

[71] Ruschewitz U. *Binary and ternary carbides of alkali and alkaline-earth metals*. Coord Chem Rev 2003; 244:115-36.

[72] H. J. Yang, Y. T. Pei, J. Th. M. De Hosson, *oxide-scale growth on Cr_2AlC ceramic and its consequence for self-healing,* Scripta Materialia 69 (2013) 203-2060.

[73] Shibo Li, Guoping Bei, Xiaodong Chen, Linquan Zhang, Yang Zhou, Mirza Mackovic, Erdmann Spiecker, Peter Greil. *Crack healing induced electrical and mechanical properties recovery in a Ti_2SnC ceramic*. Journal of the European ceramic Society 36 (2016) 25-32.

[74] K. Ando and W. Nakao. *Increasing the Reliability of Ceramics Composites Using Self-crack Healing*. ICSHM2013, PP: 844-554.

[75] Wataru Nakao, Koji Takahashi and Kotoji Ando. *Self-Crack-Healing Behavior of Mullite/SiC Particle/SiC whisker Multi-Composites.* Advances in Technology of Materials and Materials Processing, 6 [2] (2004) 236-239.

[76] Ki Woo Nam. *Effect of the crack healing of SiC according to Times of SiO_2 Colloid Coating*. Journal of Power Technology. Volume 2013. Article ID 695895. 5 Pages.

[77] *Simple and low cost crack healing of ceramic-based composites*, Journal of the American Ceramic Society, Osaka University, 2018.

[78] T. Osada, ICSHM 2013, *Kinetic Model for self-crack healing in ceramics and possibility of turbine blade Applications.*

[79] J. Song, T. Barriere, B. Liu, J. C. Gelin. *Numerical simulation of sintering process in ceramics powder injection moulded components*. AIP Conference Proceedings 908, 1111 (2007);

[80] L. Jun, Z. X. Zheng, H. F. Ding and Z. H. Jin. *Preliminary study of the crack healing and strength recovery of Al_2O_3-matrix composites*. Fatigue Fract Energy Mater Struct 27, 89-97, 2004 Blackwell Publishing Ltd.

[81] Linda Bontemaa, Cees Kwakernaak, Sybrand Van der Zwaag, Willem G. Sloof. *Selection of healing agents for autonomous healing of alumina at high temperatures*. Journal of the European Ceramic Society 36 (2016), 4141-4145.

[82] Wataru Nakao, Shuntaro Muri, Jun Nakamura, Koji Takahashi, Masahiro Yokouchi and Kotji Ando. *Self-crack-Healing Behavior of Mullite/SiC Particle/ ceramic springs*. J. Am. Ceram. Soc. 89 [4] 1352-1357 (2006).

[83] Volkan Kilicli, Xiaojun Yan, Nathan Salowitz, and Pradeep K. Rohatgi. *Recent Advancement in Self-healing Metallic Materials and Self-Healing Metal Matrix Composites*, JOM, Vol. 70, No.6, 2018.

[84] Xiu-Ping Zhang, Jia-Huo Ouyang, Zhan-Guo Liu, Yu-Jin Wang, Ya-Ming Wang, Yu Zhou. *Crack-healing ability and strength recovery of different hot-pressed TZ3Y20A-SiC ceramics by heat treatment in air*. Materials and Design 67 (2015) 324-329.

[85] Francois O. Mear, Rendaad Podor, Heikki, Suhonen, and Lionel Montagne. *2D and 3D observation and mechanism of Self-Healing in Glass-Boron composites, Sundra Castanie*. J. Am. Soc. 99 [3] 849-855 (2016).

[86] Ever J. Barbero and Kevin J. Ford. *Characterization of Self-Healing Fiber-Reinforced Polymer-Matrix Composites with Distributed Damage,* Journal of Advanced Materials, Vol 39, No. 4, Oct 2007.

[87] Z. Ilhan, A. Hornes, N. Sata, O. Freitag, A. Ausar, G. Schiller, A. Friedrich, V. Guski, U. Weber, A. Krebs, S. Schmauder. *Self-healing plasma sprayed ceramic coatings*. ITSC 2015-Proceedings of the International Thermal Spray Conference, May 11-14, 2015, Long Beach, California, USA, A. McDonald, A. Agarwal, G. Bolelli, A. Cocustell, Y. C. Lau, F. L. Toma, E. Turuner, C. Widener, 20125. ASM International.

[88] Nasiru Zakari Muhammad, Arezou Shafaghat, Ali Keyvanfar, Muhd Zaimi Abd-Majid, S. K. Ghoshal, Seyed Esmaeil Mohammadyan Yasouj, Abideen Adekunle Ganiyu, Mostafa Samadi Kouchaksaraei, Hesam Kamyab, Mohammad Mahdi Taheri, Mostafa Rezazadeh Shirdar, Ronald McCaffer. *Tests and methods of evaluating the self-healing efficiency of concrete: A review*. Construction and Building Materials 112 (2016) 1123-1132.

[89] Wataru Nakao and Shihomi Abe. *Enhancement of the self-healing ability in oxidation induced self-healing ceramics by modifying the healing agent*. Smart Mater-Struct. 21 (2012) 025002 (7pp).

[90] Ki Woo, Nam, Jong Soon Kim. *Critical crack size of healing possibility of SiC Ceramic*s. Materials Society and Engineering A 527 (2010) 3236-3239.

[91] E. Baranger, C. Cluzel, P. Ladeveze, and a. Mouret. *Identification and validation of A Multiphysics Macro-model for the Lifetime Prediction of Self-healing Ceramic matrix Composites*

[92] Shingo Ozaki, Toshio Osada, Wataru Nakao. *Finite element analysis of the damage and healing behavior of self-healing ceramic materials.* International Journal of Solids and structures, 100-101 (2016) 306-318.

[93] Willem G. Sloof, Ruizhi Pci, Samuel A. McDonald, Julie L. Fifer, Lu Shen, Linda Boatemma, Ann-Sophie Farle, Kun Yan, Xun Zhang, Sybrand van der Zwaag,

Peter D. Lee, & Philip J. Withers. *Reported crack healing in MAX phase ceramics revealed by 4D in situ synchrotron x-ray tomography microscopy.*

[94] Willy Kunz and Hagen Klemm. *Self-healing EBC Materials for Gas Turbine Applications*. 2017, Ceramic transaction 263: 173-185. ch18. Book: Advances in High Temperature Ceramic Matrix Compo Sites and Materials for Sustainable Development; Ceramic Transactions, Volume CCLX111.

[95] S. Yoshioka, W. Nakao. *Strength Recovery and crack filling Behavior of Al_2O_3/TiC Self-Healing Ceramics.* 2017, Ceramic Transactions 263: 243-251. Book: Advances in High Temperature Ceramic Matrix Compo Sites and Materials for Sustainable Development; Ceramic Transactions, Volume CCLXIII.

[96] Martin Stumpf, Tobias Fey, Leuchi Kakimoto, and Peter Greil. *Nb_2AlC-Particle induced accelerated crack healing in ZrO_2-matrix composites.* 2018, Ceramics International 44 (16): 19352-19361.

[97] G. M. Song, W. G. Sloof, S. B. Li, S. van der Zwaag. *Crack healing advanced machinable high temperature Ti_3AlC_2 Ceramics*. International Conference on Self-Healing Materials. 1-9. 2007.

[98] D. S. Burton, X. Gao, L. C. Brinson. *Finite element simulation of a self-healing shape memory alloy composite*. Mechanics of Materials 38 (2006) 525-537.

[99] Jie Kong, Chunjia Kuo, Fei Liu, Fang Ye, Xingang Luan, Nan Tian, Yongsheng Kiu, Han Zhang, Junwei Gu, and Yasheng Tang. *High temperature Self-healing SiBCN ceramics derived from hyperbranched polyborosilazanes*. 2018

[100] Son Thanh Nguyen, Tadachica Nakayama, Yuichi Otsuka, Lingfeng He, Tsuyoshi Takahashi, and Koichi Niihara, *Self-healing Behavior and Strength Recovery of ytterbium disilicate ceramics reinforced with Silicon Carbide nanofillers.* Journal of the European Ceramic Society 39 (10), 2019.

[101] Son Thanh Nguyen, Tada Chika Nakayama, Hisayuki Suematsu, Koichi Niihara, Tsuneo Suzuki, and Hirokazu Iwasawa. *Self-crack Healing Ability and Strength Recovery in Ytterbium Disilicate/silicon Carbide Nanocomposites*.

[102] Wataru Nakao, Kotoji Ando, and Koji Takahashi. *Self-healing of surface cracks in structural ceramics. Advanced nanomaterials* , 2010.

[103] Michael Wade Keller, Mathew Douglass Crall. *Self-healing composite materials*, 2017. Book: Reference Module in Materials Science and Materials Engineering.

[104] Linda Boatemaa, Myrthe Bosch, Ann-Sophie Farle, Guo-Ping Bei, Sybrand van der Zwaag, and Willem G. Sloof. *Autonomous high-temperature healing of surface*

cracks in Al_2O_3 containing Ti_2AlC particles. 2018. J Am Ceram Soc 101 (12). PP: 5684-5693.

[105] Madhan Mohankumar, A. N. Shankar, T. S. Karthik, R. Saravanakumar, Hemakesavulu Oruganti, S. Venkatesa Prabhu, N. Rakesh. *A Comparative Study on Crack-Healing Ability of Al_2O_3/SiC Structural Ceramic Composites Synthesized by Microwave Sintering and Conventional Electrical Sintering* Advances in Materials Science and Engineering, Vol. 2021 Article ID 3170697, 8 Pages, 2021.

[106] Wang, B.; Tu, R.; Wei, Y.; Cai, H. *Self-Healing of SiC-Al2O3-B4C CeramicComposites at Low Temperatures*. Materials (2022), 15 (2), 652;

[107] Meng, Z. Kim, T. W., Lee, S. M. et al. *Crack healing in the SiC-SiC ceramic matrix composites fabricated with different process.* J. Korean Ceram. Soc. 58, 86-93 (2021).

[108] Shingo Ozaki, Marika Nakamara & Toshio Osada. *Finite element analysis of the fracture statistics of self-healing ceramics.* Science and Technology of Advanced Materials. 2020, Vol. 21, No. 1, 609-625.

[109] Camillus Sunday Obayi and Paul Sunday Nnamchi (November 26th 2020). *Exploits, Advances and Challenges in Characterizing Self-Healing Materials*, Advanced Functional Materials, Nevin Tasaltin, Paul Sunday Nnamchi and Safaa Saud, Intechopen,

[110] Rois Flores, Marta & Moscato, Simone & Serna, P & Ferara, Liberato. (2015). *Self-healing capability of concrete with crystalline admixtures in different environments.* Construction and Building Materials.

[111] Jeffusion, Anthony & Juvierre, E & Freeman, Brubech & Zaoui, Ali & Koenders, Eduardus & Ferrara, Liberato. (2017). *Research Progress on Numerical Models for self-healing cementitious materials.* Advanced materials interfaces.

[112] Yige Li. *A review: Novel Routes towards the Realization of self-healing Function in Cementitious Materials*, 2018. IOP Conf.: Mater. Sci. Eng.

[113] Gurkan Yildirim, Ozlem Kasap Keskin, Suleyman Bahadir Keskin, Mustafa Sahmaran, Mohamed Lachemi. *A review of intrinsic self-healing capability of engineered cementitious composites: Recovery of transport and mechanical properties.* Construction and Building Materials 101. (2015) 16-21.

[114] Kunamini Vijay, Meena Murmu, Shirish V. Deo. Bacteria based *self-healing concrete- A review.* Construction and Building Materials 152 (2017) 1008.

[115] Nehdi, Moncef. *Innovative crack-healing hybrid fibre reinforced engineered cementitious composite*. Construction and building materials. (2017).

[116] Zhang, Hao & Liu, Yibin & Hou, Chunping & Ma, Yong & Zhang, Baoliang & Zhang, Hepeng & Zhang, Qiuyu. *Low-maintenance superamphiphobic coating based on a smart two-layer self-healing network.* Surface and coatings Technology. (2017).

[117] Robert Davies, Anthony Jefferson. *Micromechanical modelling of Self-healing cementitious materials.* International Journal of Solids and Structures

[118] Liberato Ferrara, Visar Krelani, Fabio Moretti, Marta Roig Flores, Pedro Serna Ros. *Effects of autogenous healing on the recovery of mechanical performance of High Performance Fibre Reinforced Cementitious Composites (HPFRCCs): Part 1. Cement and Concrete Composites* 83 (2017) 76-100.

[119] Jishen Qiu, Han Srang Tan, En-Hua Yang. *Coupled effects of crack width, slag content, and conditioning and healing on autogenous healing of engineered cementitious composites.* Cement and Concrete Composites 73 (2016) 203-212.

[120] Haoliang Huang, Guang Ye, Chunxiang Qian, Erik Schlangen. *Self-healing in Cementitious Materials: Materials, Methods and Service Conditions.* Materials and Design 92 (2016) 499-511.

[121] A. Beglarigale, D. Eyice, Y. Seki, H. Yazici. *Optimization of Morphology of Sodium Silicate/Polyurethane Microcapsules used for self-healing in cementitious materials*, 13th International congress on Advances in Civil Engineering, 12-14 September 2018, Izmir/Turkey.

[122] Benoit Hilloulin, Damien Hilloulin, Frederic Grondin, Ahmed Loukili, Nele De Belie. *Mechanical regains due to self-healing in cementitious materials: Experimental measurements and micro-mechanical model.* Cement and Concrete Research 80 (2016) 21-32.

[123] N. Kringos & A. Scarpas, T. Pauli & R. Robertson. A thermogravimetric approach to healing in Bitumen. Advanced testing and characterization of Bituminous Materials- Loi zos part, Scarpas & Al-Qadi (eds.), 2009 Taylor & Francis Group. London, JSBN.

[124] B. Hilloulin, F. Grondin, M. Matallah, A. Loukili. Modeling *of autogenous healing in ultra-high performance concrete*. Cement and Concrete Research 61-62 (2014) 64-70.

[125] Hickman SH, Evan B. *Influence of geometry upon crack healing rate in calcite*. Phs Chem Minerals (1987) 15: 91-102.

[126] Hoosian, M. R., Sultana, R., Patwary, M. M. et al. *Self-healing concrete for sustainable buildings. A review*. Environ Chem Lett (2022).

[127] McDonald S. A., Coban S. B., Sottos N. R et al. *Tracking capsule activation and crack healing in a microcapsule based self-healing polymer.* Sci Rep. (2019) 9: 17773.

[128] Toohey KS, Sottos NR, Lewis JA, Moore JS. White SR. *Self-healing materials with microvascular network*. Nat Mater 2007; 6:581-5.

[129] Hamilton AR, Sottos NR, White SR. *Self-healing of internal damage in synthetic vascular materials*. Adv. Mater 2010; 22:5159-63.

[130] Pingkarawat, Khomkrit & Wang, Chun & Varley, Russell & Mouritz, A. P. (2013). *Healing of Fatigue delamination cracks in carbon-epoxy composite material systems and structures.* 25.75-86.

[131] S. van der Zwaag, N. H. van Dijk, H. M. Jonkers, Phili. Trans. R. *Self-healing behavior in man-made engineering materials: bioinspired but taking into account their intrinsic character*. Soc. A (2009) 367, 1689-1704.

[132] Jong Se, Takahashi, K., Guo, Z., Wang, Y., Bolanose, E., Hamann-Schalfner, C., Thomas Hahn, H. (2008*). Towards development of a self-healing composite using a mendable polymer and resistine heating*, journal of composite materials, 42 (26), 2869-2881.

[133] The self-healing of epoxy resin blended with thermoplastics through adding thermoplastic additives (EMAA) /polyethylene-co-methacrylic and PE GMA /Polyethylene –co-glycidyl/ methacrylate /EVA –Ethylene Vinyl acetate and ABS –acylonitrile butadiene styrene to heal the cracks in the epoxy resin network and heal the delamination in carbon epoxy composite.

[134] Cohader, Amael & Branfoot, Callum & Rae, Steven & Bond, Ian & Michael, Veronique. (2018). *Self-healing materials. Progress in self-healing fiber reinforced composites*. (Adv. Mater. Interfaces 17/2018). Advanced Materials Interfaces.

[135] Henghua Jin, Chris L Mangun, Anthony S Griffin, Jeffrey S Moore, Nancy R Sottos, Scott R White. Microcapsules: *Thermally stable Autonomic Healing in Epoxy using a Dual Microcapsules System* (Adv. Mater. 2/2014). Advanced materials 26 (2): 193.

[136] You Chun Zhang, Antonius A. Boethius, and Francesco Picchioni. *Thermally Self-healing Polymeric Materials: The Next Step to Recycling Thermoset Polymers?* Macromolecules 2009, 42, 1906-1912.

[137] S. R. White, N. R. Sottos, P. H. Geubelle, J. S. Moore, M. R. Kessler, S. R. Sriram, E. N. Brown, & S. Viswanathan. *Autonomic healing of polymer composites.* Nature, Vol. 409, 15 Feb 2001. Macmillan Magazine Ltd.

[138] Sathiskumar A. Ponnusami, Jayaprakash Krishnasamy, Sergio Turteltaub, Sybrand van der Zwaag. *Modelling of the self-crack healing in ceramics/a cohesive-zone crack healing model for self-healing materials*. International Journal of Solids and Structures 134 (2018) 249-263.

[139] Wang, Chun & Sidhu, Komal & Yang, Tao & Zhang, Tin & Shaaks, Robert. (2012). *Interlayer self-healing and toughening of carbon fibre/epoxy composites Part A.* Applied Science and Manufacturing. compositesa. 2011.11.020.

[140] Russell J. Varley and Grace Parn. *Thermally activated healing in a mendable resin using a non-woven EMAA fabric.*

[141] Shuo Liu and Weiwei Guo. *Anti-biofouling and Healable Materials: Preparations,* Mechanisms and Biomedical Applications. Adv. Funct. Mater. 2018, 18, 1800596.

[142] Zhang, Hao & Tao, Jiaojun & Zhang, Baoliang & Zhang, Hepeng & Zhang, Qiuyu. (2017). *Designed fabrication of robust, rapid self-healable, superamphiphobic coatings by liquid-repellent- 'glue+particles' approach & Design*. matdes. 2017.09.002.

[143] Pingkarawat, Khomkrit & Wang, Khun & Varley, Russel & Moaritz, A. P.. (2013). *Thermoplastic Fibre Stitching. A new self-healing materials for carbon epoxy composites.*

[144] Ladani, Ray & Pingkarawat, Kkomkrit & T. T. Ngayen, Alex & Wang, Chun & P. Mouritz, Adrin. (2018). *Delamination toughening and healing performance of woven composites with hybrid Z. fibre reinforcement. Composites part A*: Applied Science and Manufacturing. compositesa. 2018.04.028.

[145] Pingkarawat, Khomkrit & Wang, Chun & Varley, Russel & Mouritz, A. P. (2013). *Healing of Fatigue delamination cracks in carbon- epoxy composite using mendablepolymer stitching*. Journal of intelligent materials systems and structures. 25. 75-86.

[146] Chen, Kunlin & Wu, Yi & Zhou, Shxue & Wu, Limin. (2016). *Recent Development of Durable and self-healing surfaces with special wettability.* Macromolecular Rapid Communications. 37.

[147] Noordwijk aan Zee, The Netherlands, F. Micciche, H. Fischer, R. Varley, and S. van der Zwaag. *Self-healing Barrier Coating using an Expandable Phase, proceedings of the First International Conference on Self-Healing Materials*, 18-20 April 2007.

[148] Lv Z, Li S, Chen H. (2017). *Analytical model for effects of capsule shape on the healing efficiency in self-healing materials*. PloS ONE 12 (11): e0187299,

[149] Steven D. Mookhoek, Patrick J. Colver, Hartmut R. Fischer, Stefan A. F. Bon and Sybrand van der Zwaag. *The Creation of High Aspect Ratio Capsules to Improve the Efficiency of Self-Healing Polymer Systems.* Proceedings of the First International Conference on Self-Healing Materials, 18-20 April 2007. Noordwijk aan Zee, The Netherlands.

[150] B. J. Blaiszik, N. R. Sottos, S. R. White. *Nanocapsules for self-healing materials.* Composite Science and Technology 68 (2008) 978-986.

[151] Steven D. Mookhoek, Hartmut R. Fischer, Sybrand van der Zwaag. *A numerical study into the effects of elongated capsules on the healing efficiency of liquid-based systems.* 2009, Computational Materials Science, Volume 47, Issue 2, December 2009, Pages 506-511.

[152] Christopher Igme Idumah. *Novel trends in Self-healable polymer nanocomposites* Journal of Thermoplastic Composite Materials, 2019.

[153] Farhad Alizadegan, S. Mojtaba Mirabedini, Shahla Pazokifard, Saba Goharshenas Moghadam, Ramin Farnood. *Improving the self-healing performance of polyurethane coatings using PU microcapsules containing bulky-IPDI-BA and nano-clay*. Progress in Organic Coatings 123 (2018) 350-361.

[154] Jose Martinez Lucci, R. S. Amano and Pradeep Rohatgi. *Computational Analysis of Self-healing in a Polymeric Matrix with Microvascular Network.* DETC 2008-50148, PP-409-417; Vol.3

[155] Iee Lee Hia, Eng Seng Chan, Siang-Piao Chai, Pooria Pusbakhsh. *Novel Repeated Self-healing Epoxy Composite with Alginate Multicore Microcapsules. 2018. Journal of Materials Chemistry A. Microcapsules: Thermally stable Autonomic Healing in Epoxy using a Dual Microcapsules System (Adv. Mater. 2/2014).* Advanced materials 26 (2): 193.

[156] Henghua Jin, Chris L. Mangun, Dylan S. Stradley, Jeffrey S Moore, Nancy R. Sottos, and Scott R. White. *Self-healing thermoset using encapsulated epoxy –amine healing chemistry.*
Another citation:
Self-healing Materials-pioneering research in the Netherlands, S. van der Zwaag, and E. Brinkman (eds.) IOS Press. © 2015. The cracks and IOS Press.

[157] Sathiskumar A. Ponnusami, Sergio Turteltaub, Xan Zhang & Ping Xiao. *Modelling Crack Propagation in Particle-dispersed Self-healing thermal Barrier Coatings.* Self-healing materials-pioneering research in the Netherlands.

[158] M. Abdolah Zadeh, S. van der Zwaag & S. J. Garcia. *Corrosion protective sol-gel coatings reversible tetra-sulphide groups, self-healing materials*, pioneering research in the Netherlands, S. van der Zwaag, E. Brinkman (eds.) IOS Press. © 2015, the authors and IOS Press.

[159] Nan Zhong, Ugo Lafont, Santiago J. Garcia & Sybrand van der Zwaag. *Self-restoring thermal interface materials based on intrinsic healing polymer matrices*, self-healing materials-pioneering research in the Netherlands, S. van der Zwaag, E. Brinkman (eds.) IOS Press. © 2015, the authors and IOS Press

[160] An, S.; Yoon, S. S.; Lee, M. W. *Self-Healing Structural Materials*. Polymers 2021, 13, 2297.

[161] Michael Nosonovsky, Pardeep K-Rohatgi, SS Materials, V-152. / Nosonovsky M., Rohatgi P. K. *Thermodynamic principles of self-healing metallic materials,* Biomimetics in materials Science, PP 25-51. (2011).

[162] N. H. van Dijk, S. van der Zwaag, *Self-healing Phenomena in Metals*, Advanced Materials. 2018. Advanced Materials Interfaces 5 (17)

[163] Michael V. Manuel and Gregory B. Olson, *Proc. Biomimetic self-healing metals*. 1st Intl. Conference on Self-healing Materials. 2007.

[164] D. S. Burton, X. Gao, L. C. Brinson. *Finite element simulation of a self-healing shape memory alloy composite*, Mechanism of materials 38 (2006) 525-537.

[165] Stefano Danzi, Volker Schnabel, Johannes Gabl, Alla Sologubenko. *Rapid on-Chip Healing of Metal Thin Films*. Henning Galinski and Ralph Spolenak, Adv. Mater. Technol. 2019, 4, 1800468.

[166] Sung Hun Cho, Tohru Sekino, Shengfang Shi, and Tomoyo Goto. *Electrochemically Assisted Room-Temperature Crack Healing of Ceramic-Based Composites.* Journal of American Ceramic Society/J. Am. Ceram. Soc. 2019; 1-11. Shi S., Goto T, Cho S., Sekino T.

[167] S. Thomas, N. Birbilis, M. S. Venkatraman, I. S. Cole. *Self-repairing oxides to protect zinc: Review, discussion and prospects*. Corrosion Science 69 (2015) 11-22.

[168] Nosonovsky M., Rohatgi P-K.. *Encapsulating a low melting point metal in a micro spheres that can act as a barrier between the low melting and the high melting point metal alloy during the casting. Biomimetics in Material Science (Self-Healing, Self-Lubricating and Self-Cleaning Materials*), springer, (2012).

[169] E. W. Lee, j. Cook, A. Khan R. Mahapatra and J. Waldman. *The oxidation resistance of $MoSi_2$ composites*, Journal of Materials, PP.54-57, March 1991.

[170] M. D. Sachs and j. A. Posh. *Decomposition of mullite*, J. Am. Ceram. Soc. 55 [2] 98-101, (1972).

[171] R. F. Dav. J. I. A. Aksay, and J. A. Posh. *Decomposition of mullite,* J. Am. Ceram. Soc., 55 [2] 98-101 (1972).

[172] E. W. Lee, J. Cook, A. Khan R. *The oxidation resistance of $MoSi_2$ Composite,* Journal of Materials, PP. 54-57. Mahapatra and J. Waldman.

[173] C. D. Wirkus and D. R. Wilder. *High temperature oxidation of molybdenum disilicide,* J. Am. Ceram. Soc., 49 [4] 173-77 (1966).

[174] Van der Zwaag S. *Self Healing Materials An Alternative Approach to 20 Centuries* of Materials Science, 2007:1-18.

[175] Pete Greil. *Self-Healing Engineering Ceramics with Oxidation Induced Crack Repair.* Adv. Eng. Mater. 2019, 1901121.

[176] Greil, P. *Generic principles of crack-healing ceramics.* J Adv Ceram. 2012; 1: 249–267.

[177] Boatemaa L, Kwakernaak C, van der Zwaag S, Sloof WG. *Selection of healing agents for autonomous healing of alumina at high temperatures*. J Eur Ceram Soc. 2016; 36: 4141-4145.

[178] L. Boatemaa, S. van der Zwaag, and W. G. Sloof. *Self-healing of Al_2O_3 containing Ti microparticles.* Ceramics International 44 (2018)11116-11126.

[179] C. G. McKamey, P. F. Tororelli, J. H. DeVan, and C. A. Carmichael. *A study of pest oxidation in polycrystalline $MoSi_2$*. J. Mater. Res., Vol. 7, No. 10, Oct 1992.

[180] T. S. R. Ch. Murthy, R. Balasubramaniam, B. Basu, A. K. Suri, M. N. Mungole. *Oxidation of monolithic TiB_2 and TiB_2-20% $MoSi_2$ composites at 850 ºC*. Journal of the European Ceramic Society 26 (2006) 187-192.

[181] P Srikari Tantri, Anup K Bhattachanga and Sheela K Ramasesha. *Synthesis and properties of $MoSi_2$ based engineering ceramics.* Proc. Indian Acad. Sci. (Chem. Sci.), Vol. 113, Nov 5 & 6, Oct-Dec 2001, pp 633-649.

[182] T. C. Chou and T. G. Neih. *New observations of $MoSi_2$ pest at 500 ºC*. Scripta Metallurgica et Materialia. Vol. 26, pp. 1637-1642, 1992.

[183] Katsuyuki Yanagihara, Toshio Maruyama & Kazuhiro Nagata. *High temperature oxidation of Mo-Si-X intermetallic (X= Al, Ti, Ta, Zr and Y).* Intermetallics 3 (1995) 243-251.

[184] S. Knittel, S. Mathieu, M. Vilasi. *The oxidation behavior of uniaxial hot pressed $MoSi_2$ in air from (400-1400) ºC*. Intermetallics 19 (2011) 1207-1215.

[185] A. Stergiou, P. Tsakiropoulos & A. Brown. *The intermediate and high-temperature oxidation behavior of $Mo(Si_{1-X}\ Al_X)_2$ intermetallic alloys.* Intermetallics 5 (1997) 69-81.

[186] Katsuyuki Yanagihara, Kazuhiro Nagata and Toshio Maruyama. *The role of microstructure on pesting during oxidation of $MoSi_2$ and $Mo(Si,\ Al)_2$ at 773K.* Oxidation of Metals, Vol. 47, No 5. ¾, 1997.

[187] Katsuyuki Yanagihara, Toshio Maruyama & Kazuhiro Nagata. *Effect of third element on the pesting suppression of Mo-Si-X intermetallics (X= Al, Ta, Ti, Zr and Y).* Intermetallics 4 (1996) S 133-S 139.

[188] Mohan G. Hebsur. *Pest Resistant $MoSi_2$-based Materials containing in-situ Growth β-Si_3N_4 Whiskers.* US 6,391,811 B1. May 21, 2002.

[189] T. C. Chou and T. G. Nieh. *Mechanism of $MoSi_2$ Pest during low temperature oxidation*. J. Mater. Res., Vol. 8, No.1, Jan 1993.

[190] K. Natesan, S. C. Deevi. *Oxidation behavior of Molybdenum Silicides and their composites*. Intermetallics 8 (2000) 1147-1158.

[191] Houan Zhang, Hejian Wu, Jia Lin, Siyong Gu, Lei Yu. *Low temperature oxidation behavior of CNTs/$MoSi_2$ Composites*. Advanced Materials Research. ISSN: 1662-8985, Vol. 983, pp 116-120.

[192] www.Manualslib.com

[193] Hongfei Cheng, Yi Zhou, Qinfu Liu. Kaolinite *Nanomaterials:Preparation, Properties and Functional Applications. Nanomaterials from Clay Minerals. A New Approach to Green Functional Materials*. Micro and Nano Technologies. 2019. PP 285-334.

[194] Brindley, G. & Keith Robinson. (1946). *The structure of kaolinite.* Mineralogical Magazine and Journal of the Mineralogical Society, 27(194), 242-253.

[195] U. Sutharsini, M. Thanihaichelva, R. Singh. *"Two-Step Sintering of Ceramics" In Sintering of Functional Materials*, edited by Igor Shishkovsky. London: IntechOpen, 2017.

[196] M. Ghazali Kamardan, N. Hidayah A. Zaidi, M. Noh Dalimin, A. Mujahid A. Zaidi, S. Bahrin Jamaludin and M. Mahadi A. Jamil. *The Sintering Temperature Effect on the Shrinkage Behavior of Cobalt Chromium Alloy*. Am. J. Applied Sci. 7 (11):1443-1448, 2010.

[197] Souhir Mankai, Jamel Mcliouli, Jalila Sghaier, and Didier Lecomte. *Determination of porosity from shrinkage curves during sintering of granular materials.* www. tandfonline.com/Idrt.

[*] Hammood I, Barber G, Wang B. *A review of some of experimental and numerical studies of self-crack-healing in ceramics.* Int J Ceramic *Eng Sci* 2020;2:274–291.